Assessing and mitigating risk to amphibian populations from shifting anthropogenic stressors

by

Rylee Garrett Murray

B.Sc., Thompson Rivers University, 2011

Thesis Submitted in Partial Fulfillment of the
Requirements for the Degree of
Doctor of Philosophy

in the
Department of Biological Sciences
Faculty of Science

SIMON FRASER UNIVERSITY
Spring 2023

Declaration of Committee

Name:	**Rylee Garrett Murray**
Degree:	**Doctor of Philosophy**
Title:	**Assessing and mitigating risk to amphibian populations from shifting anthropogenic stressors**
Committee:	**Chair: Vicki Marlatt** Associate Professor, Biological Sciences
	Wendy Palen Supervisor Professor, Biological Sciences
	Jonathan Moore Committee Member Professor, Biological Sciences
	Joshua Malt Committee Member Section Head British Columbia Ministry of Water, Land and Resource Stewardship
	David Green Examiner Professor, Biological Sciences
	Amanda Bates External Examiner Professor, Biology University of Victoria

Abstract

Human disturbances to landscapes resulting in habitat degradation and fragmentation frequently drive wildlife population declines by altering demographic rates. A deep understanding of the specific mechanisms that reduce survival of individual life history stages, and the magnitude of the response, is critical to mitigating drivers of decline. I explore how a range of anthropogenic stressors scale to the level of emergent population dynamics using individual level physiological responses and stage-structured demographic models to improve predictions for three conservation challenges: 1) understanding impacts to amphibian populations affected by river hydropower development, 2) forecasting the magnitude and impact of climate change for populations of an amphibian whose range spans across 16^{o} of latitude, and 3) identifying the impact and most effective mitigation strategies for amphibian populations subject to increasing road mortality. I use estimates of individual-level physiological traits to predict how anthropogenic changes in thermal habitat for Coastal tailed-frog (*Ascaphus truei*) will affect population-level vulnerability from 1) river diversion hydropower dams, and 2) accelerating climate change. I demonstrate that *A. truei* populations in British Columbia are subject to the equivalent of 50-years of climate warming in rivers where river diversion hydropower dams operate. I find that across the *A. truei* range, from Northern California to Northern British Columbia, that populations at the southern range boundary have higher immediate vulnerability to climate change. However, faster rates of temperature change in the north, compounded with adaptations to lower temperatures, causes accelerating risk to northern populations. Equally important to forecasting population vulnerability is identifying and evaluating methods to reverse population declines. I use demographic models to elucidate the potential for reducing extinction risk to migrating populations of Northern red- legged frogs (*Rana aurora aurora*) subject to increasing road mortality by evaluating the effectiveness of two commonly employed mitigation strategies, road-side fencing and wildlife underpasses. I find that the combination of two mitigation structures effectively reverse current population declines for *R. aurora*, but when I account for increasing vehicle traffic in the

future, predict that additional mitigation will be required to prevent population declines and local extinction. In this thesis, I use physiological and demographic models to improve our understanding of the magnitude of current anthropogenic stressors to wild amphibian populations, but also highlight that modern stressors are frequently non-stationary, and present unique challenges to population-scale predictions.

Keywords: River diversion hydropower; climate change; habitat fragmentation; thermal performance; demographic modeling; amphibian decline

To Alexis and Kane, and Ruby, who I hope this piece may contribute even an infinitesimal fragment in allowing their dreams come true.

"We have to dream in order to survive."

(Gates McFadden as Dr. Beverly Crusher)

Acknowledgements

I have learned a lot about biology, ecology, and conservation throughout my academic career, and a lot about myself: my motivations and passions. It would not have been possible without the love and support of so many people; namely the amazing and influential women of my life who I draw so much inspiration. First, I would love to thank my senior supervisor, Wendy Palen, who early on recognized my hard work, dedication, and curiosity and later was a constant and understanding support when things were tough. Your confidence, intellect, and humour revitalize me every time we talk, and I hope to receive and benefit from your mentorship for a long time into the future. Purnima Govindarajulu, Barb Beasley, and Mo Ryan have also been influential, strong, independent women that excite me about being a conservationist and always brighten my day. Amanda Kissel, she took a chance on me and I learned so much from her. Mentor, friend, role-model: your calm, rational, empathetic, and hilarious personality is the foil to my whirlwind, and yet without you I would not be the person I am today; I've changed so much because of you. And combined with Lindsay "Linda" Davidson, and Michelle "Seegs" Segal, the three make up an indestructible support group and family. Outside of academia, my Gramma, Phyllis, my parents, Kelly and Daryl, my Aunty Tracey, and my surrogate parents Kris Weatherman and Brian Groome, all have been my caregivers even in my adult years, and great inspiration and sounding board for all my weird ideas and opinions, and have all encouraged curiosity my entire life. To Jessica, my longest and best friend, whose own journey through academia in the Fine Arts contributed inspiration and encouragement: that I might be able to also follow my curiosity through such an endeavour. And Kerry, alongside Jess, you two are solid through it all. Your pragmatism and humour are essential to me. Camille, who I deeply love beyond words, opened a new world of partnership, compassion, and exploration that was essential in the completion of this thesis and in making me who I am today.

Thank you to Jon Moore and Josh Malt for being a part of my supervisory committee over the past eight-and-a-half years. Your encouragement, critiques, and praise were always welcome when I would be hard on myself and forget what I was doing. And what you both taught me with respect to stream ecology and wildlife management greatly improved this thesis.

This work would not have been possible without the financial support from the Gordon and Betty Moore Foundation, the Canadian National Sciences and Engineering Research Council, Society for Little Amphibian Tragedies & Clayquot Biosphere Trust, Habitat Conservation Trust, British Columbia Ministry of Transportation and Infrastructure, British Columbia Ministry of Water, Land, and Resource Stewardship, Parks Canada, and the U.S. National Sciences Foundation. Thank you to my collaborators and co-authors at Colorado State University who made the full vision of Chapter 3 come to fruition.

I would also like to thank the large number of incredible people who've helped my research as field technicians, volunteers, and confidentes: Danielle Courcelles, Griffin Dare, Chloe Reid, Michael Arbeider, and Kara Hall: we made great teams of young and budding scientists. Thanks to all the members of the Palen Lab that helped with ideas, study design, statistics, and were company in many field trips: Viorel Popescu, Pascale Gibeau, Dan Greenberg, Gavia Lertzman-Lepofsky. And a special thanks to Cherie McKeeman, who's co-passion for frogs with external genitalia has been a great source of field help and encouragement over the years.

And finally, although my immaturity at the time stopped me from asking permission: I'd like to acknowledge that this work took place on the stolen, and in some cases collaboratively used, land of the Xa' xsta, Yuułu?iɬ?ath, and the Tsimshian, specifically the Kitselas and Kitsumkalum First Nations in what we now call British Columbia, and the nations who rightfully own the land in what we now call the coastline of Northern California and Central Oregon.

Table of Contents

List of Tables

List of Figures

Chapter 1. General Introduction

1.1. Scales of shifting human stressors

> Was it actually possible to know the future? Not simply to guess at it; was it possible to know what was going to happen, with absolute certainty and in specific detail?
>
> *Louise in Ted Chaing*
> *Story of Your Life, 2002*

The myriad ways in which ecosystems are influenced by humans have been accelerating since the Late Pleistocene and have caused shifts in millennia-held ecological regimes, and wildlife losses likely resulting in the sixth mass extinction sometime after the 2100s CE (Braje and Erlandson 2013). Understanding the rate at which biodiversity has been lost since during and after the last glacial maximum (Meltzer 2020) has hinged upon our knowledge that many human influences have continued to act as stressors to wildlife across a range of scales in space (local to landscape) and time (days to millennia; pulse to press), and affected ecosystems across multiple levels from metabolism and physiology to communities (Simmons et al. 2021). However, not all of human history is mired in negative impacts; despite the heavy use of natural resources by populations in the millions (Thornton 2005), indigenous peoples of what is now called North America stewarded the land across space and time that actually increased native biodiversity (Armstrong et al. 2021, Hoffman et al. 2021). However, since at least 17th century CE after the publication “Sylva” (Evelyn 1664), that advocated for land stewardship and protecting biodiversity in the face of dwindling European forests (Hemery 2014), most European-based cultures have found it difficult to balance land-use and conservation. Furthermore, the multiple scales at which humans impact wildlife and ecosystems means that stressors are not static, and therefore should be understood and not mitigated as such. Currently, the ways in which we try to avoid, mitigate, compensate, and ultimately manage cumulative antagonistic or synergistic human stressors have been usually singular and small in scale spatiotemporally (Antwi et al. 2022). For example: governments are increasingly outsourcing research and monitoring efforts to private biological contracting companies that are not interested in, nor have the capacity to implement studies at anything but the basest scales (Darimont et al. 2018, Westwood et al. 2019a). Space- and time- series data exist mostly for economically important species and habitats (Magurran et al. 2010) and still are rarely used to be critical of current practices and inform decisions that would effectively protect habitat,

populations, and biodiversity beyond current levels of stressors (García-Barón et al. 2021). Meanwhile, calls to integrate rigorously collected data (Westwood et al. 2019b) with new ideas on the implementation of conservation across multiple scales are leading to positive forecasts of conservation efficacy (Bennett et al. 2021). However, in North America, neoliberalism has stagnated the already taxonomically biased conservation funding (Government of Canada 2018, Echols et al. 2019, Fletcher 2020, Buxton et al. 2021), and so conservationists, particularly of non-economically important taxa, need to advocate and embrace techniques that allow for rapid assessment of species non-stationary situations at multiple scales in space and time.

Robust and effective techniques that can evaluate population and species vulnerability to stressors across spatiotemporal scales exist, but need to be used more regularly, outside the confines of ivory tower research, and results interpreted in new ways to make outside the box predictions of how species will be impacted by the negative effects of human activity or our interventions. For example: techniques that measure physiological responses to- or traumatic outcomes from- ecosystem change that scale from individual survival (Régnière et al. 2012) to emergent population dynamics (Merow et al. 2014) allow us to make multi-spatiotemporal-scale predictions beyond the confines of our study systems (Meltzer 2020). Particularly, when we compare population predictions over time, or current and near- future environment with species tipping points (e.g. physiological constraints) at multiple-spatiotemporal-scales, we can gain an understanding of the speed and acceleration of change, and can better predict relative vulnerability of populations and species in the distant future at local, to regional, to landscape scales (Turner et al. 2020). Furthermore, these scale independent conclusions at the population level, the level at which we practice most conservation (Pickett et al. 1992), can also scale to species and landscapes, and when combined with predictions of environmental factors, climate, and time.

To explore the concept of using scale independent measures of species responses to changing environments and to make predictions about vulnerability across multiple scales, I aim to answer two questions concerning major drivers of amphibian decline (Stuart et al. 2004). 1) how does population vulnerability from changing temperatures because of direct resource exploitation at local scales compare to population and species vulnerability across a species range when coupled with global climate change and scaled to near- and distant- futures and 2) how do our predictions of population vulnerability, and subsequently mitigation of habitat degradation, change when we consider the non-stationary level of stress imposed by a static footprint on habitat? I focus on amphibians because they are a taxonomic group that is for the

most part not-economically important and therefore under-represented in conservation (Wright et al. 2020), and who's complex lifecycle warrants continued exploration into how multiple stressors at different life stages and scales can scale to emergent population dynamics (Campbell Grant et al. 2020). The effects of resource development and climate change in tandem is a timely question that seeks to understand, in part, the cumulative effects of our quest for renewable energies on ectotherms, such as amphibians. Furthermore, despite the surge in climate change research (Taylor et al. 2021), loss of suitable habitat is still the largest driver of amphibian declines (Stuart et al. 2004, Campbell Grant et al. 2020), and thus understanding the nuanced ways in which habitat alterations causes declines is still of grave importance if we wish to succeed in our conservation goals.

Understanding causal mechanisms of declines using species physiological constraints has been important to rapidly assess species vulnerability to environmental change and the consequences of conservation actions that scale easily to populations and species (Wikelski and Cooke 2006). Because understanding how climate change contributes to biodiversity loss is of particular importance in recent decades, thermal physiology is one mechanistic way we can assess species responses (Chown 2012). Furthermore, for ectotherms, population growth is highly linked to thermal physiology, such that populations and species that experience temperatures beyond physiological limits are likely in decline (Deutsch et al. 2008, Angilletta 2009, Ma et al. 2015), thus presenting an opportunity to make predictions by scaling up from individuals to populations. I use estimates of individual-level physiological traits to predict how changes caused by humans in thermal habitat for Coastal tailed-frog (*Ascaphus truei*) will affect population-level vulnerability from 1) river diversion hydropower dams), and 2) accelerating climate change. I use estimates of local and regional responses to changing temperatures to make predictions about how human stressors effect population growth, and assess the speed at which vulnerability across multiple scales is changing. By doing so, I attempt to understand how regional climate adaptation links with changing human stressors to make distant future predictions of population and species vulnerability outside the time range of current climate models. However, the effects of habitat degradation also change with time, and I address how such changes impact individual survival and scale to populations across a species range that experience similar types of habitat degradation. Furthermore, I illustrate a unique situation of how the effects of seemingly static forms of habitat degradation can increase over time and may thwart conservation efforts.

While changes to environmental temperatures likely effect thermal physiology across all life stages similarly (González-Tokman et al. 2020, Dahlke et al. 2020, De Souza Jensen & Greenberg *in prep.*) and allow us to make predictions about population decline even for species with complex life-cycles, the specific use of stage-based demographic models allows us to understand the contribution to population vulnerability of stressors that may only impact some life-stages (Villellas et al. 2015). I further my exploration of scaling impacts on individuals to populations and species, and the concept that using changing predictions of species vulnerability over time helps us to better understand the actual effects of conservation efforts. I use estimates of road crossing mortality of Northern red-legged frog juveniles and adults whose migration corridor is bisected by a highway with increasing vehicle traffic to illustrate the potential for a static footprint (a highway) to have non-stationary impacts to population vulnerability over time (increased traffic). Furthermore, I assess whether conservation efforts based on current levels of impact have the ability to mitigate future increases in human activity.

Chapter 2. Downstream warming from diversion dams reduces thermal safety margin for Tailed-frog (*Ascaphus truei*) larva

2.1. Abstract

The life history and physiology of riverine species is fundamentally shaped by natural flow and temperature regimes. During seasonal low flows, river diversion hydropower dams often remove a large proportion (up to 90%) of natural streamflow, resulting in reaches with dramatically reduced discharge. Such conditions have the potential to create negative effects for stream biota by changing downstream thermal regimes and either exceeding species thermal performance optima (T_{opt}) or reducing the thermal safety margin (TSM) between ambient environmental temperatures and physiological limits. Neither the effect of reduced discharge from diversion dams on downstream water temperature nor the subsequent ecological and physiological impacts on stream biota have been evaluated. Here we quantified the magnitude of warming above and below four diversion dams in British Columbia, Canada, and predicted the impact of dam-induced warming for the thermal performance of Coastal Tailed frog (*Acaphus truei*) larva. *A. truei* have high overlap with existing and future diversion dams in the region, are listed as a species of 'special concern', and spend multiple years in high-gradient streams as larvae. Using laboratory-based thermal performance experiments at six temperatures, we estimated the thermal performance curves and T_{opt} for three *A. truei* populations. We compared *A. truei* T_{opt} to summer water temperatures – sampled between June and September - measured above and below four diversion dams in the region. We estimated the thermal optimum for *A. truei* larva was 23°C across all three populations. We found that daily mean water temperatures in the average diversion reach (2.9 km downstream of dams) were 0.3°C warmer than the natural expected warming, and that summer temperatures never exceeded T_{opt} in either environment. However, the TSM, measured as the difference between observed ambient mean maximum daily temperatures and T_{opt}, was reduced by 5% to as little as 6°C downstream of diversion dams. This study supports the conclusion that diversion dams do not currently put *A. truei* larva at risk of exceeding physiological thermal limits. However, warming due to water diversion is likely to compound the risk posed to *A. truei* from additional climate-induced warming in the next century.

2.2. Introduction

Streams and rivers of temperate regions are threatened by growing human appropriation of freshwaters for agriculture, human consumption, and hydro-electric generation (Poff et al, 1997), as well as by climate-driven reductions in snowpack and glaciers that feed them (Barnett et al, 2005; Caissie, 2006; van Vliet et al, 2013). In contrast, the magnitude, variability, and seasonality of natural flow regimes in rivers structure riverine ecosystems and have shaped the life history and physiology of stream biota (Poff et al, 1997). Hydro-electric and storage reservoirs (Jackson et al, 2001) are known to alter natural flow regimes and change sedimentation rates, downstream water temperatures, and total water availability (Poff & Ward, 1989), which in turn decreases the viability and persistence of many downstream populations (Gibeau & Palen 2020, Gibeau & Palen 2021). River diversion dams have emerged as an alternative to large storage hydro-electric dams (Anderson et al, 2006; Abbasi & Abbasi, 2011), are often smaller and occur higher in watersheds than reservoir hydropower dams (Anderson et al, 2006; Wohl, 2006) and they remove a portion of existing streamflow (called the diversion reach) for downstream electrical generation and subsequently return the water to the channel. As a result, river diversion hydropower dams are expected to have fewer downstream impacts because they more closely mimic natural flow regimes and have little impact on overall water availability, but empirical data are limited (Gibeau et al. 2017) and transferability of findings from studies on large storage hydropower is low (Connors et al, 2014). During seasonal low flows, discharge in diversion reaches can be a small fraction (as low as 10%) of natural streamflow which has the potential to cause localized pronounced changes to discharge variability due to operational fluctuations of the dam. Seasonal variation in flow regime is changed in river diversion dams by reducing magnitude or truncating periods of high flow (Poff et al, 1997), in some cases leading to earlier onset of dry season low flow conditions (Lewis et al, 2004). Variability within seasons may be dampened as operators take advantage of short periods of increased water availability (e.g. rain events), or fluctuations in power generation can introduce variability when natural regimes would be relatively stable (e.g. dry seasons; Poff et al, 1997). While changes in yearly and seasonal variation in discharge may have overall permanent impacts on some stream characteristics, such as sedimentation and channel morphology (Poff et al, 1997; Fuller et al, 2014), there are unknown consequences for other abiotic factors such as temperature regimes, which are dependent on discharges and may be transitory and compounded during certain seasons (Wohl, 2006).

Concurrent with the rapid adoption of river diversion hydropower, anthropogenic climate change is expected to result in warmer temperatures, and shift seasonal patterns of precipitation that in part drive the hydrology of streams. In temperate regions where snowmelt is integral for streams and rivers (Mote et al, 2005; Stewart et al, 2005; Hamlet et al, 2005; 2007) reductions in snowpack of >50% over the last 50 years caused by increasing air temperature and changes to precipitation (Mote et al, 2005; Hamlet et al, 2005) are causing snowmelt and spring freshet to end earlier and longer periods of summer low flows (Hamlet et al, 2007). Climate change projections forecast continued warming (Stocker et al, 2013) with temperatures too high for much of the precipitation to fall as snow during winters, resulting in a transition from snow-dominated precipitation to rain-dominated precipitation in many watersheds in the US and Canadian northwest (Elsner et al, 2010; Schnorbus et al, 2014). During winter and spring, increases in surface water run-off could change the timing of high flow events, yet further impacts may arise when melting of reduced snowpacks and glaciers in the spring lead to earlier, smaller, and shorter freshet and an increase in the length and severity of summer low flow and drought periods (Mote et al, 2005; Hamlet et al, 2005; 2007; Isaak et al, 2016) similar to downstream reaches in systems with operating river diversion hydropower dams. Thus, studying the impacts of river diversion hydropower dams may also foreshadow impacts from climate change.

River diversion hydropower dams can divert up to 90% of the water during annual periods of low discharge, and during the summer months the added removal of water has the potential to compound the effects of seasonally high air temperatures on stream water. Water temperature in streams is affected by multiple factors including air temperature, water source (ground water, snow or glacier melt, rain water), friction, exposure to sunlight, and discharge (Vugts, 1974; Sinokrot & Stefan, 1993; Caissie, 2006; Dewson et al, 2007; Cole & Newton, 2013). While atmospheric conditions (solar radiation, air temperature, precipitation, melting snow or ice), topography (shading by vegetation or mountains, latitude, elevation), and streambed characteristics (hyporheic exchange, groundwater, conduction with sediments) play the most notable roles in how water temperatures warm, stream discharge (speed, volume, friction with streambed) significantly influences warming rates, mostly through the changes in heat capacity at different volumes of water (Caissie, 2006). Thus, the construction of river diversion hydropower dams, which is often associated with reduced canopy cover along the diversion reaches due to road and penstock construction could cause increased solar radiation and air temperature (Cole & Newton, 2013), and has the potential to significantly increase

temperatures in the streams. In addition, smaller volumes of water traveling through river channels are expected to be influenced to a greater degree by solar radiation and experience higher rates of atmospheric heat transfer (lower heat capacity) resulting in higher downstream temperatures (Sinokrot & Stefan, 1993; Caissie, 2006; Dewson et al, 2007). Little research has been done to understand the impacts to warming rates when diversion reaches have as much as 80 – 90% of discharges removed during the summer months, and the risk that increased temperatures pose to stream biota (Connors et al, 2014).

Ectotherm physiology is shaped by ambient environmental temperatures over evolutionary timescales (Angilletta et al, 2002), which causes differences in locomotive performance across temperatures and translates into changes in predation risk, foraging ability, fecundity, and population growth rates (Fry & Hart, 1948; Levins, 1968; Lynch & Gabriel, 1987; Huey & Kingsolver, 1989; Gilchrist, 1995; Watkins, 1996; Schulte et al, 2011). Relationships between locomotion and temperature (Thermal performance curves; TPCs; (Watkins, 1996; Köhler et al, 2011) are useful for estimating physiological metrics such as thermal performance optima (T_{opt}), critical thermal maxima (CT_{max}), critical thermal minima (CT_{min}), and thermal performance breadths (Huey & Stevenson, 1979). These metrics are related to, among other ecological pressures, climatic evolutionary history, and life-history traits (Andrews & Schwarzkopf, 2012). By combining TPCs with estimates of thermal change to an ectotherms environment, we can calculate thermal safety margin (TSM; degrees between environmental temperature and T_{opt}) to estimate climate vulnerability (Deutsch et al, 2008). Because metabolic costs for individuals beyond T_{opt} can collectively result in negative population decline (Deutsch et al, 2008; Estay et al, 2010) and local population extinction (Sinervo et al, 2010) estimates of T_{opt} provide a means to predict population viability in the face of environmental temperature changes.

Here we add to a growing body of knowledge and evidence for increased temperatures as a mechanism of habitat fragmentation (Tuff et al. 2016) by estimating the thermal vulnerability of a cold water adapted amphibian larva, *Ascaphus truei* (Coastal Tailed frog) to anthropogenic stream warming caused by river diversion hydropower dams in southwestern British Columbia. We collected empirical data on environmental stream temperatures upstream and downstream of four hydropower diversion dams, and used these data to estimate the specific contribution of river diversion hydropower dams to downstream warming. We conducted thermal performance experiments on three populations of *A. truei* larvae to estimate TPCs and T_{opt} across a range of controlled temperatures (2-28°C). We combined estimates of T_{opt} with the

observed warming downstream of dams to predict the vulnerability of *A. truei* to the effects of anthropogenic warming by dams more broadly in the region. We hypothesized that reduced discharge in diversion reaches would cause stream temperatures to warm at a faster rate than similar reaches not influenced by diversion dams, and we evaluated the vulnerability of *A. truei* larvae to warming temperatures by estimating whether summertime mean daily and mean maximum diversion reach temperatures exceeded the T_{opt} for larval *A. truei* or caused reductions in TSM that would put larvae at further risk to warming.

2.3. Methods

2.3.1. Study system

We evaluated the effect of temperature regimes in streams affected by river diversion hydropower for larval *A. truei*, a cold-water adapted amphibian endemic to the Pacific Coast, ranging from Northern California to the North Coast of British Columbia, and categorized by the Committee on the Status of Endangered Wildlife in Canada (COSEWIC) as 'Special Concern' (COSEWIC, 2011). *A. truei* reproduction is relatively low (<100 eggs per clutch), larval period is long, lasting 3 – 4 years in the northern latitudes of their range, adults are long-lived, and all life stages are cold-adapted to high velocity high gradient streams (Daugherty & Sheldon, 1982), suggesting that both *A. truei larvae* and *A. truei* populations may be especially vulnerable to changing environmental and thermal conditions (de Vlaming & Bury, 1970; Brown, 1975; Hossack et al, 2013).

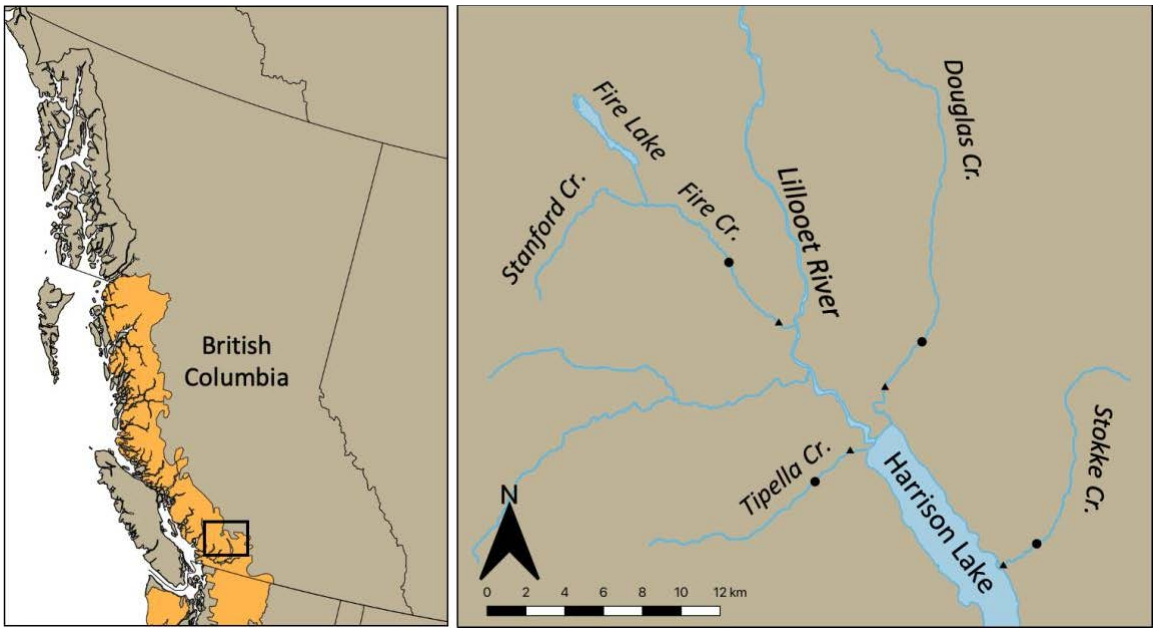

Figure 2-1 Map of the upper Harrison Lake watershed situated in southwestern British Columbia within the *A. truei* range (orange), including study streams with operating hydroelectric diversion dams. *A. truei* larva were sampled from populations at Tipella, Stokke, and Fire above the dams (dots), and temperature was sampled at 5 sites above and 5 sites below the dams to just above the powerhouses (triangles) on each of the three larvae sampling streams plus a fourth stream with a dam, Douglas.

We monitored the temperature of four high gradient streams in the Harrison River watershed (Fire, Tipella, Douglas, and Stokke), situated approximately 95km northeast of the Fraser River delta in southwest British Columbia (Figure 2-1). Watersheds ranged from 63 – 105km^2, with mean annual discharges of 4.6 – 6.5 m^3/s, and mean gradients of 4.5 – 12.5%. An operating river diversion hydropower dam, also called Run-of-River hydropower, is present on each stream with diversion reaches of reduced streamflow extending from 2.1 – 4.3km downstream of each dam (Table 2-1). During the summer months streamflow in these and other streams in the region is generated from melting snowpack, glacial runoff, rainfall, and groundwater (Fuller et al, 2014). Peak seasonal air temperatures and solar radiation combined with receding summer hydrographs result in the warmest stream water temperatures of the year between June and September. During this time, channels are typically stable, and biofilm growth and biological productivity is highest, making it a critical time of year for most stream biota and for larval *A. truei* foraging and growth.

Table 2-1 **Distances associated with stream reaches. Distance from headwaters (km) of each stream is defined as the point at which the last major tributary enters the mainstem of the stream above the dam. Diversion reaches start below the dam to the point at which water is returned to the stream at the powerhouse.**

Stream	Watershed size (km^2)	Distance from 'headwaters' to dam (km)	Length of diversion reach (km)
Tipella	63.2	4.0	2.3
Stokke	73.9	1.9	2.1
Fire	105.2	4.6	4.3
Douglas	102.6	1.7	3.0

2.3.2. Stream temperatures

To estimate the effect of river diversion hydropower dams and reduced discharge on downstream temperatures, we collected hourly temperature (^oC) between the months of June and September 2015. In each stream, we monitored temperature in ten locations, five points upstream and downstream of the diversion dam, radiating out at 0.1km, 0.4km, 1.0km, 1.5km, and either just below the headwaters (the point of confluence upstream of the dam with the first major tributary of similar stream order) or just above the power house (where water is returned back to the stream), except at Fire Cr. where only three points were used upstream (0.1km, 1.0km, 3.0km) due to equipment failure. We used temperature loggers (Maxim/Dallas Semiconductor) installed at a depth of 55-65cm as close to the centre of the thalweg as possible attached to rebar that we hammered into the streambed substrate (Figure 2.1).

We used multiple linear regression in program R (R Development Core Team 2016) to estimate the degree of natural warming that occurs with distance down watersheds (e.g, from headwaters to confluences with higher order streams), while also estimating the specific contribution of the presence of the diversion dam (i.e. diversion of >50% of summer streamflow; Appendix A, Table S1, Figure S1). We used empirical data on the difference in mean daily temperature at downstream sampling locations from the temperature recorded at the headwaters, the distance downstream from the headwaters of the sampling location, and whether it was above or below the dam (i.e. in the diversion reach), to create a global model to estimate the rate of warming per downstream kilometer. All combinations of variables and interactions were considered to generate candidate models and models were evaluated using

second order Akaike's Information Criteria (AICc) to correct for small sample size (5 models). The top model was used to predict the natural background rate of stream warming per kilometer downstream, and the increased warming rate due to the presence of the dam. We then used observations of daily mean (± CI; $T_{i,mean}$) and maximum (± CI; $T_{i,max}$) temperatures of the warmest summer month for each stream from sampling points directly above the dams to predict both the natural background temperatures (T_{nat}) and the magnitude of additional warming created by the dam (T_{dam}) at 0, 2.9, and 4.3 km downstream of the dam, representing the immediate effect of the dam, and the average and maximum length of diversion reaches represented by the river diversion hydropower operations in these streams, respectively.

2.3.3. Thermal physiology experiments

To estimate the response of larval *A. truei* locomotion to water temperature and estimate T_{opt}, we collected 30 larvae (Gosner stage 30-36; Gosner, 1960) from each of three populations coinciding with three of our study streams (Tipella, Fire, Stokke) during August and September 2015. The following year in October 2016 we gathered another 15 individuals (Gosner stage 26-45; Gosner 1960) from each of the streams to test their critical thermal maxima (CT_{max}) which is an estimate of the species upper thermal limit, the temperature which the larvae can experience briefly and still recover, and can help us characterize the steepness of the thermal performance curve at the temperatures exceeding T_{opt}. The CT_{max} estimates obtained were also later used for further studies on range-wide differences in *A. truei* thermal physiology. After removal from the streams, larvae were transported indoors and kept in separate 500L fiberglass tanks lined with cobbles, filled with re-circulating dechlorinated water. Individuals used for thermal performance assay were left to acclimate for >3weeks at ~8.3 °C (95% CI +/- 0.8°C; Table S2) and fed puréed spinach baked on ceramic tiles, replaced continuously throughout the acclimation period. Larvae collected for CT_{max} estimates in 2016 followed a protocol 72-hour acclimation protocol in an oxygenated 8°C water bath.

2.3.4. Thermal performance assays

To determine thermal optimum (T_{opt}) for each population, we created six temperature treatments ranging from 2 - 28 °C (Table 2.2). We used recirculating chilled water, 200W aquarium heaters, and digital thermostats to maintain constant water temperature in each treatment. Dissolved oxygen was maintained above 85% saturation using compressed air and aquarium air stones. Each population was assayed separately over the course of three days.

Larvae were randomly assigned to temperature treatment (n = 5) and after a brief acclimation (30 min) were released and held at the treatment temperature for 6 hours. Because death was not the intended endpoint of our assays, observations of death or indicators of near death (loss of righting reflex) were used to adjust the maximum temperature treatment for subsequent assays. For example, one larva died at 27°C in the Tipella Creek trial, therefore the maximum temperature for the Stokke Creek assay was reduced to 26°C. Burst swimming speed of larvae was tested by placing individuals in a v-shaped plexiglass channel with 2 cm of water and a startle response was generated with a weak (100V, 150 milliamp, 15 millisecond) electrical stimulus (S88 Grass Stimulator) using stainless steel electrodes on either side of their tails. Each trial was recorded with a high resolution (720p) digital camera at high speed (240fps). After each trial, each larva was weighed (mg) and their volume (ml) measured. Larvae were only used once, and individuals were euthanized at the conclusion of the experiments.

Table 2-2 Mean temperatures (°C) recorded during six-hour exposures to a range of six temperatures to create thermal performance curves for three populations of *A. truei* larvae

Population	Mean temperatures for thermal performance assay (°C)					
Tipella	1.9	8.4	16.1	20.1	23.8	26.7
Stokke	2.1	10.0	16.1	20.1	24.0	26.0
Fire	2.2	10.0	16.1	20.1	23.8	28.0

To estimate CT_{max} of *A. truei* larvae in streams of the South Coast, individuals were placed in separate flow-through containers and submerged in an oxygenated 8°C water bath for a five minute rest period after which it was heated at a constant rate (Dallas and Rivers-Moore 2012) of 0.3°C/min using a 500-watt submersible aquarium heater. We recorded the water temperature (°C) at which individuals stopped responding to a tactile stimulus and lost the ability to right themselves (LRR; Lutterschmidt and Hutchison 1997, Angilletta 2009) and were returned to cooler water to recover. Following testing, larvae were measured (length, mm), and euthanized using benzocaine and preserved in formalin and 95% EtOH. Averaqe CT_{max} was calculated for each of the populations and for the South Coast region, and CT_{max} of each individual was included in the data for creating thermal performance curves; see blelow.

We calculated maximum velocity (V_{max}) within the first half second after forward motion was initiated by analyzing the highspeed videos using Digitizing Tools software (Hedrick, 2008) implemented in MATLAB. V_{max} was calculated as the maximum distance (pixels) travelled between adjacent frames divided by the time period between frames (250 milliseconds; 240fps), within the first 120 frames (one half second). We fit a single regional (South Coast BC) thermal performance curve to V_{max} for all individuals (n = 90) from all three sampled populations (Tipella, Fire, Stokke) to a modified beta curve (Yin et al. 2003) Equation (1) and estimated parameters (specifically, T_{opt}) using maximum likelihood with the bbmle package (Bolker and Team 2017) in R (R Core Team 2019).

$$V_{max} = p_i + (p_{max} + (p_{max} - p_i)\left(1 + \frac{t_{opt} - t}{t_{opt} - t_m}\right)\left(\frac{t - t_i}{t_{opt} - t_i}\right)^{\left(\frac{t_m - t_i}{t_{opt} - t_m}\right)} \quad (1)$$

Where p_i is the performance at the lowest temperature (set as a constant – the average performance of each population in the 2°C treatment), t_i the lowest temperature (2°C), and t_m the inflection point where the rate of change of performance starts to decrease towards t_{opt}, the temperature at p_{max} (maximum performance). We included data points from CT_{max} trials to anchor the curves where performance equals zero. Others have successfully used gaussian curves (Angilletta 2006) and generalized additive models (Gerick et al. 2014) to model thermal performance, however, these models do not allow for statistical estimation of key parameters of the curve (T_{opt}) with error.

2.3.5. Comparison of environmental temperatures and performance

To estimate the impact of diversion dams and reduced discharge on *A. truei* swimming performance and thermal safety margin (TSM), we compared predictions of natural background (T_{nat}) and dam induced (T_{dam}) daily mean (± CI) and maximum (± CI) temperatures of the warmest summer month at 0, 2.9km, and 4.3km downstream of the dam, to the thermal performance curve, and estimated T_{opt} for *A. truei* larvae. We calculated the mean and minimum TSM (°C) for natural background and dam induced warming by subtracting the predicted mean and maximum temperatures for each of the distances downstream from T_{opt}, and the reduction in TSM by subtracting the TSM predicted in the presence of a dam from the TSM predicted after natural background warming.

2.4. Results

2.4.1. Stream temperatures

Stream temperatures varied throughout the summer and differed between above and below dam reaches (Table 2-3). The highest summer temperatures observed in each stream were on average 0.8°C warmer below dams than above dams, where maximum temperatures observed above dams ranged from 13.5 to 17.5 °C, and below dams ranged from 15.0 to 18.0 °C. The top model (AICc w = 1; Appendix A, Table S3) to predict the rate of downstream warming included all variables: distance from headwaters (km), sampling location (above or below dam), and the interaction between distance and sampling location. Above the dams, streams warmed by 0.17 °C ± 0.02 95% CI per km. Daily mean temperatures were 0.21°C ± 0.08 warmer immediately below dams, and warmed an additional 0.06°C ± 0.02 per downstream km more than the natural rate of warming documented above dams (Figure 2-2; Appendix A, Table S4).

Table 2-3 Summer stream temperatures (°C) and variability (± 1SD) from June to September observed above and below the dam in each watershed. Temperatures are the minimum, maximum, and daily mean observed during the sample period.

	Above dam			Below dam		
Stream	Min Temp (°C)	Mean Temp (± 1SD)	Max Temp	Min temp	Mean Temp (± 1SD)	Max Temp
Tipella	7.0	10.2 (± 1.0)	13.5	8.0	11.2 (+ 1.0)	15.0
Stokke	7.0	11.9 (± 1.5)	17.5	7.5	12.8 (+1.4)	18.0
Fire	7.5	11.0 (± 1.4)	16.0	8.0	12.4 (+ 1.6)	16.0
Douglas	7.5	12.4 (± 1.8)	17.5	7.5	13.1 (+ 1.8)	17.0

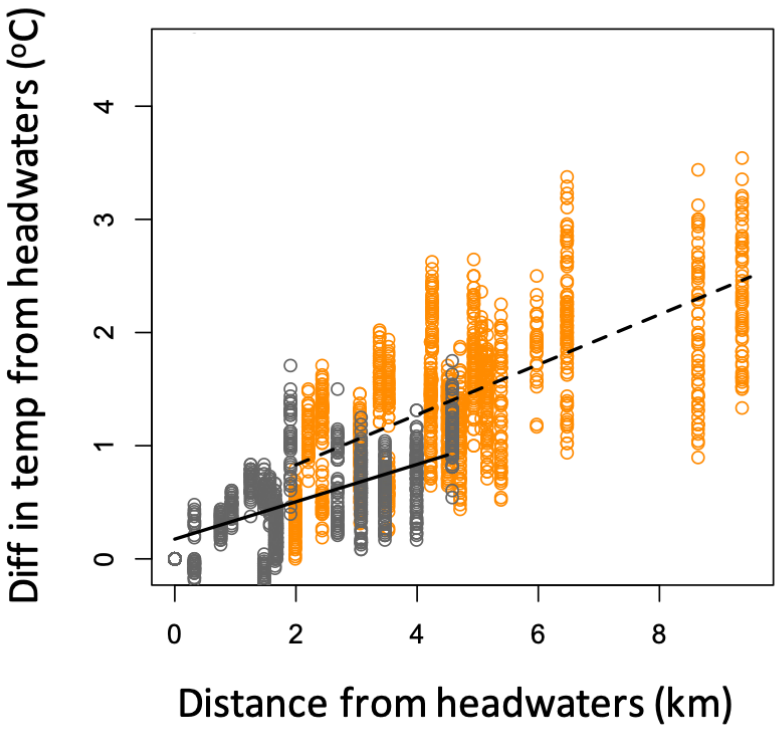

Figure 2-2 Observed differences in daily mean stream temperature (°C) sampled on four streams in southwest British Columbia, above (black) and below (orange) hydropower diversion dams. Predicted differences in daily temperatures shown as best-fit lines above (solid) and below dams (dotted).

The daily mean and maximum temperatures of sampling points directly upstream of the four dams for the warmest month were $T_{i, mean}$ = 12.5 °C ± 3.0 and $T_{i, max}$ = 13.9 °C ± 3.2 respectively. Using these starting temperatures we predicted the temperature at 0, 2.9, and 4.3km downstream without and with a dam by using the warming rates estimated for above dam (0.17 °C per km) and diversion reaches (0.06°C plus 0.21°C per km) respectively (Figure 2.2; Appendix A, Table S5). T_{dam} at 0km was 0.2°C ± 0.1 warmer than T_{nat} and steadily increased downstream and at a faster rate than $T_{nat,}$ at 2.9km and 4.3km until mean T_{dam} = 13.4°C ± 3.3 and maximum T_{dam} = 15.0°C ± 3.5, which were 0.5°C ± 0.1 warmer than the expected T_{nat} for that point in the stream (Figure 2-3).

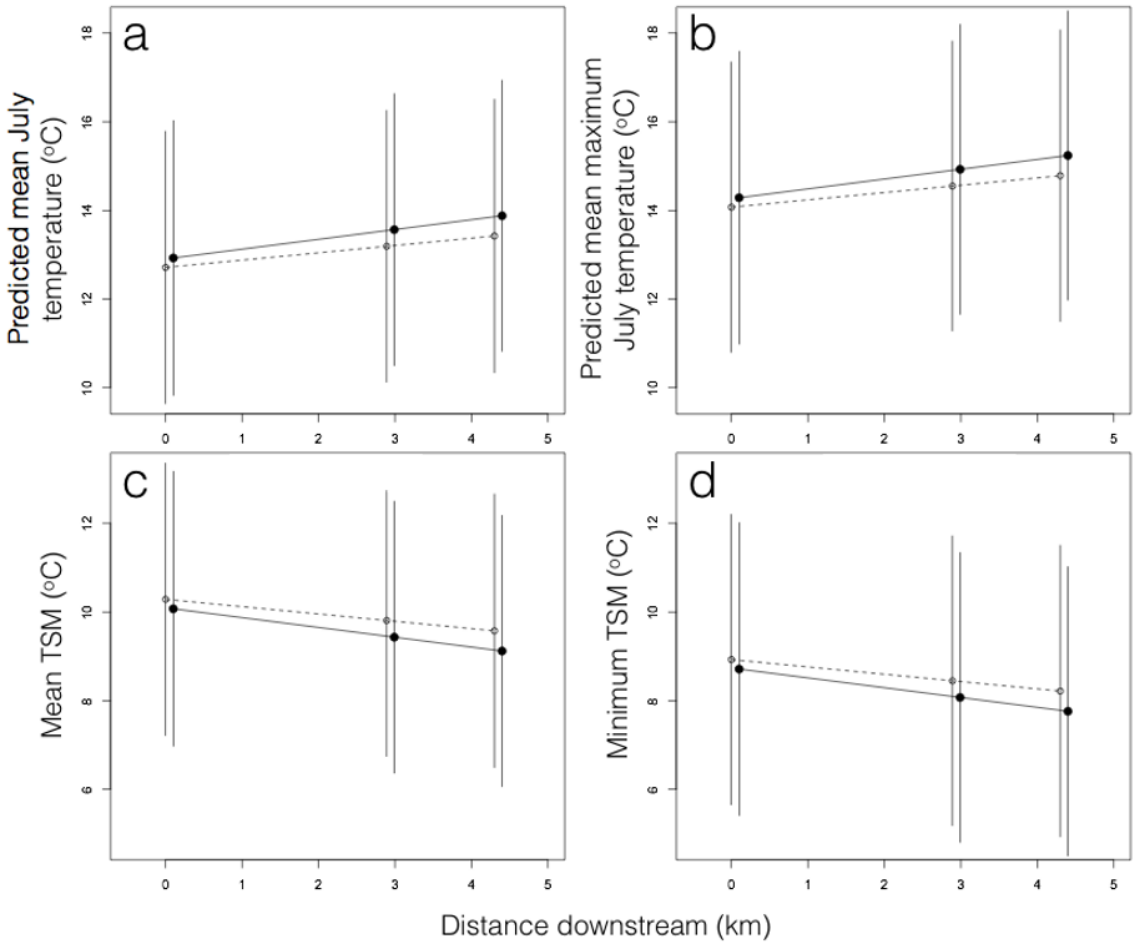

Figure 2-3 Predicted mean (a) and maximum (b) July temperatures (°C) and associated mean (c) and minimum (d) thermal safety margins (TSM) for streams without (open circles, dotted line) and with river diversion hydropower dams (black dot, solid line) with 95% CI (whiskers), immediately below (0km) the average position of dams on streams, and at the end of the average diversion reach (2.9km), and the longest diversion reach (4.3km) observed in the four study streams.

2.4.2. Physiological Assays

The thermal performance curve we characterized using the V_{max} data from the burst swimming trials in combination with the separate CT_{max} assays is congruent with the expected asymmetrical ectotherm performance curve (Angiletta 2009; Figure 2-4). Using the maximum likelihood results of the parameters estimate for Equation (1), T_{opt} = 22.9°C (16.4 – 24.3°C) 95% CI with maximum burst swimming speed within the first one half second of swimming to be V_{max} = 189 cm/s (161 – 199 cm/s). We estimated the critical thermal maximum for *A. truei* to be

CT_{max} = 31.2ºC (± 0.2ºC), but four larvae died in the performance assays in two of the hottest temperatures: three from Fire Creek (28 ºC) and one from Tipella (27ºC). No larvae died in the trials for Stokke Creek, where the maximum temperature treatment was reduced to 26 ºC.

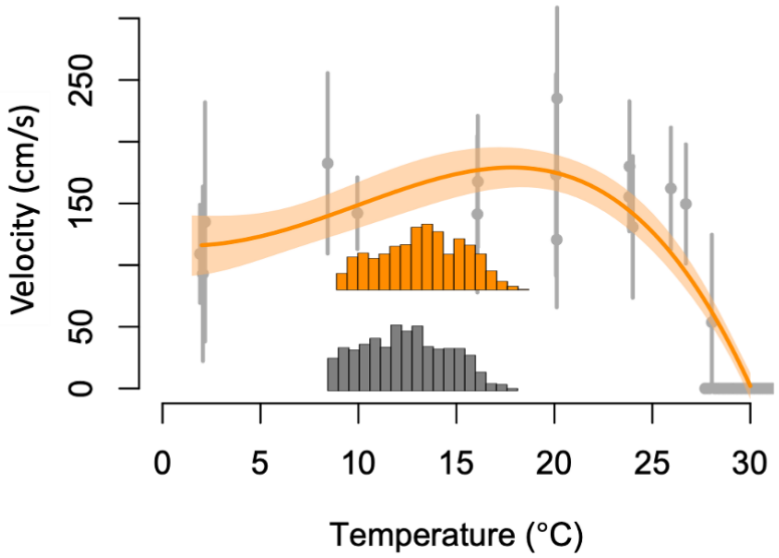

Figure 2-4 Thermal performance curve (average burst swimming velocity; cm/s) and 95% CI of *A. truei larva*, averaged across 90 individuals from three populations tested at six temperatures with average burst swimming velocity ±95% CI across the 15 larvae (5 larvae, 3 streams) tested per temperature (except 5 larvae per treatment 26-28ºC; grey dots/whiskers). Frequency histograms of maximum daily temperatures (ºC) logged over 88 summer days between 25 June – 21 September 2015 across all four streams above (grey) and below (orange) hydropower diversion dams.

2.4.3. Comparison of environmental temperatures and performance

Using the predicted mean daily temperatures in reaches above and below the four river diversion hydropower dams and our predicted T_{opt} = 22.9ºC, we estimated the TSM to naturally decrease by 5.6% at 4.3km downstream from a point on a free flowing stream (Figure 2-3). However, in *A. truei* habitat downstream a dam, TSM was predicted to be reduced by 7.2% at 2.9km and a further reduced by 3.3% at 1.4km further downstream, for an overall 10.5% reduction in TSM over the total 4.3km downstream from a dam. By comparing the reduction of TSM on a dammed stream compared to a free flowing stream, we estimate that river diversion

hydropower dams reduce TSM by almost 1.05 times faster than the natural flow regime for these systems of 4.3km. And by the end of the longest diversion reach we sampled (6.1km) the TSM would be eroded by a net 11% and would be warming at a rate 1.11 times faster than the natural flow regime.

2.5. Discussion

We identified an increased risk from warming stream temperatures caused by river diversion hydropower dams to a temperate stream dwelling ectotherm. The risk to populations of *A. truei* larva depends on their longitudinal position in the stream and spatially explicit predictions of temperature changes that hinge upon the length of water diversion. We predict that populations across four dammed streams are not likely to experience thermally limiting conditions due to operation of river diversion hydropower dams based on how temperatures change downstream of dams (Figure 2-4). However, while *A. truei* larva in free flowing streams have TSMs (using T_{nat}) of 8.2°C - 7.8°C, which provide a buffer to exceeding physiological limits in case of extreme warming events, we predict that the increased rate of warming below dams erodes TSM immediately by 0.2°C directly below the dam, and at a rate of ~ 0.1°C/km throughout the diversion reach (Figure 2-3). These warming rates lead to a high proportion of the populations of A. truei larva that inhabit dammed streams at temperatures warmer than expected (Table 2-1), with TSMs eroded throughout the length of diversion reaches that we studied by 0.2°C – 0.6°C, which puts larva at further risk to increased warming from other sources, such as climate change. If we consider other existing river diversion hydropower operations in southwestern British Columbia with known populations of *A. truei*, for which our longest diversion reach represents the 75th percentile of the range, and for which the average and maximum diversion reach lengths are 3.6km and 6.1km, TSM may be currently eroded for *A. truei* larvae by as much as 0.4 – 1.0°C, leaving populations of larvae in those streams at similar or greater risk.

Among other anthropogenic drivers of temperature in streams, river diversion hydropower stands to play a significant role by affecting fundamental characteristics of streams that are integral to natural temperature regimes. Solar radiation is a dominant component of downstream warming, however, other atmospheric, topographical, and geological characteristics are important, including air temperature, continued downstream input of water fed by precipitation, snowpack or glacier melt, and groundwater, and discharge (Poole & Berman, 2001; Caissie, 2006). Our result that reducing discharge significantly in streams

causes a moderate increase in warming is consistent with other research for second to third order streams such as those in our study (Poole & Berman, 2001). Changes in land use, such as forestry, change the biotic influence that ecosystems have on stream temperature by decreasing vegetation and canopy cover over streams and increasing solar radiation input (Gray & Edington, 1969; Johnson & Jones, 2000). But also, the reduction of canopy on the land mass can mean that precipitation run-off, an often important influx of water for many streams, is warmed faster by solar radiation and increased soil temperatures (Moore & Spittlehouse, 2005) which has a much higher influence on stream temperature than changes in discharge (Poole & Berman, 2001). The influence of dams on temperature regimes globally is significant as millions of rivers worldwide are under some form of regulation through damming or diversion, most of which cause change in downstream water temperatures (Poff & Hart, 2002). However, effects of regulation are highly variable depending on the type of dam and it's intended use (Poff & Hart, 2002) whereas the release of water below many large hydroelectric dams is colder than would naturally occur, reservoirs or diversions for agriculture or human consumption can cause significant warming (Caissie, 2006). However, most of these impacts occur in higher order streams (Poff & Hart, 2002; Wohl, 2006) thus making comparisons between river diversion hydropower and effects of impacts like storage for agriculture, human consumption, or storage hydropower difficult (Connors et al, 2014). Yet, the magnitude of warming observed in our study may be easily comparable to the effects of anthropogenic climate change to water temperatures in cold, mountain streams in temperate regions. As air temperatures over the last half century in the northwestern US have increased by 0.21^{o}C/decade, stream temperatures have increased by half that (Isaak et al, 2016). While these estimates of stream warming did not take into account changes in hydrology (ie. reduced flow or changes to rain/snow input), snowpacks have been in decline over the past century in the region, leading to concurrent reductions in stream flow (Barnett et al, 2008). Based on these findings, the diversion of water below dams leading to a ~0.5^{o}C increase in mean and maximum temperatures (and subsequently a reduction in TSM of our focal species of 0.5^{o}C) could be equivalent to 50 years of climate warming and reductions in snowpack, thus suggesting that river diversion hydropower may have a much greater influence on thermal regimes than climate change alone.

Changes to discharges play a variable role in stream warming that may not be generalizable across streams in regions or worldwide as river diversion hydropower is developed to meet the needs of renewable energy in many jurisdictions. In this study we predicted the warming rate of above dam and diversion reaches without the use of discharge

data as a way to generalize the effects of diversion dams, but many streams are expected to have significantly faster or slower warming rates depending on geography, stream size, and minimum discharge requirements. In British Columbia, diversion dams have been increasing across the landscape for over 50 years and minimum discharges do not consider temperature, instead focus on water availability for life history requirements, habitat, and behavior of salmonid fishes (Hunter, 1992; Hatfield et al, 2003). Across the globe, river diversion hydropower in temperate regions could affect maximum temperatures similar to our study system by compounding the impacts of dry and warm seasons on stream temperatures, although the magnitude of the effects will vary greatly across years as temperate systems are highly variable due to climate variability that acts across years and decades. However, effects of reduced discharge may be sustained longer throughout the year in tropical regions due to lack of seasonality, and across years as climates at lower latitudes are less variable (Pesquera & Tejedo, 2016).

We compared our estimated thermal performance curve for *A. truei* larvae to observed and predicted temperatures in reduced discharge stream reaches to estimate the risk posed by river diversion hydropower dams by decreasing TSM. Using mean maximum temperatures of the warmest month, a better indicator for current and future risk posed to ectotherms (Gerick et al, 2014), we found that *A. truei* larvae TSMs were 23 – 46% larger in current natural environments (without diversion dams) than tadpoles of wetland associated species of southern British Columbia (*Spea intermontana* TSM = 3.2 °C, *Pseudacris regilla* TSM = 3.8 °C, *Rana aurora* TSM = 3.7 °C), which are predicted to be at significant risk of range retraction due to climate change by the 2050's and 2080's (Gerick et al, 2014). Thermal physiology and TSM has been used effectively for over 35 years (Huey & Stevenson, 1979) as a framework for assessing vulnerability and extinction risk to changes in environmental temperatures (Sinervo et al, 2010) because they relate metabolic processes to population demographic rates (Deutsch et al, 2008) whereby risk is increased as TSM decreases, which could lead to stochastic events or, over time, sustained temperatures, that would reduce population viability. Past predictions of ectotherm vulnerability to climate change at lower latitudes (i.e. tropics) posited a greater risk because of their narrow TSMs compared to temperate species, which should be buffered physiologically with larger TSMs (Martin & Huey, 2008; Deutsch et al, 2008; Huey et al, 2009; Duarte et al, 2011; Gallagher et al, 2015). However, TSMs are a proxy for climate variability in species evolutionary past (Angilletta et al, 2002), suggesting that temperate species have evolved wide TSMs because of the much larger range and variability of temperatures

experienced not only seasonally, but across years, decades, centuries etc. compared to tropical species (Janzen, 1967; Pesquera & Tejedo, 2016). Environmental temperatures are often compared to thermal physiology as decadal means, or even over the short period of time in which a study has taken place, which in temperate regions, most likely does not account for extreme events associated with climate trends that occur over much larger time scales. Thus, TSMs for temperate species may be just as 'narrow' as those for tropical species, and an erosion of TSM by half a degree by diversion dams could put the species at high risk considering climate variability over larger timescales. Furthermore, although we predict a small increase in water temperature due to river diversion hydropower, it's an incremental change that could cause potential compounding or synergistic reductions in TSM with future climate warming and changes in land use.

2.5.1. Conclusions

Our study adds to the body of knowledge of anthropogenic impacts to the world's flowing water by estimating the effects of water regulation in cold, mountainous streams on their cold adapted biota. Subsequently, we provide insights into the future of streams by considering the effects of climate change on water availability in temperate regions and use diversion dams as a natural experiment. By focusing on abiotic anthropogenic impacts, such as temperature, we are able to establish mechanistic cause and effect relationships by understanding how changes will effect the physiology of the organisms of conservation concern (Cooke et al, 2013). These relationships can be used to forecast future impacts, or explain previous or currently witnessed species declines (Wikelski & Cooke, 2006). Our results suggest that warming temperatures caused by reduced discharges by dams may not appreciably increase the vulnerability of *A. truei* larva but the additive or synergistic effect of climate change is still yet to be examined, although it appears that temperatures in mountainous streams may be of less concern (Isaak et al, 2016). Yet that is not to say that the reduction of discharge in these ecosystems is not of importance. As we search for ways to generate sustainable (zero emission, low ecological footprint) energy, and increasingly turn to small diversion dam schemes, we still know little about their effects. While induced warming may not exceed physiological limits, further work is required to understand the potential impacts to bioenergetics demands and density effects due to increasing temperatures and shrinking habitat. Effects of temporal changes in discharges to habitat and behavior, are also of importance to population viability, for all species.

Chapter 3. Physiological traits reveal population-level climate vulnerability of a widely distributed amphibian (*Ascaphus truei*)

3.1. Abstract

Marine and terrestrial ectotherms from low latitudes are hypothesized to be more vulnerable to climate change than high-latitude counterparts because thermal niches are narrower toward the equator. Less well known is the latitudinal pattern of climate vulnerability for populations within species with broad geographic ranges. Here, we estimated the critical thermal maximum (CT_{max}), thermal optimum (T_{opt}), and thermal breadth (TB_{80}) for populations of Coastal tailed frog (*Ascaphus truei*), which span 16 degrees of latitude and 1,500 m of elevation in Western North America and predicted the consequences of thermal trait variability under future climate scenarios. We found that CT_{max} was relatively unchanged across the species' range, but both T_{opt} and TB_{80} varied with respect to latitude and elevation. Thermal niches were 3.1-3.6 times wider at higher latitudes (TB_{80}) skewed towards lower temperatures, and thermal optima (T_{opt}) were 1.4 times higher at lower latitudes. We estimate that 2080s temperatures (RCP 4.5) will exceed T_{opt} more frequently (compared to current climate) for both southern (2 times) populations and northern (9 times) populations, with high uncertainty in predictions for high latitude populations. Our results suggest that thermal trait variation exhibited by populations of a single species mirrors patterns documented among species. However, while southern populations are at most immediate risk to continued thermal change, vulnerability is increasing fastest for northern populations due to the combined effect of population-level differences in physiology and large regional differences in changing thermal regimes.

3.2. Introduction

Climate change is driving the loss of species and populations (Wiens 2016), yet predicting which regions and species are most vulnerable is still in its infancy (Dillon et al. 2010, Vasseur et al. 2014). Across the globe, better predictions of climate risk for both endo- and ectotherm taxa have been generated by an understanding of species specific thermal physiology (Huey et al. 2012). Broadly, vertebrate ectotherm species found at lower latitudes are known to experience a narrower range of annual temperatures than higher latitude counterparts, as the latter experience large shifts in temperatures with seasons. Such

contrasting patterns in thermal niche breadth has served as the basis for the climate variability hypothesis (CVH), which posits that larger environmental variation at high latitudes has driven broader thermal physiological niches, and conversely that lower environmental variability at low latitudes has led to narrower thermal physiological niches (Janzen 1967). Empirical studies spanning marine, terrestrial, and freshwater ecosystems have supported the CVH (Brattstrom 1965, Brattstrom 1968, Feder 1978, van Berkum 1988, Addo-Bediako et al. 2000, Deutsch et al. 2008, Sunday et al. 2011, Shah et al. 2018), and many have concluded that tropical species are therefore more vulnerable to small absolute changes in temperature with climate change (Deutsch et al. 2008, Tewksbury et al. 2008). Within temperate latitudes (23.5 – 66.5 degrees latitude), species thermal niches also increase with latitude (Brattstrom 1965, Sunday et al. 2011, 2014), but those at mid-latitudes may have the highest climate vulnerability, arising from a combination of high temperatures and relatively narrow (compared to high-latitude) thermal niches (Pinsky et al. 2019). However, the pattern of increasing thermal niche breadth for ectotherms with increasing climate variability has not been well evaluated for populations within a species. Understanding population level differences in physiology may provide the means to more accurately predict species' responses to accelerating climate change (Ames et al. 2020), while controlling for phylogeny.

Predicted climate vulnerability of different ectotherm species is often based on physiological traits estimated from a single or few populations within a species' range (Angilletta 2009). However, for wide ranging species, climate vulnerability may differ among populations depending on how physiological traits vary with respect to local or regional climate. The few studies that have evaluated population level differences in physiological traits (for ectotherms) find little evidence that thermal traits correlate with proxies for climate variability such as latitude or elevation, possibly due to limited environmental gradients within the ranges tested and high connectivity between populations (Gaitan-Espitia et al. 2014), or because thermoregulatory behaviors may buffer differences in environmental conditions reducing selection in physiological adaptation (Buckley et al. 2015). However, populations of closely related species have shown regional differences in thermal physiology across such proxies as latitude and elevation (Gutiérrez-Pesquera et al. 2016, Shah et al. 2018). While in general, climate is warming fastest within arctic latitudes and slowest at equatorial latitudes (Burrows et al 2011), species range boundaries are shift to higher elevations (Isaak et al. 2016) and higher latitudes (VanDerWal et al. 2013). Studies that have evaluated regional differences in changing climate and the consequences for biota (risk of extinction, disappearing climate envelopes), predict that

populations will shift in latitude (Sunday et al. 2015) or elevation (Isaak et al. 2016) to avoid extinction, but most have not considered the potential for intraspecific differences in thermal physiology. In contrast, mechanistic models of population level climate vulnerability have successfully predicted extinction risk using single estimates, species averages (when more than one population has been studied), or phylogenetic reconstruction of physiological traits (Sinervo et al. 2010), suggesting the simplifying assumption of using non-population specific estimates of physiological traits may be robust. However, if there are substantial differences in traits among populations combined with region or landscape specific climate change, simplifying models would inaccurately estimate complex patterns of population vulnerability, especially for wide-ranging species spanning large environmental gradients. Measuring population level physiological traits may improve the accuracy of predictions of climate risk, and may be especially useful where the historic environmental variability that shaped species physiology is decoupled from that predicted in the future (Rohr and Raffel 2010).

Climate variability, characterized by the difference between maximum and minimum temperatures (or deviation from average temperatures), is known to have shaped the breadth of species' thermal niches, which in turn defines key physiological thresholds. For example, lizards that experience more variable body temperatures can sprint at maximum speed over a wider range of temperatures than species whose body temperatures rarely fluctuate (van Berkum 1988). Physiological traits used to define species' environmental niche include thermal optimum and critical thermal maxima and minima. Thermal optimum (T_{opt}) is the temperature that maximizes individual performance and fitness, and has been related to population-level measures, where population growth rates decline as temperatures exceed T_{opt} (λ<; Deutsch et al. 2008). Critical thermal maximum (CT_{max}) is the maximum temperature at which performance is possible (Angilletta et al. 2002). Temperatures above CT_{max} cause acute mortality, and temperatures between T_{opt} and CT_{max} cause chronic physiological stress. Theory as well as empirical data suggest that species-level CT_{max} should be positively correlated with T_{opt} as well as temperature variability (Clusella-Trullas et al. 2011), Similarly, species-level T_{opt} is known to increase with mean annual temperature across the species range (van Berkum 1988, Angilletta et al. 2002), and is higher with more frequent high temperatures (Higgins et al 2014) or higher thermal variability (Clusella-Trullas et al. 2011). Thermal physiology that closely matches environmental temperatures is thought to allow individuals to acquire resources and avoid predators (Christian and Tracy 1981, Mitchell and Angilletta 2009) by optimizing metabolic activities and maximizing locomotion (Zhang and Ji 2004). Species' thermal niches can be

narrow if temperatures are relatively stable and predictable. Terrestrial ectotherm species that experience a broader range of annual temperatures must maintain the same average range of metabolic and biological functions between upper and lower critical limits as species that live in stable warm environments (Payne and Smith 2017). Thus, thermal breadth (TB_{80}), the range of temperatures over which an individual can maintain 80% maximal performance (growth, reproduction, or locomotion), is wider for species that experience higher variability in temperature, especially when average temperatures are much lower than T_{opt} (Angilletta et al. 2002). However, when temperatures regularly exceed T_{opt}, species-level TB_{80} is also wider such that species can take advantage of higher temperatures and complete basic functions without incurring the physiological costs typical beyond T_{opt} and below TB_{80} (Buckley and Huey 2016). While these patterns have been described among species, the same environmental forces have the potential to act on populations, especially for species with large geographic ranges that encompass broad climatic gradients, and where populations are relatively isolated (Angert et al. 2011). In particular, population-level CT_{max} may be expected to vary inversely with latitude; CT_{max} could be higher for populations occurring at lower latitudes where frequent high temperatures select for higher thermal tolerance (Brattstrom 1965, Sunday et al. 2011, 2014). For population-level T_{opt}, large (seasonal) temperature variation and extremes at high latitudes (as opposed to more stable temperatures at low latitudes) may drive stable T_{opt} (Buckley and Huey 2016) across the range of the species . Further, we expect that population-level thermal breadth (TB_{80}) should increase with latitude because of increasing climate variability (Buckley and Huey 2016), similar to the patterns described for species-level TB_{80}. Most of our hypotheses here stem from species comparisons; however, and need to be confronted with data from populations within a species. We expect that (isolated) populations differ in their thermal physiology given that the same climatic forces likely act on traits similarly. Yet, populations' shared evolutionary history and (modest) connectivity may be expected to result in similar thermal traits, suggesting that species level traits may be reasonable predictors of climate risk.

The temperate Pacific Coast of North America (30-50° N latitude) spans considerable gradients in environmental conditions that lead to substantial regional climatic variation. Seasonal variability in temperature within this region scales with latitude, where higher latitudes (50°N) experience a wider range of annual temperatures (particularly sub-zero), and southern latitudes reach higher maximum temperatures for longer periods of time. Such gradients provide an opportunity to evaluate the degree to which biogeographic proxies for differences in

environmental conditions (latitude, elevation) predict population-scale differences in thermal physiology. Here, we tested whether key thermal physiological traits (T_{opt}, CT_{max}, TB_{80}), frequently used to predict climate change vulnerability, vary predictably with latitude and elevation, sampling populations across the range of the Coastal tailed frog (*Ascaphus truei*), from Northern California to Northern British Columbia (spanning 16° latitude, 1200m elevation). Further, we combined population-level estimates of T_{opt} with regional climate models to make first-order predictions of population climate vulnerability in the 2080s. In particular, we tested the assumption applied by many climate envelope models (*sensu* Gerrick et al. 2014) that thermal physiology among populations is constant. As an approximation of thermal vulnerability, we calculated the frequency with which future ambient air temperatures are predicted to exceed T_{opt} in the 2080s (RCP 4.5) because such temperatures are associated with reduced individual fitness (Angilletta 2009), as well as population-level decline and local extinction (Deutsch et al. 2008, Sinervo et al. 2010). We hypothesized that population specific thermal traits vary along latitudinal and elevational gradients as described above, and such differences, combined with regionally variable climate forecasts will better predict population-level climate vulnerability across the *A. truei* range.

3.3. Methods

3.3.1. Study sites and species

We collected *A. truei* larvae from streams at high and low elevations (Table 3.1, Appendix B Table S1) throughout the species range (Figure 3.1) in 2015 - 2017. *A. truei* are a cold-water adapted amphibian endemic to high velocity streams of the Pacific Coast of North America (Figure 3.1). They are listed as a species of 'Special Concern' in Canada and California, and 'Sensitive' in Oregon (COSEWIC 2012, Thomson et al. 2016, Oregon Department of Fish and Wildlife 2019). *A. truei* are long-lived amphibians (15-20 years) with relatively low fecundity (<100 eggs per clutch), and a protracted larval period lasting 2 – 4 years. All life stages, eggs, larvae, and adults, are adapted to cold high gradient streams (Daugherty and Sheldon 1982), suggesting that *A truei* may be especially vulnerable to changing environmental and thermal conditions (de Vlaming and Bury 1970, Brown 1975, Hossack et al. 2013).

Table 3-1 Details of study populations, and number of larvae tested.

Region	Population	Number of larvae		Elevation (m)	Elevation Category
		CT_{max}	TPC		
N.BC	Elendsen	38	38	230	Low
	Kitimat	22	38	179	Low
	Kleanza	26	23	623	High
	Shames	25	27	700	High
S.BC	Fire	27	30	380	Low
	Stokke	28	30	378	Low
	Tipella	28	27	336	Low
OR	Augusta	12		1253	High
	Bear	47	30	332	Low
	Bulldog	12		1191	High
	Cripple	13		451	Low
	Flunky	12		533	Low
	Hardy	20		1220	High
	Kink	24		695	Low
	Lamb Butte	38		1187	High
	Lookout (low elevation)	13		577	Low
	Lookout (high elevation)	63	30	1055	High
	Marten	37		406	Low
	North Fork Steelhead	12		577	Low
	Ore	13		506	Low
	Salmon	12		609	Low
	Shellrock	13		1159	High
	Tidbits	96	36	748	High
N.CA	Jiggs	25	34	144	Low
	Noyo	24	35	33	Low
	Stoney	12	14	1538	High
	Trinity Alps	8	28	1531	High

*Because the upper elevational limit for the species decreases with increasing latitude (*M.Todd, pers. comm.*) we defined the low and high elevational limits differently for each region.

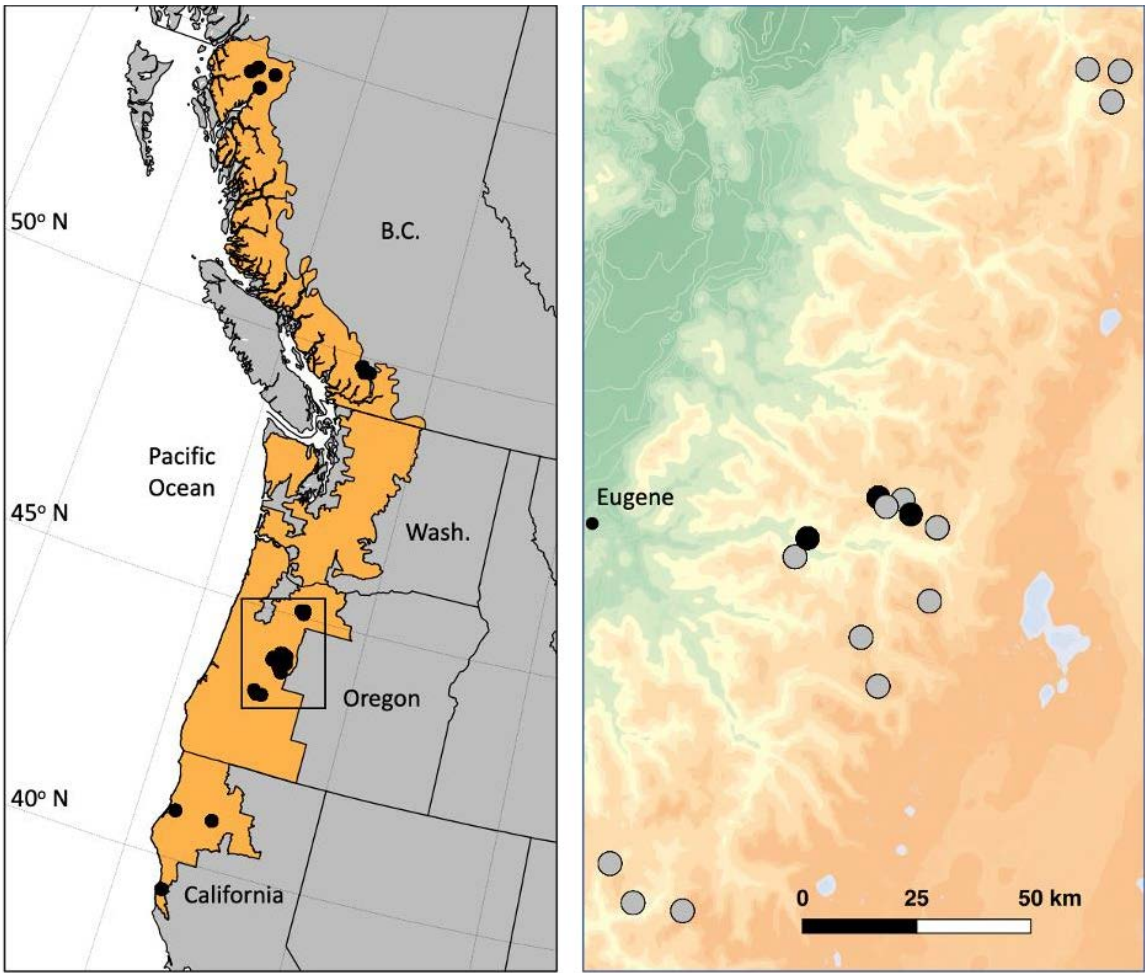

Figure 3-1 **Map of 27 populations (black dots) across the range of *A. truei* (orange) in Northern California (N.CA), Oregon (OR), and Southern and Northern British Columbia (S.BC, N.BC) from which we collected larvae to test thermal physiology (*left panel*). Right inset represents OR populations where both CT_{max} and T_{opt} were tested (n = 3, black dots), and where only CT_{max} was tested (n = 16, grey dots), across a range of elevations (332m - 1253m).**

3.3.2. Thermal physiology experiments

To characterize the thermal physiology and climate vulnerability of *A. truei* populations across the species range, we conducted lab experiments to estimate three key physiological traits; critical maximum temperature (CT_{max}), thermal optimum (T_{opt}), and thermal breadth at 80% of maximum performance (TB_{80}). We estimated population-specific thermal performance curves (TPC) using individual burst swimming performance trials to derive estimates of T_{opt} and TB_{80}. We evaluated whether differences in population-level physiological traits relate to the

environmental gradients present across the *A. truei* range and used these estimates as the basis for mechanistic predictions of population-level vulnerability to future warming.

3.3.3. Critical maximum

To understand the degree to which *A. truei* populations are adapted to regional and local climates, we measured the CT_{max} of 722 individual *A. truei* larvae (Table 3.1) from 27 populations ranging from Northern California to Northern British Columbia (Figure 3.1) and across a range of elevations (Appendix B, Table S1). We hypothesized, similar to patterns documented among species, that CT_{max} would be under strong regional and local adaptive pressure (or be released from such; Bennett et al. 2021) due to differences in water and riparian air temperature across the *A. truei* range.

We measured CT_{max} following a 72-hour acclimation period in an oxygenated 8°C water bath. We tested a minimum of 8 individuals (8-96, median=24, mode=12) of varying age and size (Gosner stage 26-45; Gosner 1960), housed in separate flow-through containers, from each population (Table 3.1). We recorded the water temperature (°C) at which individuals responded to a tactile stimulus and lost the ability to right themselves (LRR; Lutterschmidt and Hutchison 1997, Angilletta 2009). We used submersible 500-watt aquarium heaters (16C-2, Dwyer Instruments Inc.) to raise water temperatures in test aquaria at a rate of 0.3°C/min (Dallas and Rivers-Moore 2012). After exhibiting LRR, larvae were returned to cooler water, in which all individuals used in the analysis recovered. Following testing, larvae were measured (length, mm), and euthanized using benzocaine and preserved in formalin and 95% EtOH.

3.3.4. Thermal performance

In a subset of *A. truei* populations (n = 15, Table 3.1), we evaluated whether T_{opt} and TB_{80} are related to environmental conditions that vary with latitude and elevation (Table 3.1). We measured the burst swimming performance of approximately 30 individuals of Gosner stage 30-36 (Gosner 1960) per population at six temperatures ranging from 2 – 27°C (+/- 0.6 °C) to estimate population-specific thermal performance curves. Individuals were acclimated for 21 days at 10°C after collection from the field and fed natural biofilm on rocks collected from nearby streams, supplemented with puréed spinach dried onto ceramic tiles. Larvae were then randomly assigned to one of the six test temperatures and housed in mesh containers (15.5 x 15.5 x 8.5cm) floated in oxygenated aquaria for 6 hours. Cool temperature treatments (2°, 10°C)

were created with aquarium chillers (Coralife ½ hp), and warm temperature treatments (16, 20, 24, 27°C) with 200-watt aquarium heaters connected to digital thermostats (Inkbird ITC-306T). Burst swimming speed was tested by placing individuals in a v-shaped plexiglass channel with 2 cm of water, and a startle response was generated with a weak (100V, 150mA, 15ms) electrical stimulus (S88 Grass Stimulator) using stainless steel electrodes on either side of the tail (Figure S1). Trials were recorded using high-resolution (720p) high-speed (240fps) digital cameras. Larvae were only tested once. Following each trial, larvae were weighed (mg) and volume measured (ml) and allowed to recover.

3.3.5. Statistical analyses

We tested the effect of latitude, elevation (high/low), their interaction, and age class (cohort, Appendix B, Figure S2) on individual CT_{max} using linear mixed effects regressions using the package lme4 (Bates et al. 2015) implemented in program R (R Core Team 2019). We evaluated population and year for inclusion as random effects to account for non-independent measures of CT_{max} (testing multiple individuals per population) and slight differences in experimental protocol and personnel between years. We ran all possible combinations of fixed effects (10 models), and averaged the set of models with a cumulative AICc weight of 0.95 (Burnham and Anderson 2004) and present the 'full' model average coefficients which assumes that a variable is included in every model, but in some models the corresponding coefficient is set to zero.In order to estimate T_{opt} and TB_{80} for each test population, we constructed thermal performance curves of how maximum swimming velocity (V_{max}) changed with test temperature (2 – 27°C). Videos of individual burst swimming were analyzed using Digitizing Tools software (Hedrick, 2008), implemented in MATLAB. V_{max} was calculated as the maximum distance (pixels) travelled between adjacent frames divided by the time period between frames (250 milliseconds; 240fps), within the first 120 frames (1/2second). We fit thermal performance curves to V_{max} for all individuals in all populations using a modified beta curve (Equation (1); Yin et al. 2003). We estimated parameters (specifically, T_{opt}) using a maximum likelihood with the bbmle package (Bolker and Team 2017) in R (R Core Team 2019). We used this equation because we are able to statistically estimate T_{opt} rather than guessing the estimate from a graph (Angiletta 2006).

$$V_{max} = p_i + (p_{max} + (p_{max} - p_i)\left(1 + \frac{t_{opt} - t}{t_{opt} - t_m}\right)\left(\frac{t - t_i}{t_{opt} - t_i}\right)^{\left(\frac{t_m - t_i}{t_{opt} - t_m}\right)}$$

(1)

Where p_i is the performance at the lowest temperature (set as a constant – the average performance of each population in the 2°C treatment), t_i the lowest temperature (2°C), and t_m the inflection point where the rate of change of performance starts to decrease towards t_{opt}, the temperature at p_{max} (maximum performance). We included data points from CT_{max} trials to anchor the curves where performance equals zero. Others have successfully used gaussian curves (Angilletta 2006) and generalized additive models (Gerick et al. 2014) to model thermal performance, however, these models do not allow for statistical estimation of key parameters of the curve (T_{opt}) with error. Using the thermal performance curves described above, we also calculated TB_{80} for each population, defined as the range of temperatures corresponding to 80% of p_{max} on either side of T_{opt}.

To test our predictions of T_{opt} and TB_{80} with latitude, elevation (high/low), and the interaction between the two, we used simple linear regression (R Core Team 2013). We ran all possible combinations of latitude and elevation, including an interaction (5 models), and averaged the set of models with a cumulative AICc weight of 0.95 (Burnham and Anderson 2004) to describe the drivers of each physiological trait and present the 'full' model average coefficients which assumes that a variable is included in every model, but in some models the corresponding coefficient is set to zero..

3.3.6. Climate Forecasts

Using one common measure of environmental restriction, environmental temperatures in exceedance of T_{opt} (Angilletta 2009), we used population differences in *A. truei* thermal physiology combined with local climate forecasts to predict future climate vulnerability. We extracted locally downscaled maximum monthly contemporary (1981 – 2010) and future (2080's, RCP4.5) air temperature for the months of May - September (Climate NA database, Wang et al. 2016) for 4, 401 recorded locations *of A. truei,* downloaded from the Global Biodiversity Information Facility (GBIF). Because *A. truei* are riparian specialists, we grouped all GBIF locations by region (N.CA, OR, S.BC, and N.BC) within 1.5 degrees north or south of the centre of our study sites in each region, and applied a correction factor to transform air temperatures from Climate NA to riparian air temperatures using riparian and nearby weather station daily maximum air temperatures (Appendix B, Figure S3). Using estimated riparian air temperatures in the 2080s at the 4, 401 locations paired with elevation obtained for each

location from a digital elevation model, we calculated the frequency of exceedance, i.e., the proportion of months across all locations within each region that exceeded the regional – (N.CA, OR, S.BC, and N.BC) and elevation – specific (high or low) mean population value of T_{opt}. We also calculated the percent change in the frequency of exceedance of T_{opt} for each region according to Equation (2):

$$\frac{freq\left(Exceed\ T_{opt}\ Future\right) - freq\left(Exceed\ T_{opt}\ Contemporary\right)}{freq\left(Exceed\ T_{opt}\ Contemporary\right)} \times 100 \quad (2)$$

Where $freq$ is the number of months (May to September) that mean maximum temperatures at each of 1000 randomly chosen riparian sites within each region (N. CA, OR, S. BC, N. BC) exceed that region's predicted T_{opt}:

$$\frac{\sum_{i=0}^{n_{sites}} n_{months}\ Exceed\ T_{opt}}{n_{sites}\ x\ n_{months}} = freq\left(Exceed\ T_{opt}\right) \quad (3)$$

3.4. Results

3.4.1. Effects of latitude and elevation on thermal physiological traits

We found that individual CT_{max} varied between 24 - 31°C across the species' range as well as differences in the shape of each population's TPC (Figure 3.2; Appendix B, Table S3, Figure S4). The linear mixed effects model competition indicated support for latitude, elevation, and their interaction as predictors of CT_{max} among populations of *A. truei*, and for the inclusion of population and year as random effects (Table 3.2). The top-ranked model included only an intercept, but models including latitude, elevation, and their interaction had substantial weight, and were included in the model average (Table 3.2). In our average model (4 models, *cumulative AICc w* $\leq$ 0.95), the effect of the interaction of low elevation and latitude on CT_{max} was 1.8 times greater than the effect of high elevation and latitude (Figure 3.3). However, we found that the effects of latitude and elevation were small relative to the range-wide average CT_{max} for *A. truei*, such that CT_{max} across the range increases by 0.7°C across 16° latitude at low elevation but decreases by 0.6°C across the range at high elevations (Figure 3.4). At

approximately the mid-point of the range (~48° latitude), CT_{max} for populations at low and high elevations are predicted to be equal (29.1°C +/- 0.6 SE).

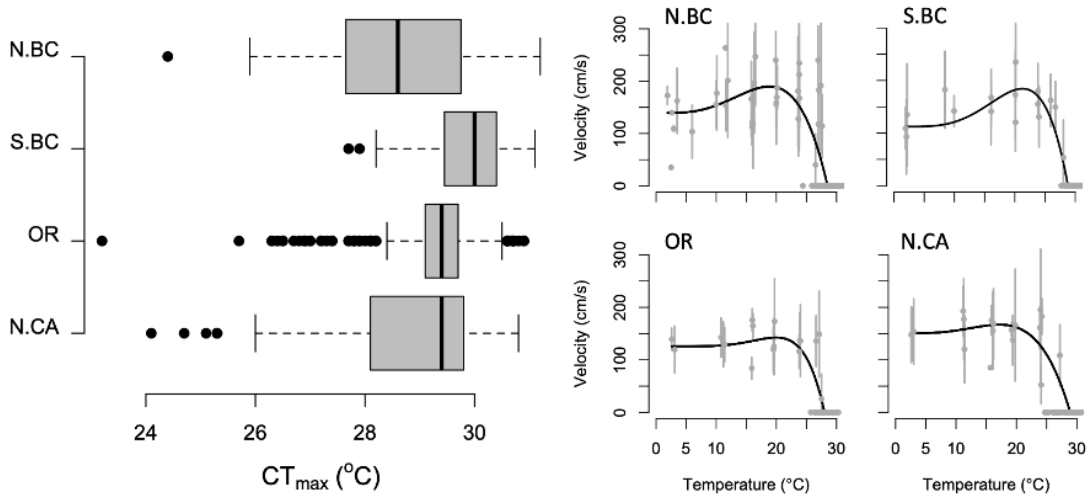

Figure 3-2 **CT_{max} (*left panel*) and thermal performance curves (TPC; *right panel*), used for estimating T_{opt} for *A. truei* in four regions (N.CA, OR, S.BC, N.BC). Boxes show median plus 50% of the data, whiskers are 1.5 times the interquartile range, and dots are extreme values. Values for CT_{max} are estimated at the individual level while TPC (T_{opt}, TB_{80}) are estimated at the population level (Figure S4) and here on the regional level (See also Table 3.1).**

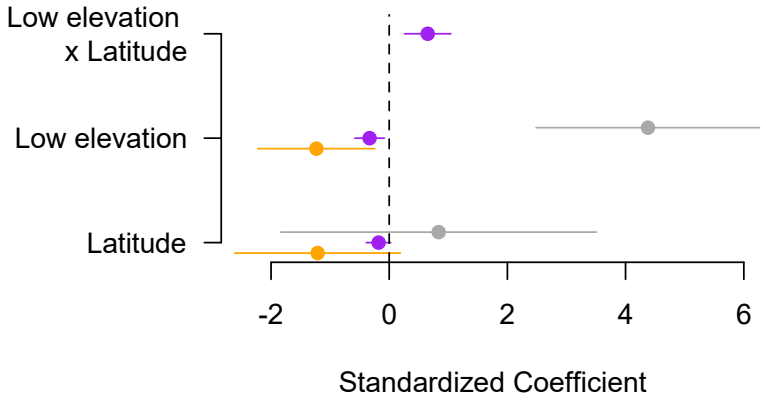

Figure 3-3 **Standardized model averaged coefficients (± 95% CI) for models describing thermal physiology metrics (CT_{max}, purple; T_{opt}, orange; TB_{80}, grey) as a function of latitude, elevation, and their interaction. Latitude alone is equivalent to latitude at high elevation.**

Table 3-2 **Model selection tables using Akaike Information Criterion corrected for small sample size (AICc) for the linear mixed effect model used to describe CT_{max}, and the linear models used to describe T_{opt} and TB_{80}. The top models (Cumulative *weight* < 0.95, shaded models) were used in a model average to predict each physiological trait.**

Physiological trait	Fixed effect parameters	Random effect parameters	k	ΔAICc	AICc *weight*	*R^2
CT_{max}	*Null*	Population + Year	4	0.00	0.52	0
	Latitude	Population + Year	5	2.06	0.19	0.01
	Elevation	Population + Year	5	2.46	0.15	0.01
	Elevation + Latitude + Elevation*Latitude	Population + Year	7	4.11	0.07	0.03
	Elevation + Latitude	Population + Year	6	4.73	0.05	0.01
	Cohort	Population + Year	5	6.82	0.02	0
	Latitude + Cohort	Population + Year	6	8.94	0.01	0.01
	Elevation + Cohort	Population + Year	6	9.25	0.01	0.01
	Elevation + Latitude + Elevation*Latitude + Cohort	Population + Year	8	10.90	0.00	0.03
	Latitude + Elevation + Cohort	Population + Year	7	11.58	0.00	0.01
T_{opt}	*Null*		2	0.00	0.53	0
	Latitude		3	1.50	0.25	0.11
	Elevation		3	2.35	0.16	0.05
	Elevation + Latitude		4	4.77	0.05	0.14
	Elevation + Latitude + Elevation*Latitude		5	8.57	0.01	0.19
TB_{80}	Latitude		3	0.00	0.63	0.3
	Null		2	2.26	0.20	0
	Elevation + Latitude		4	3.70	0.10	0.31
	Elevation		3	5.01	0.05	0.03
	Elevation + Latitude + Elevation*Latitude		5	6.52	0.02	0.39

*Marginalized R^2 for linear mixed effects models (CT_{max}), multiple R^2 for linear models.

**Conditional

Using Equation (1) we fit thermal performance curves to larval *A. truei* burst swimming data for each population (Appendix B, Figure S4) and used the parameter estimate for T_{opt} from the non-linear maximum likelihood estimator. The linear model competition indicated support for including latitude and elevation as important predictors of T_{opt} among populations of *A. truei.* The top-ranked model included only an intercept, but models with latitude and elevation had substantial weight, and were included in the model average (Table 3.2). In our average model (3 models, *cumulative AICc w* $\leq$ 0.95), latitude and elevation had equal effect on T_{opt} (Figure 3.3), where T_{opt} decreases by 2.2°C across 16° latitude, and decreases by 1.2°C at lower elevations such that, southernmost populations (N.CA) at high elevations had the highest T_{opt} (23.2°C +/- 1.1 SE), and northernmost populations (N.BC) at low elevations had the lowest T_{opt} (19.8°C 0.9 SE; Figure 3.4). We used the population specific TPCs to estimate TB_{80} and found that in a model competition of all possible combinations of latitude, elevation, and their interaction, increasing latitude was the strongest predictor of wider thermal breadths (TB_{80}; ΔAIC = 0, *w* = 0.63; Table 3.2). In the model average for TB_{80} (3 models, *cumulative AICc w* $\leq$ 0.95) the effect of latitude was 5.2 times greater than the effect of elevation (Figure 3). We found that TB_{80} narrowed by 0.8°C at high elevation and widened by 8°C across 16° latitude, such that, TB_{80} was 3.8°C (+/- 2.8 SE) in the southernmost low elevation populations, and was 3.1 times wider (11.7°C, +/- 2.4 SE) in the northernmost low elevation populations (Figure 3.5). Because TPCs are asymmetric, with a steep decline in performance beyond T_{opt}, TB_{80} is also asymmetric (Appendix B, Figure S4). Therefore, wider TB_{80} are skewed towards cooler temperatures (Figure 3.4).

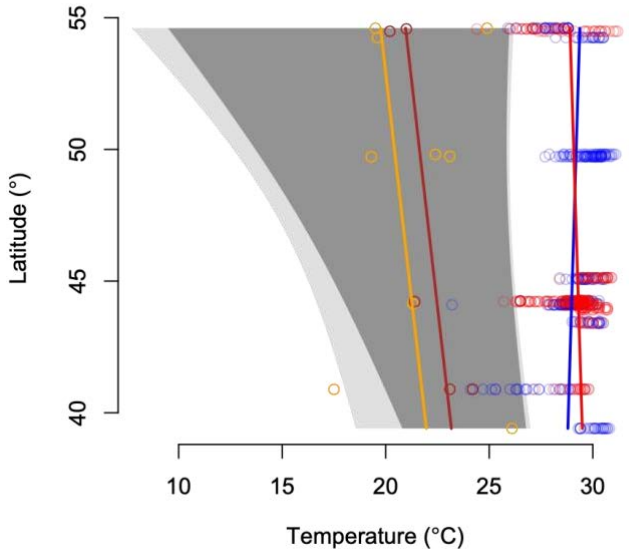

Figure 3-4 **Thermal traits (CT_{max}, T_{opt}, TB_{80}) of *A. truei* populations across latitude, spanning N.CA (39° latitude) to N.BC (55° latitude); showing predicted mean (line) from model results for CT_{max} at high (red) and low (blue) elevation, and T_{opt} at high (brown) and low (orange) elevation. Shading indicates 95% CI of TB_{80} at high (dark grey) and low (light grey) elevations.**

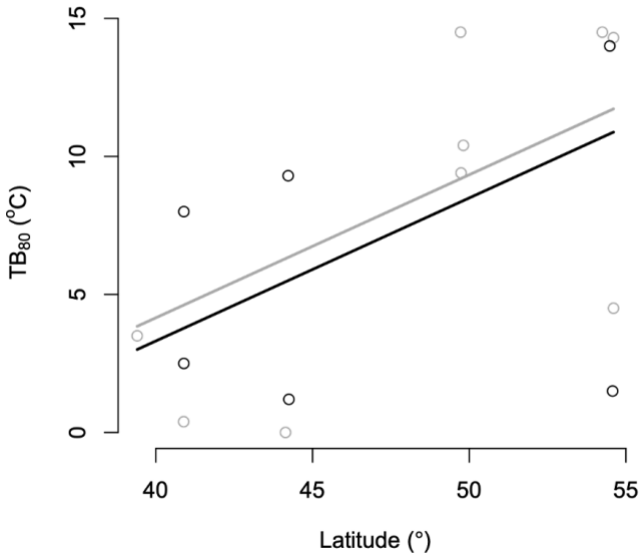

Figure 3-5 **Population estimates of TB_{80} with latitude (16 °) for larval *A. truei* (r^2 = 0.2). Lines indicate model average estimates for high (dark grey) and low(light grey) elevation.**

3.4.2. Predicted climate vulnerability

Locally downscaled climate models for western North America from Climate NA (RCP4.5; Wang et al 2016) corrected to estimate riparian air temperatures in the 2080's (Appendix B, Figure S3) suggest that average riparian air temperatures (May - September) will increase by between 2.4 – 3.4ºC in each of our study regions (N.CA 3.4º, OR 3.1º, S.BC 3.0º, and N.BC 2.4º C; Figure 3.6). We found that the number of months within each region with riparian air temperatures exceeding population average T_{opt} will increase in the future, with low latitude populations exceeding T_{opt} more frequently than high latitude (Figure 3.6). As expected, during contemporary climate (1981 - 2010), the number of months with maximum temperatures exceeding T_{opt} for all elevations declines with increasing latitude, and where temperatures in S.BC (high elevation) and N.BC (low and high elevation) do not exceed population T_{opt} at all. However, while the number of months that exceed T_{opt} (Equation 2; 3) in the future (2080s) is highest at the southernmost low elevation populations (N.CA = 0.42), the frequency of exceeding T_{opt} in these populations is only 1.9 times greater in the future compared to contemporary climate. In contrast, future temperatures in northern populations (low elevation) are predicted to exceed T_{opt} only occasionally (S.BC = 0.027, N.BC = 0.15), but populations are predicted to experience the largest relative change in frequency of exceedance across the species range (S.BC, low elevation 3.5 x higher 2080's versus contemporary climate). Therefore, we find that the southernmost low elevation populations (N.CA) are 2.3 times more vulnerable to physiologically limiting temperatures in the future (N.CA = 0.42, N.BC = 0.18) than the northernmost populations, but that vulnerability is increasing 2.8 times faster in northern populations than southern (increase in frequency of exceedance for N.CA low elevation = 90%, increase in frequency of exceedance for S.BC low elevation = 256%).

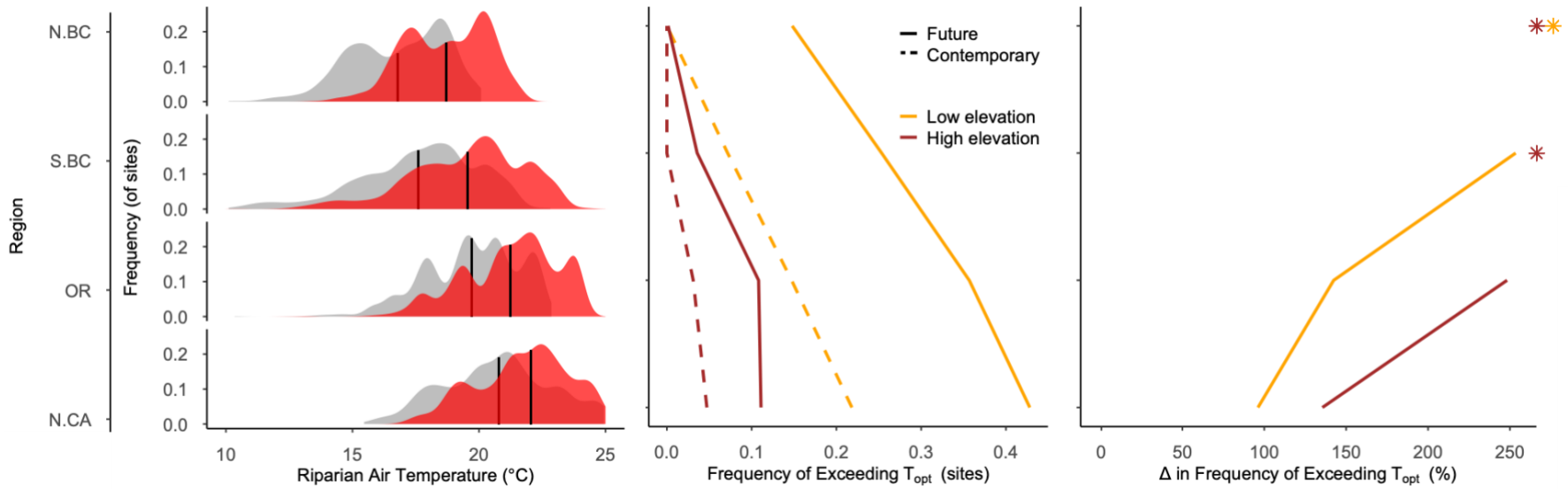

Figure 3-6 **Range, frequency, and mean (bars) of 1981-2010 contemporary (grey) and future (2080s, RCP 4.5, red) average monthly maximum air temperatures for the summer period (May – September) generated from 4, 401 known locations of *A. truei* and grouped by study region (N.CA, OR, S.BC, and N.BC; *left panel*), the frequency of months at sites that exceed T_{opt} at high (brown) and low (orange) elevations by region, under current (dashed line) and future climate (2080's, solid line); *middle panel*, and the predicted percent change in the frequency of months at sites that exceed T_{opt} for high (red) and low (orange) elevation in the 2080's by latitude; *right panel*. Note: T_{opt} is exceeded for the first time in N.BC in the 2080's at low elevation and in N.BC and S.BC at high elevation indicated by an asterix representing an infinite increase compared to current.**

3.5. Discussion

Our results offer insight into regional adaptations in the thermal physiology of a wide-ranging amphibian, which in turn are likely to influence population-level climate vulnerability across the species' range. We found population variation in three physiological traits (T_{opt}, CT_{max}, TB_{80}), by latitude and elevation, with differences across 16° of latitude in TB_{80} (8°C) and T_{opt} (3.4°C), and modest variation in CT_{max} (0.7°C; Figure 3.4). As predicted, population average CT_{max} (high elevations) and T_{opt} decline with latitude, while TB_{80} broadens and is skewed toward colder temperatures at higher latitudes. These results suggest that intraspecific trends in thermal physiology may be similar to those documented among diverse ectotherm species (Brattstrom 1965, Sunday 2011). However, the relatively modest variation we observed in CT_{max} and T_{opt} may also reflect that the adaptation of thermal traits in particular may be slow relative to behavioral thermal regulation (Angiletta 2009). Using these estimates of thermal traits as a basis for predicting climate vulnerability, we confirm that by the 2080s low latitude *A. truei* populations (N.CA, OR) are more likely to experience temperatures exceeding T_{opt} compared to high latitude populations, mirroring general predictions for wide-ranging ectotherms (Tewksbury et al. 2008, Buckley et al. 2015a, Buckley and Huey 2016). However, we find that the rate of change in our vulnerability metric (exceeding T_{opt}) over the coming decades indicates that northern populations are experiencing a faster rate of change in the occurrence of physiologically limiting conditions compared to their southern counterparts. Because of lower thermal limits in the north, our results provide cause for concern that regional thermal adaptation may not rescue populations from climate change-driven environmental limitation and local extinction, especially for populations at low elevations. However, we did find that populations at high elevation have higher T_{opt} which may provide a buffer from the effects of accelerated warming, and these areas may represent refugia for the species at both low and high latitudes.

Our results provide support that the same latitudinal and elevational forces that shape thermal physiology across species are also likely at work among populations of this wide-ranging amphibian. Population-based thermal limits, thermal breadth, and thermal optimum all varied in somewhat predictable ways based on our predictions of latitudinal and elevational trends in mean maximum and annual temperatures, and temperature variation. While comparisons of diverse vertebrate taxa suggest that CT_{max} is relatively invariant with respect to latitude, it has been shown to decline with elevation (Shah 2017), and the effect of elevation is

largest for species at mid-to-high latitudes because the elevational gradient in climate (temperature) that single species inhabits is steeper in these regions (Sunday and Bennett 2019). Here, we show that *A. truei* populations exhibit relatively modest but clear patterns in thermal limits across latitude (Figure 3.4). Our results indicate that CT_{max} increases with latitude for low elevation populations of *A. truei* but decreases with latitude for those at high elevation. We hypothesize that these contrasting patterns may arise from unmeasured, but important environmental differences across the species range that vary with latitude and elevation in complex ways. For example, in Northern California, *A. truei* at low elevations live in closed canopy streams and riparian corridors buffered from high temperatures as they receive little solar radiation and are often influenced by cold marine air. In contrast, in British Columbia many populations at low elevation live in open canopy streams or riparian areas widened by high-flows during spring run-off, and receive intense direct solar radiation coinciding with peak annual temperatures (Dupuis and Steventon 1999) that may drive selection for slightly higher thermal limits (CT_{max}; Mitchell and Angilletta 2009, Buckley and Huey 2016). However, we documented relatively modest variation in CT_{max} which may be explained by recent research that suggests CT_{max} for most species is physiologically constrained (Bennett et al. 2021). Constant CT_{max} across latitudes has been documented across populations of other ectothermic species with wide ranges (Frazier et al. 2006, Gaitan-Espitia et al. 2014, Buckley et al. 2015b). This also provides support for the hypothesis that CT_{max} is shaped by maximum temperatures (Angilletta et al. 2002, Buckley and Huey 2016, Kingsolver and Buckley 2017), and that extreme (not mean) high temperatures across a species range are relatively constant (Addo-Bediako et al. 2000, Ghalambor 2006, Clusella-Trullas et al. 2011, Vaughan et al. 2013) because the mean highest (or extreme) temperatures for similar habitats across the globe tend to be relatively invariant regardless of latitude (Bozinovic et al. 2014). However, mean and extreme low temperatures are variant across latitudes (Bozinovic et al. 2014) and therefore measures of thermal breadth (TB_{80} or CT_{max} - CT_{min}) are known to widen for species at higher latitude (Brattstrom 1965, Tewksbury et al. 2008, Sunday et al. 2011, Bennett et al. 2021) because individuals must maintain relatively high performance during much of the year when they are experiencing lower temperatures than their southern counterparts. This broadening of the temperatures experienced and at which individuals perform well may cause T_{opt} to decrease such that individuals spend more time near their optimum performance given that a larger proportion of their year is spent at lower temperatures at higher latitudes. In fact, we found support for reduced T_{opt} at high latitudes. Furthermore, the trend of declining T_{opt} among populations of *A. truei* with increasing latitude also mirrors trends across species (Brattstrom

1965, Sunday et al. 2011) and has been documented for seven populations of crabs (Gaitan Espitia et al. 2014). However, our results suggest a modestly higher T_{opt} for high elevations is a relatively novel finding, yet consistent with other research that shows a shorter growing season at high elevation with less variable temperatures necessitates a higher T_{opt} with a narrower TB_{80} (Huey and Kingsolver 1993, Higgins et al. 2014). While our results suggest clear and biologically relevant latitudinal and elevational gradients exist among populations of *A. truei*, there remains considerable unexplained variation (R^2 for top models: CT_{max} = 0.72, TB_{80} = 0.30, T_{opt} = 0.0; Table 2) in thermal traits within each region.

Variation in thermal traits among *A. truei* populations likely arise from broad scale climatic and biogeographic conditions such as temperature and seasonality, as well as species ecology and life history, such as changes in habitat types, predators, and differences in time spent in aquatic and terrestrial life stages, which are also expected to influence the climate vulnerability of populations. Here we used two common but simple climate proxies, latitude and elevation, to represent gradients in biogeography, species ecology, and life history and evaluated their correlation with variation in thermal physiological traits. However, strong correlations between local- rather than regional- scale climatic variables (e.g. stream temperature, MAT) and key physiological traits may indicate local adaptation (Huey & Kingsolver 1993, Buckley et al. 2015) that runs counter to our expectations based on simple latitudinal and elevational climate gradients (Isaak et al. 2016). Range-wide analysis of biogeographic and latitudinal climate correlates for *A. truei* indicates that climate across such broad scales may work in tandem (e.g. 30 year extreme maximum temperature, mean temperature of the warmest month) or antagonistically (e.g. glacier and snow cover, mean maximum summer temperature) in shaping thermal physiology, especially given heterogeneity at the site/population level (Appendix B, Table S2). These climate correlates may help explain some of the variation we observed in population level thermal traits, however, we were unable to include them explicitly in our analysis either because they are interpolated across landscapes, not elevation specific, or exhibit collinearity with latitude or elevation. In addition, we also collected *in-situ* stream temperature for one year in 22 of our 27 study populations (2016 – 2017) and found that mean annual and maximum summer stream temperatures had no correlation with latitude and only weak correlation with elevation (Appendix B, Figure S5), further suggesting that local stream temperatures may be decoupled from broad-scale patterns in air temperature. We posit that riparian and terrestrial thermal environments, rather than stream temperatures, are more likely to have shaped the thermal physiology of *A. truei*, as

stream temperatures are not expected to be thermally limiting and individuals spend the majority of their lifespan in terrestrial environments (de Vlaming and Bury 1970, Dupuis and Steventon 1999). Furthermore, while regional to local climate shapes thermal physiology for populations, the degree to which they also play roles in thermal acclimation and plastic responses is not known. We acclimated individuals for three to 21 days (at 8°C for CT_{max} and 10°C for T_{opt}) in all of our experiments in order to measure thermal traits at a common baseline across populations. Despite the potential for climate heterogeneity and experimental artifacts (acclimation, plastic responses) to mask trends in thermal physiology, we show statistical support for predictable population-level variation across 16° of latitude and 1500m of elevation. When combined with predicted rates of thermal change occurring in each region, we show that regional thermal adaptation gives rise to clear differences in future climate vulnerability.

We found that due to differences in regional thermal physiology and climate change forecasts, vulnerability is highest for populations at low latitudes, while the rate of increase in vulnerability is highest for high latitude populations. While most forecasts estimate vulnerability to changing climate by comparing current or future temperatures with estimates of CT_{max} for species and populations, we use the frequency of exceeding T_{opt} , a more conservative measure that has also been related to long-term population viability, as populations that regularly experience temperatures beyond T_{opt} have negative population growth or higher extinction probabilities (Deutsch et al. 2008, Sinervo et al. 2010, Huey et al. 2012). Life history and population dynamics play an important role in shaping thermal physiology (Kingsolver and Buckley 2017, Rohr et al. 2018) as such, T_{opt} is shaped by the upper limits of long term average maximum temperatures such that individuals may complete important biological tasks with relative efficiency with few metabolic costs when temperatures exceed average temperatures (Buckley and Huey 2016). This in turn leads to life history trade-offs, a change in development time with a concurrent change in temperature (Sinervo 1990, Van Der Have 2002, O'Regan et al. 2014, Carbonell and Stoks 2020) so that individuals can avoid and/or recover from abnormally hot temperatures and live to reproduce or make-up for lost fitness in the future (Angilletta 2009). However, when temperatures chronically exceed T_{opt}, individuals slowly incur metabolic costs that translate to reduced fitness (increased bioenergetic demands, reduced ability to obtain resources, reduced lifetime fecundity), leading to population declines that scale with the magnitude of exceeding T_{opt} (Angilletta 2009, Ma et al. 2015). However, using T_{opt} estimated from locomotive trials may not be the most accurate proxy for fitness (Angiletta 2002) because animals rarely use maximal locomotive performance in the wild to escape predation or

find shelter and food (Jayne & Irschick 2000). While locomotor capacity considers whole-organism performance (Bennett & Huey 1990), it evaluates a somewhat isolated physiological process much like tests on, for example, heart rate or muscle fibre twitch that rarely have evolutionary trade-offs (Garland 1988) but are required for strong selection and optimization. As such, T_{opt} estimated from locomotion may be higher than that derived from true whole-organism metrics because individuals tend to perform well at many temperatures, often well beyond the range of normal bodily and environmental temperatures with no trade-offs (Huey & Hertz 1984, Huey et al. 1989, Huey & Kingsolver 1993). In contrast, growth rate is a more sensitive measure of thermal optima and breadth because it incorporates variable, chronic, and acute temperatures over longer time periods alongside bioenergetics and food availability and has a direct correlation to lifetime fitness and stronger trade-offs resulting in faster adaptation and evolution (Angiletta 2002). While locomotion derived T_{opt} may actually confer a higher threshold (Hertz et al. 1989) in which to compare changing environmental temperatures and make conclusions about population or species vulnerability than that derived from growth, it's utility lies in it's speed in estimation (quick laboratory experiments as opposed to longer growth, survival, or fecundity experiments), and it's adaptive (while slow) response to thermal environments (Huey & Kingsolver 1993) which allows us to make relative, as opposed to precise, comparisons of vulnerability among and across species.

In contrast, using CT_{max} forecasts rapid declines as individuals that experience temperatures that exceed critical limits are rarely given chances to recover. While chronically hot temperatures exceeding CT_{max} would without a doubt cause rapid declines, it would only take a few extreme events causing mass mortality to bring populations to local extinction. Further, predictions of forecast maximum and extreme temperatures used to compare to CT_{max} are less reliable than those of mean temperatures (de Perez et al. 2018) which are more suited to comparing to T_{opt}. Regardless of our choice of physiological metric, predictions of vulnerability across species (southern, often tropical, compared to northern, often temperate; Brattstrom 1965, Deutsch et al. 2008, Tewksbury et al. 2008, Huey et al. 2009, Dillon et al. 2010, Sunday et al. 2011) using either CT_{max} or T_{opt} are consistent with our findings for populations among species: that trailing edge (southern) populations are more likely to experience unsuitable thermal conditions than leading edge (northern) populations. However, our predictions using T_{opt} are more sensitive as vulnerability is antagonized by the combination of changing climate and differences in thermal physiology, showing how important sensitive life history and physiological traits play across populations in the species range in determining vulnerability. For *A. truei*,

while we predict that southern populations are the most at risk to continued climate change, it is unlikely that overall they are currently in decline, as the majority of summer growing season temperatures (May - September) are below T_{opt}. However, under current conditions, the cumulative frequency of all southern populations exceeding T_{opt} is over 40% of summer months, suggesting that some populations experience higher and lower frequencies, and that currently some populations may already be in decline because of the added physiological costs of being beyond T_{opt} throughout much of the summer growing season. We expect that our estimates of relative climate vulnerability may also be conservative, as changing thermal environments mediated by species or population physiology is only one of many types of environmental limitation. In particular, simultaneous changes in water availability (Lertzman-Lepofsky et al. 2020, Greenberg and Palen 2021) and habitat loss (Hof et al. 2011) may compound the effects of warming temperatures and accelerate species' range shifts in both terrestrial and freshwater environments (Sunday et al. 2015, Lertzman-Lepofsky et al. 2020). Furthermore, rates of change, such as climate velocities, help to further our predictions of species declines or range shifts and this is the utility of the second part of our vulnerability analysis that addresses the trends in the rate of change in vulnerability across the species range.

Species vulnerability to decline from human impacts is not increasing linearly with time (Lee and Jetz 2008) nor does an impact change at the same rate across the globe, e.g. rates of climate change between the poles and equator (Burrows et al. 2011). But forecasting and representing non-linear vulnerability increase across space and time can be challenging. Here we show that the near future (2080s) vulnerability for the most vulnerable populations of a species could be outpaced by the far future (beyond 2080s) vulnerability of the populations with the lowest current and near future vulnerabilities because of differences in changing climate by region combined with population differences in thermal physiology. While southern populations of *A. truei* (N. California and Oregon) experience temperatures (currently and 2080s) exceeding population-level T_{opt} more frequently than northern populations (S. and N. British Columbia), the rate at which that frequency is changing is 2.8 times faster for northern populations. Using this relative measure, our results suggest that the climate vulnerability of northern populations of *A. truei* is increasing much faster than those in the south. Our analysis suggests that the current climate vulnerability of this species is low and population decline is low for most populations in the 2080s (i.e., majority of temperatures below T_{opt}). Currently we are limited to forecasting vulnerability using climate models that do not extend past the 2080s, but this comparison allows us to forecast vulnerability using current rates of change beyond current models of climate

change. Other rates of change have been used to forecast vulnerability and range shifts beyond current models, but often suggest hope for rescue from shifting climate. For example, rates of climate change are four times greater in the north compared to equatorial regions (Stuecker et al. 2018) which have led some to suggest that there is room for temperate cold adapted species ranges to shift north (Sunday et al. 2012), which would not likely happen within the current model time frame (except marine ectotherms which more closely match climate velocities due to vagility and few barriers to movement in the marine environment). However, because of global change, synergies (Coristine and Kerr 2011) occurring between the combination of lower thermal limits in northern populations, and human impacts such as accelerated climate change that may outpace lower latitude summer temperatures due to changes in the intertropical convergence zone and loss of ice and snow (Spicer et al. 2013), and a higher degree of habitat degradation in some northern biomes previously thought to be 'intact' despite being over-represented in land conservation (Riggio et al. 2020), may render range shift a non-viable option to rescue species. Furthermore, because species' average thermal physiology is often skewed to more closely fit southern thermal regimes due to over-filling of niches at higher latitudes (Sunday et al. 2012) northern populations are less likely to be triggered to expand leading to a net loss of range as southern edges retract (Coristine and Kerr 2015).

Here we generated a robust dataset to estimate the trends in thermal physiological traits for a broadly distributed species (*A. truei*). Our results have expanded our understanding of the range of thermal trait variation possible within a species. While caution is warranted in interpreting our specific vulnerability analyses, we propose that our results offer a unique perspective on the vulnerability of species and populations to the accelerating impacts of climate change. Such impacts are not unique to our study system or even climate change, as similar conclusions have been made in other realms: as high density human settlement overfishes stocks at lower latitudes in the Northeast Atlantic and pushes exploitation and human activity north, the combination of climate change, increased pollutants, and fishing pressure increases both exposure and risk to fisheries non-linearly (Lee and Jetz 2008), suggesting that the vulnerability of species and populations to a multitude of human impacts may be worse than our current near future predictions. While important for understanding how species physiology is shaped by climate, we further hope that our approach may be valuable by helping to identify populations and regions that might benefit from additional conservation resources. Such strategies could include protecting or restoring corridors of habitat across elevation to allow for local-scale range expansion (Thompson and Gonzalez 2017), or the protection of northern

populations at highest future risk of compounding anthropogenic effects from climate change and industrial development (Leroux and Kerr 2013, Chisholm 2022).

Chapter 4. Predicting the effects of road mortality and mitigation on an at-risk amphibian with increasing human activity

4.1. Abstract

Human disturbances to landscapes result in habitat loss, degradation, and fragmentation, and frequently drive wildlife population declines by altering demographic rates and movement. Many costly conservation efforts are focused on reducing the direct mortality to individuals when habitats are fragmented or migration corridors are blocked, yet the consequences for population viability are rarely measured. Here we analyzed 15-years of road mortality and mitigation data for a frog population (*Rana aurora aurora*) in which some individuals must cross a highway to complete their annual life-cycle. We used a stochastic matrix population model to estimate how road mortality affects the population growth rate (λ) and 30-year probability of extinction, and whether commonly employed mitigation efforts (roadside fencing and underpass structures) can reverse such effects under both current and future (2040s) vehicle traffic. Our models predict that the *R. aurora* population is declining at a rate of 2% per year (λ = 0.98) under 'current' rates of vehicle traffic compared to a hypothetical 'wild' population without road mortality (λ = 1.02). We find that the addition of roadside fencing and an underpass can mitigate such declines, leading to a 1% annual population increase (λ = 1.01) and a 30% lower risk of extinction compared to a population without any mitigation. While mitigation appears to partially offset the negative effects of road mortality, when we incorporate future (2040s) predictions of increased traffic, mitigation is no longer able to prevent population declines (λ = 0.98). The results of our study suggest that mitigation of road mortality is a viable option to reduce road mortality and extinction risk of *R. aurora* populations, but without improvement, mitigation alone cannot compensate for future pressures caused by increased traffic.

4.2. Introduction

Human disturbance to landscapes causing habitat loss, degradation, and fragmentation is a major cause of wildlife population declines and biodiversity loss (Stuart et al. 2004, Rybicki and Hanski 2013, Haddad et al. 2015, Newbold et al. 2015, Gonçalves-Souza et al. 2020) often by changing population and meta-population dynamics such that both survival and colonization

is decreased (Hanski 1998, Gu et al. 2002, Wiegand et al. 2005). While the sum total of habitat loss has been estimated to have the greatest impact on most species, (Bender et al. 1998), populations of species that require seasonal movement between ecotones to acquire resources within otherwise contiguous habitat are expected to be at elevated risk of extinction when habitat fragmentation occurs (Harding 2002). The elevated risk to migrating populations is attributed to the reduction in connectivity when anthropogenic edges act as barriers to movement or as sources of mortality (Serieys et al. 2021). As such, many conservation tools designed to mitigate habitat fragmentation and reduced connectivity focus on the creation of wildlife corridors to allow for seasonal movement and reduce human-wildlife conflict (Henry et al. 1999, Raimer and Ford 2005). For example, habitat fragmentation by roads resulting in reduced connectivity (Shepard et al. 2008) and direct mortality is a major cause of population decline (Czech and Krausman 1997, Forman and Alexander 1998, Fahrig and Rytwinski 2009, Laurance and Balmford 2013), and has been effectively mitigated by fencing and crossing structures, particularly for large mammals (Carroll et al. 2001, van der Grift et al. 2013, Sijtsma et al. 2020). However, reduced habitat connectivity and direct mortality also impact smaller bodied animals, such as small mammals (Rico et al. 2007), birds (Kociolek et al. 2011), and amphibians (Cushman 2006). Our understanding of the impacts of road mortality on population persistence is especially limited for amphibians, and the effectiveness of mitigation measures even more so (Beebee 2013, Petrovan and Schmidt 2019). Roads have been hypothesized to act as severe barriers to wet-skinned amphibians in particular because the often high solar radiation and dry substrate interrupt movement (Semlitsch et al. 2007, Van Buskirk 2012) in the same way that hot, dry, clear cut forests reduce habitat permeability (Popescu and Hunter Jr. 2011). The resulting fragmentation can limit dispersal from natal wetland habitats, lead to loss of genetic diversity (Reh and Seitz 1990, Lesbarrères et al. 2006) and an increased risk of extinction due to stochastic events (Wilcox and Murphy 1985).

The impacts of roads to herpetofauna has largely focused on correlational studies of population decline (Fahrig et al. 1995), genetic isolation (Reh and Seitz 1990, Vos et al. 2001), or local extirpation (Puky 2003). In contrast, the impact of fragmentation from roads on large mammals is better documented. Studies have linked reductions in habitat permeability to changes in demographic rates and reduced population persistence because of significant road mortality or increased genetic isolation from reduced migration (Fahrig and Rytwinski 2009, Bond and Jones 2013, Polak et al. 2014). While few studies have linked mortality from road crossing to amphibian population decline (Fahrig et al. 1995), the cumulative impacts of road

mortality and reduced connectivity are expected to put amphibians at greater risk of population vulnerability when roads bisect habitat and migration corridors (Semlitsch et al. 2007, Perumal et al. 2021). However, for some amphibians, road mortality losses may be complicated by strong density-dependent survival in later life stages, where the decreased abundance of dispersing juveniles and migrating adults may be compensated for by higher per capita growth, survival, or reproductive output (Vonesh and De la Cruz 2002, Harper and Semlitsch 2007). Therefore, understanding whether impacts to individuals (e.g., road mortality) scale to the level of emergent population dynamics is central to assessing risk, and requires more than mortality surveys and correlational studies. While some modeling studies have highlighted how roads can impact amphibian population connectivity and persistence (Jaeger and Fahrig 2004, Rytwinski and Fahrig 2013), very few empirical studies have mechanistically linked road crossing mortality of amphibians to declines in population abundance or viability (but see Gibbs and Shriver 2005, Wilkinson and Romansic 2022). Process-based measures that would allow explicit inference to population decline due to migration mortality, such as stage-based population demographic models, are methodologically challenging because they require substantial field data to parametrize (Fardila et al. 2017). However, with such data, mechanistic hypotheses can be tested regarding which components of species' life history drive population declines (Wisdom et al. 2000) and provide guidance to what combination of conservation actions could reverse them (Mills et al. 1999).

Reducing amphibian road crossing mortality using a variety of mitigation tactics and structures has been the focus of many conservation efforts (Fahrig et al. 1995, Schwarz 2001, Glista et al. 2009, Petrovan and Schmidt 2019, Denneboom et al. 2021). Fences to prevent movement and reduce mortality are often constructed along roadsides where migration is concentrated (Helldin and Petrovan 2019), but trade-offs exist as fencing can further reduce connectivity (Jaeger and Fahrig 2004), exacerbate density dependent growth and survival (Harper and Semlitsch 2007, Muths et al. 2011), and increase genetic isolation (Lesbarrères et al. 2006). Furthermore, fences may not be able to effectively compensate when populations have been depressed because of long-term road mortality or barrier effects (Eberhardt et al. 2013). Therefore, underpass structures are also frequently used to increase the permeability of landscapes bisected by roads and reduce mortality for many small bodied or highly-mobile organisms (McDonald and St Clair 2004). For many organisms, underpass structures that effectively restore connectivity do not mitigate mortality unless installed in combination with fencing in order to achieve both reduction in mortality and increased permeability (Cunnington et

al. 2014). Governments have invested in costly planning and construction of road mitigation infrastructure for many amphibian populations, including underpasses and fencing (Elton and Drescher 2019). Unfortunately, the effectiveness of such projects at reducing mortality and especially population growth is rarely evaluated (Boyle et al. 2021). Further, road mitigation actions that reduce but do not eliminate mortality may be effective at lower vehicle traffic, but increased traffic may ultimately limit efficacy.

Here, we quantitatively compared two forms of road-crossing mitigation, roadside fencing and an underpass, over a 30-year timespan for an at-risk population of *R. aurora* threatened by a highway that crosses an important juvenile and adult seasonal migration corridor. We used extensive field-collected demographic data, estimates of the number of migrating individuals, and road crossing mortality rates in stage-structured population dynamics models to determine the effectiveness of road crossing mitigation by comparing predictions of population growth and extinction risk over 30 years. We constructed a series of stochastic matrix models to compare the efficacy of each mitigation scenario at reducing 30-year extinction probability and increasing population growth rates given current traffic levels and evaluated whether mitigation would be effective given future projections for increased vehicle traffic (tourism and population growth) in the region. Finally, we estimated the elasticity of the population growth rate (λ) to variation in individual vital rates of the *R. aurora* life cycle to assess whether mitigation of the juvenile and adult life stages is likely to affect population level dynamics. We present a roadmap for determining the efficacy of two common methods of road crossing mitigation and highlight that effective mitigation requires consideration of both present impacts and how drivers of mortality may scale in the future.

4.3. Methods

4.3.1. Species range, status, and threats

The Northern Red-legged frog, *Rana aurora aurora*, is a cold-adapted species occurring along the Pacific coast of North America, west of the Cascade and Coast Mountain Ranges, from southwestern British Columbia to northwestern California. Although globally listed as “apparently secure”, the status of *R. aurora* is “Special Concern” under the federal Species at Risk Act in Canada (Environment Canada. 2016) and “Vulnerable” in Oregon and California (NatureServe 2022). Local declines and disappearances have occurred in densely human-populated areas where wetlands and forests have been lost and fragmented by urban and

agricultural development (Jennings and Hayes 1994, Blaustein et al. 1995, Lannoo 2005, Malt 2013), and where bullfrogs and sport fish have been introduced (Kiesecker and Blaustein 1997, Govindarajulu 2004, Adams et al. 2011). Roads are thought to exacerbate these threats, especially through direct mortality to juveniles and adults migrating between terrestrial and aquatic-breeding habitats (Hayes et al. 2008, B.C. Ministry of Environment and Climate Change Strategy 2020).

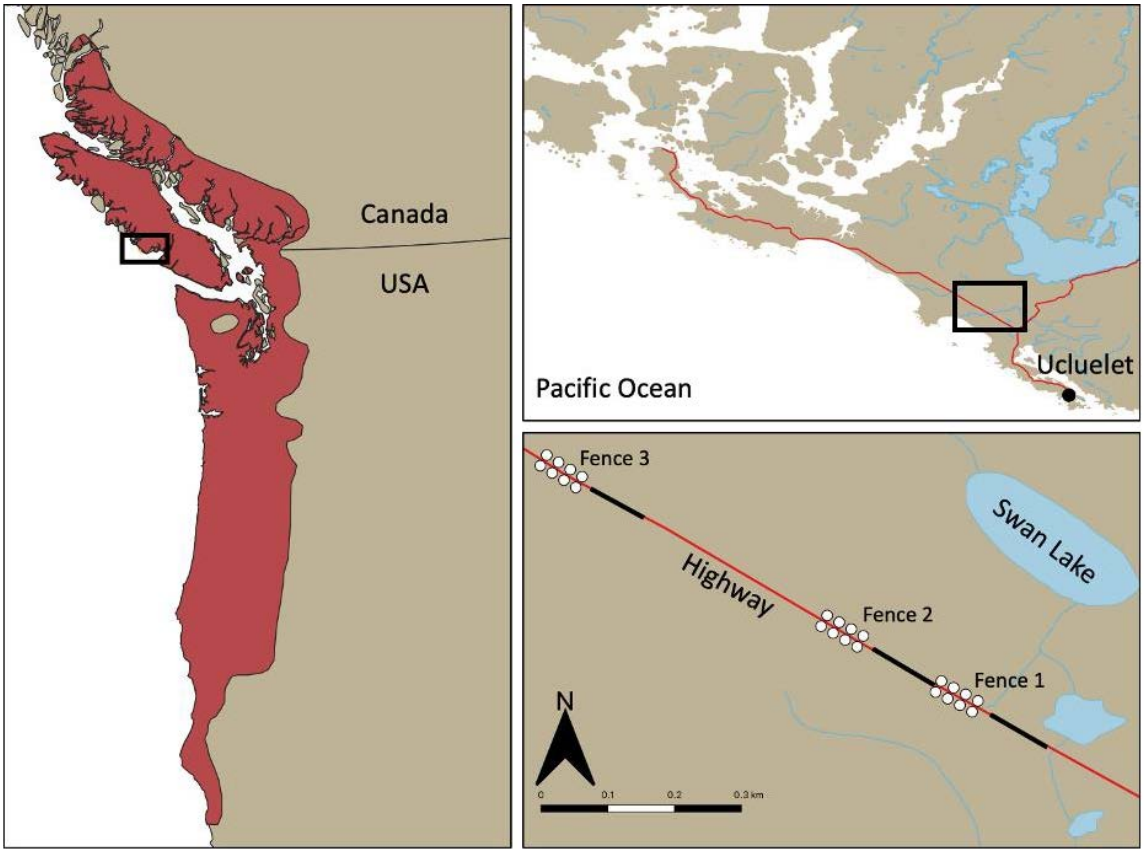

Figure 4-1 **Map of *R. aurora aurora* range (red) from Northern California to Southern BC, showing the general location of the study site on Vancouver Island (black box; left panel) on highway 4 near Ucluelet, BC (black box; top right panel), and position of three 90m fenced highway sections on east and west sides (white dots) and 90m unfenced sections before and adjacent to each fenced section (bottom right panel). The underpass was installed in in the south-east most fenced section (fence 1) of the highway.**

4.3.2. Swan Lake Study Site

We used a population at Swan Lake, British Columbia, Canada as inspiration for modelling road mortality and source of data for some (but not all) of the vital rates for a

hypothetical *R. aurora* population. We observed frequent mortality of *R. aurora* migrating across B.C. Highway 4 to breed at a 4-ha wetland, known as Swan Lake, approximately 10 km from Ucluelet, B.C. (Figure 4-1; Beasley 2006). Swan Lake is a low elevation shallow fish-less freshwater lake (< 80 cm deep) that dries to ~30% of its maximum size each summer within the Lost Shoe Creek watershed. Emergent rushes (*Juncus spp.*) are the predominant vegetation and serves as the main attachment sites for egg masses laid by *R. aurora*, as well as Northwestern salamanders (*Ambystoma gracile*), Pacific treefrogs (*Pseudacris regilla*), and Rough-skinned newts (*Taricha granulosa*). Beyond a fringe that includes shore pine (*Pinus contorta*), Pacific crab apple (*Malus fusca*), and sweet gale (*Myrica gale*), the surrounding forest is dominated by western hemlock (*Tsuga heterophylla*), western redcedar (*Thuja plicata*), and amabilis fir (*Abies amabalis*) with an understory of salal (*Gaultheria shallon*), blueberries and huckleberries (*Vaccinium sp.*), salmonberry (*Rubus spectabilis*), deer fern (*Blechnum spicant*), sword fern (*Polystichum munitum*) and a variety of mosses typical of the Southern Very Wet Hypermaritime variant of the Coastal Western Hemlock Biogeoclimatic Zone (CWHvh1; B.C. Ministry of Forests 1994). The natural history of the Squaw Flat Research Natural Area *R. aurora* population used to estimate key vital rates has been described previously (Hayes et al. 2008).

4.3.3. Matrix model

We constructed a 30-year stochastic age-based matrix model with a 1-year time interval to predict the dynamics of a female-only *R. aurora* population and estimated the cumulative extinction probability (CE) and stochastic population growth rate (λ_s) for each model scenario (Tuljapurkar 1982, Morris and Doak 2002). We assumed that up to 25% of the *R. aurora* population was subject to potential road mortality based on the geography of our study site and observations of adult migration patterns (Appendix C). We divided the life history of *R. aurora* into four annual stages, or matrix elements (a_{ij}, F_{ij}) composed of one or more vital rates (Figure 4-2). In our population simulations, embryos are laid in February and hatch into aquatic larvae in March – April, followed by metamorphosis in late summer (July – August). Newly metamorphosed terrestrial juveniles overwinter near the natal wetland to complete their first year and the first annual stage. Juveniles either (a) stay near their natal wetland and mature into adults or (b) cross the road and mature into adults before re-crossing the road to breed at Swan Lake (Figure 4-3). In spring (February), adults breed at Swan Lake and either (a) stay near Swan Lake during the summer, fall, and winter, or (b) cross the highway shortly after breeding

and return to Swan Lake in the fall before overwintering near the lake (Figure 4-2). Mean estimates of each vital rate were calculated from field experiments or surveys on *R. aurora* (Appendix C). We incorporated stochasticity into our models by calculating variances for each vital rate from our field studies or reported in the literature for closely related species (Appendix C). We ran 1,000 iterations of each stochastic simulation in MATLAB to calculate the cumulative 30-year probability of quasi-extinction ($n \leq 20$ adults females; Appendix C) and stochastic growth rate (λ_s) for each scenario. We began the population at stable-stage distribution (derived from the mean deterministic matrix and using the mean number of egg masses at Swan Lake as the abundance of adult females: 1,380). For a list of models used to parameterize each matrix model, see Appendix C, Table S1.

$$\begin{pmatrix} 0 & 0 & 0 & F_{14} \\ a_{21} & 0 & 0 & 0 \\ 0 & a_{32} & a_{33} & 0 \\ 0 & 0 & a_{43} & a_{44} \end{pmatrix} \times \begin{pmatrix} n_1 \\ n_2 \\ n_3 \\ n_4 \end{pmatrix}_t = \begin{pmatrix} n_1 \\ n_2 \\ n_3 \\ n_4 \end{pmatrix}_{t+1}$$

Transition rate	a_{ij}	Parameter equation
Wild (No road mortality)		
Embryo to Juvenile	a_{21}	$\phi_{embryo}*\phi_{larvae}*\phi_{meta}$
Juvenile	a_{32}	ϕ_{juv}
Remaining a Juvenile	a_{33}	$p_{juv}*\phi_{juv}$
Juvenile to Adult	a_{43}	$(1-p_{juv})*\phi_{juv}$
Adult	a_{44}	ϕ_{adult}
Fecundity	F_{14}	$F_{adult} * p_B *$ sex ratio
With road mortality		
Juvenile	a_{32}	$((1-\hat{p}_{rd})*\phi_{juv}) + (\hat{p}_{rd}*\phi_{juv}*\phi_{jrd})$
Adult	a_{44}	$((1-\hat{p}_{rd})*\phi_{adult}) + (\hat{p}_{rd}*\phi_{adult}*\phi_{ard}^2)$

Figure 4-2 **Matrix model structure and vital rate definitions. Here, n_i is the number of individuals in stage *I* at time *t*, F_{ij} represents per capita fecundity, a_{ij} is the transition rate from one stage to the next and is made up of component vital rates shown in the *Parameter equation* column. Φ represents survival, meta = overwintering metamorph, p_{juv} is the probability of remaining a juvenile, p_B is the probability of breeding, and $\hat{p}_{rd}$ is the proportion of juveniles and adults that cross the road with added juvenile (Φ_{jrd}) or adult (Φ_{ard}) survival.**

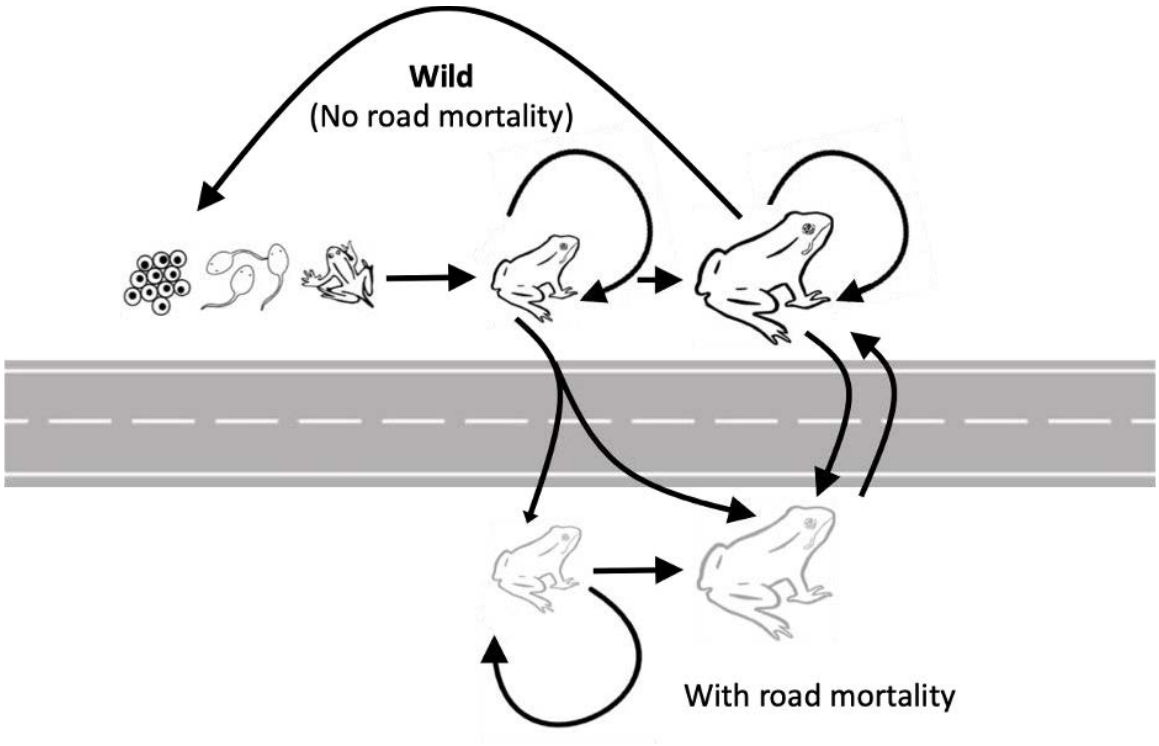

Figure 4-3 **Schematic diagram of the three stage *R. aurora aurora* matrix model with road crossing scenarios. Each arrow represents transition probabilities among the stages. The top life cycle represents a theoretical wild population that does not experience road mortality. Individuals in the first stage (embryos, larvae, and overwintering metamorphs) transition to the next stage after a 1-year time step. The arrow going from the adult stage back to stage one represents the reproductive contribution (fecundity) of the population. In a population where a proportion of the population experiences road mortality (below the road) some juveniles cross the road to complete part of their lifecycle and do not cross the road again until they have transitioned to the adult stage. Some adults cross the road after breeding and return to Swan Lake, crossing the road again, before winter sets in.**

4.3.4. Scenarios

We constructed models to estimate the population impact of current and future rates of road mortality and the ability of two types of mitigation structures (roadside fencing and underpasses) to offset those losses, resulting in 7 scenarios: a population subject to (1) road mortality at current (2005 - 2015) rates of vehicle traffic, (2) with roadside fences that inhibit crossing, and (3) with a combination of roadside fences and underpass. We also ran each of these scenarios (1-3) under predictions of future traffic (2040s; Scenarios 4-6 ; Table 1). Lastly,

we also modeled a hypothetical ‘wild’ population in the absence of any road mortality for comparison (7).

Table 4-1 Seven model scenarios used to evaluate the efficacy of road mitigation on population growth rate and 30-year probability of extinction of a, *R. aurora, population*

Scenario	Changes to survival
Current (2010 - 2015)	
1. Without mitigation	Juvenile/adult survival rates subject to road mortality at current vehicle traffic (μ = 19 vehicles/hr)
2. Mitigation fences	Juvenile/adult road mortality mitigated with roadside fences at current vehicle traffic
3. Mitigation fences + culvert	Juvenile/adult road mortality mitigated with roadside fences and an underpass at current vehicle traffic
Future (2040s)	
4. Without mitigation	Juvenile/adult survival rates subject to road mortality at future vehicle traffic (μ = 46 vehicles/hr)
5. Mitigation fences	Juvenile/adult road mortality mitigated with roadside fences at future vehicle traffic
6. Mitigation fences + culvert	Juvenile/adult road mortality mitigated with roadside fences and an underpass at future vehicle traffic
Wild	
7. No road mortality	Juvenile/adult survival rates not subject to road mortality

Table 4-2 Vital rate estimates (mean, variance) and sources.

Scenario	Vital rate	Description	Estimate	Variance
	No road mortality			
Wild	p_B	Probability of breeding[1]	1	
	F_{14}	per capita fecundity[2]	358	25553
	sex ratio		0.5	
	Φ_e	Embryonic survival[2]	0.770	0.044
	Φ_l	Larval survival[1]	0.044	0.000108
	Φ_{meta}	Metamorph survival[1]	0.413	0.00279[3]
	Φ_{juv}	Juvenile survival[1]	0.268	0.00326
	p_{juv}	Probability of remaining a juvenile[1]	0.260	
	Φ_{adult}	Adult survival[1]	0.840	0.06783[3]
	Road crossing			
	$\hat{p}_{rd}$	Proportion of population crossing the road	0.25	
Current traffic	Without mitigation			
	Φ_{jrd}	per capita juvenile road crossing survival	0.9786	0.00771
	Φ_{ard}	per capita adult road crossing survival	0.9246	0.00199
	Fence mitigation			
	Φ_{jrd}		0.9985	0.0044
	Φ_{ard}		0.9804	0.00540
	Fence + culvert mitigation			
	Φ_{jrd}		0.9985	0.00214
	Φ_{ard}		0.9962	0.00082
Future traffic	Without mitigation			
	Φ_{jrd}		0.9340	0.00771
	Φ_{ard}		0.8660	0.00199
	Fence mitigation			
	Φ_{jrd}		0.9540	0.0044
	Φ_{ard}		0.9183	0.00540
	Fence + culvert mitigation			
	Φ_{jrd}		0.9540	0.00214
	Φ_{ard}		0.9331	0.00082

Notes: [1]Hayes (*unpub.*), [2]Beasley (*this article*), [3]McCaffery & Maxell (2010)

4.3.5. Vital rates

We modelled the mean stochastic population growth rate (λ_s) and the 30-year CE of adult female *R. aurora* using annual stage-based models, in which matrix elements were made up of one or more lower level vital rates (Morris and Doak 2002). We derived vital rates for our models from a combination of our field studies and experiments with *R. aurora* and used estimates from the published literature for additional rates (Table 2). We modelled survival (ϕ) and estimated fecundity (F) and transition probabilities between stages (p; Figure 4-3) primarily

from *R. aurora* field studies in Ucluelet, BC, Canada, and Washington, USA (Appendix C), with additional information summarized from the published literature (vital rate variance; Table 4-2).

4.3.6. Mitigation experimental design

To make fair comparisons of road edge abundance and road mortality at fenced (impact) versus unfenced (control) sections, we designated 90m sections of unfenced road adjacent to fenced sections as controls that began at least 5 m away from the end of the fenced (impact; mitigated) sections (Figure 4-1). In 2011, we then installed an underpass at the southeast most section (Fence 1) as further mitigation. For the purposes of this study, and to directly compare changes to road mortality due to the impacts of our mitigation structures, we focus on the reduction in mortality at the southeastern most impact and control sections (Fence 1), but use all three fenced and adjacent control sections to estimate overall reduction in juvenile and adult survival due to the presence of the road.

4.3.7. Estimating road mortality

To estimate the per capita reduction in survival of adults and juveniles crossing the road we estimated abundance over 0.27km of road using amphibian drift fences and pitfall traps paired with surveys of carcasses found on the road at adjacent unfenced sections the morning after (nighttime) migration activity. In 2005, three 90m roadside amphibian drift fences (separated by at least 130m) with 23 pitfall traps each were installed at locations previously identified as having the highest rates of *R. aurora* migration (Appendix C, Figure S1; Figure 1). Both sides of the highway were fenced in each section. Pitfall traps were open from dusk to dawn, and amphibians captured were relocated to the opposite side of the road in the morning. Between 2005 – 2010 during peak migration seasons (spring – February to May, fall – September to November) and during summer (June to August) when weather conditions were favourable for amphibian movement (rain and overnight temperatures above >10^{o}C; n = 135 nights across all seasons and years), we conducted pitfall trapping for migrating juveniles and adults along the highway edge

We used a closed *N*-mixture model (Royle 2004) implemented in package ‘unmarked’ (Fiske and Chandler 2011) for program R (R Core Team 2014) to estimate detection, abundance, and the influence of site- and survey- level covariates on abundance and detection of juveniles and adults at the highway edge using our spatially and temporally replicated pitfall

trap data. For this model, we assume that replicated counts (each survey night) collected across sites are representative of the abundance of individuals at each location during typical spring, summer, or fall season migration. Hierarchical models of abundance (*N*-mixture models) allow for comparisons of abundances of species while accounting for spatial and temporal variation in detection probabilities (Royle 2004). We used fence ID and side of the road as predictors of abundance (because each 'site' or pitfall trap was nested as fence ID(side of road(trap))), and mean overnight temperature, overnight rainfall, and the number of hours that the trap was open as covariates for detection. We modelled juveniles and adults in each season (spring, summer, fall) separately (6 model sets total) because we hypothesized that the factors that influence detection would be different for each age class and season, and because we had different numbers of survey nights per season (spring n = 20, summer n = 18, fall n = 97). We used Akaike's information criterion, adjusted for small sample sizes (AICc; Burnham and Anderson 2002) to identify the best-supported model for detection variables for each age class and season combination, and used the side of the road and fence ID for abundance covariates in all models (Appendix C, Table S2, Table S4).

To estimate the mortality rate of animals crossing the road, we needed to compare our estimated abundances of animals at the road's edge with abundances killed on the road. To do this, we surveyed 1.69 km of the highway each morning that pitfall traps were checked (n = 135 mornings) for carcasses of *R. aurora*. However, because the carcasses of some individuals that are killed overnight may not be detected in the morning due to damage by cars, being washed away by heavy rainfall, or being removed by scavengers, we applied a modelled correction for the persistence of carcasses that varied by mean hourly traffic from dusk to dawn (BC Ministry of Transportation Traffic Data Program) and overnight rainfall accumulation (Pacific Rim National Park weather records). During a subset of nights (n = 51), we marked carcass locations on the highway and returned the following morning to catalog the persistence of marked carcasses and newly killed individuals. We used a binomial generalized linear mixed-effects model using package 'lme4' (Bates et al. 2015) implemented in R (R Core Team 2014) with traffic, rainfall, and age class as fixed effects, and day of the year as a random effect to account for pseudoreplication. We then used the age-specific model predictions of probability of persistence based on traffic and rainfall prior to morning road mortality surveys to correct the number of carcasses found in the morning only (Appendix C, Table S4, Figure S2). We used the corrected number of juveniles and adults killed nightly on the highway at fenced and un-fenced

sections to compare to our *N*-mixture estimates of abundance at adjacent fenced sections to arrive at per capita estimates of road crossing survival with and without mitigation (see below).

In order to make predictions of future road mortality as a function of traffic we used our model corrected predictions of road mortality as the response for a count based negative binomial generalized linear model with mean hourly traffic and age class as the independent variables (Appendix C, Table S5). Separately, we estimated the mean annual increase in overnight traffic over the period 2005 – 2015 (compounded annually) to predict traffic in the 2040s. We then used 2040s traffic as the input for the traffic dependent road mortality model described above to estimate future road mortality at higher (2040s) vehicle traffic and calculated the percent increase in mortality due to increased traffic compared to those in the 2005 – 2015 study period.

4.3.8. Estimating mitigation effects on road mortality

To estimate how the per capita stage-specific (juvenile, adult) mortality rates for individuals that cross the road changes in the presence of two commonly used mitigation structures (roadside fencing, underpasses), we compared our estimates of road mortality at the un-fenced (control) versus adjacent fenced (impact) sections (fence 1 - 3) in three time periods representing before mitigation (2000 - 2004), after the installation of roadside fencing (2005 - 2010), and the period after both roadside fencing and a specially-designed underpass was installed (2011 – 2015; Appendix C). This spatial and temporal structure to the road mortality data allowed us to use a Before-After Control-Impact (BACI, (Roedenbeck et al. 2007) approach to estimating how mortality changed among the three time periods.

We assumed that density at fenced sections was representative of the density of individuals attempting to cross the road at adjacent southeast unfenced control sections, therefore, we calculated the mean number of frogs killed per kilometer of road in the un-fenced sections at night throughout each of the three seasons (spring, summer, fall) to compare to mean number of frogs killed per kilometer of fenced sections at nights throughout each of the three seasons. This provided estimates of road mortality for the 'Before mitigation' period, based on the assumption that control sections would have the same level of mortality after mitigation as before, using a linear model of road mortality as a function of abundance at the road edge (Appendix C, Figure S3). Furthermore, we compared estimates of road mortality at fenced (impact) sections paired with abundance estimates at the road edge (pitfall traps on fences 1 -

3) to calculate mortality for the 'After fencing mitigation' period. Because we don't have pitfall trap data for the 'After fencing and underpass mitigation' period we used the relative change in road mortality found in the underpass section (impact; fence 1) to the paired un-fenced section (control; adjacent to fence 1) to estimate the change in mortality.

4.3.9. Wild population size

Extinction probability for a wild population is a function of population size and the rate of decline. In each model simulation, we used a starting population vector based on the mean number of egg masses found in Swan Lake (2007 – 2018) as a proxy for the number of adult females in the population multiplied through the stable age distribution calculated from the mean deterministic matrix without road mortality.

4.3.10. Elasticity Analysis

We calculated deterministic elasticity values, which provide the proportional change in lambda given a proportional change in a single vital rate, using mean values of the 'wild' population matrix (scenario 7; without road mortality). However, because populations often experience variation in multiple vital rates simultaneously and such changes violate the basic assumptions of deterministic elasticity analysis (Caswell 2010), we also conducted a simulation-based elasticity analysis in which 10,000 random matrices were created with vital rates drawn at random from uniform distributions between maximum and minimum values obtained from our studies. We used multiple linear regression of the centred and standardized randomly drawn vital rates to estimate the effect (using the regression coefficients) that each has on lambda as our simulated elasticities (Wisdom et al. 2000).

4.4. Results

4.4.1. Estimating road mortality

Using five years (2005 – 2010) of data on *R. aurora* road mortality and road crossing abundance, we estimated the impact of vehicle traffic on crossing frogs and their per capita survival rate when crossing the road. We found that currently on average 19 ($\pm$7 SD) vehicles/hour drive along the 1.69km of road that bisects the *R. aurora* migration corridor per night across all seasons, that on average 5 ($\pm$8 SD) juveniles and 9 ($\pm$7 SD) adults are killed

per night across all seasons, and that for every one vehicle/hour increase, the number of dead juveniles increases by 4% (±1 SE) and adults by 2% (±1 SE; Figure 4-4). Subsequently, we predict that individual road crossing mortality rates for juveniles is 2.14% (±0.77 SE) and for adults is 7.54% (±4.46 SE) with each crossing, and where adults migrate across the highway twice per year (away from Swan Lake in spring, back in fall) resulting in an annual road crossing survival of 97.9% for juveniles and 85.5% for adults (Appendix C, Figure S3).

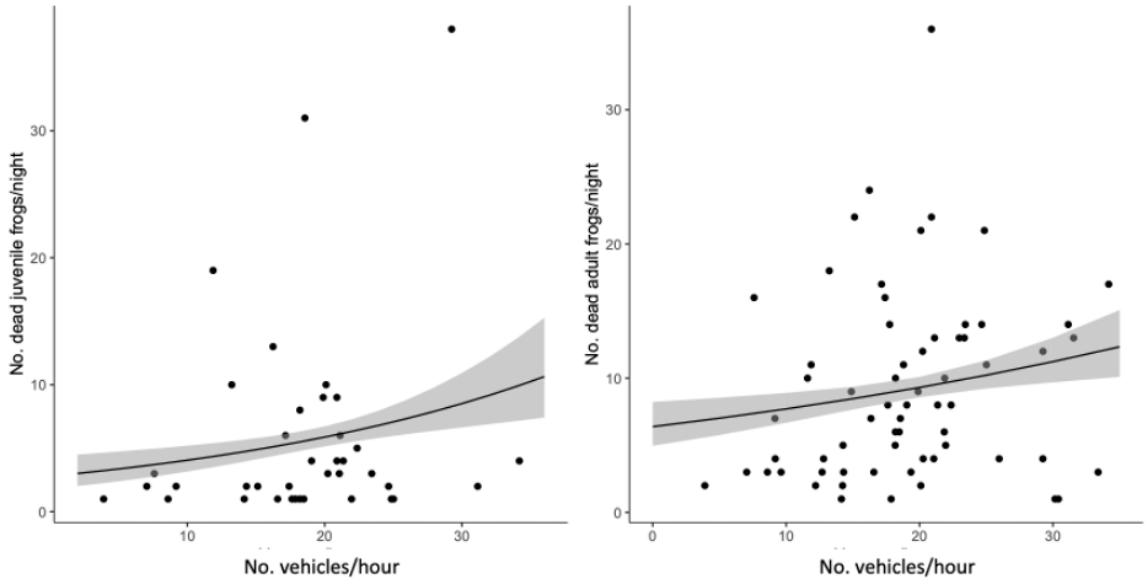

Figure 4-4 The predicted number of frogs killed on the road per night with 95% CI as a function of the hourly vehicles per night for juveniles (left) and adults (right). Mean hourly vehicle traffic for the current scenario was 19 vehicles/hour, and for the future (2040s, 160% increase) 49 vehicles/hour.

4.4.2. Estimating mitigation effects on road mortality

Using estimated abundance and road mortality data from the fence with the highest density of both juveniles and adults (fence 1), and during the fall season when the highest abundance of frogs cross the road, we compared the decrease in mortality before and after mitigation (fences, underpass), and in control (un-fenced) and impact (fenced or fenced plus underpass) to estimate changes in road crossing survival. We find that road crossing survival is increased with the installation of mitigation fencing by 93% (±9 SE) for juveniles and 74% (±9 SE) for adults compared to un-fenced sections (Figure 4-5) to 0.99 (±0.07 SE; juveniles) and 0.96 (±0.07 SE; adults; Table 4-2). We found that the installation of an underpass structure and additional fencing does not further reduce mortality of juveniles compared to only fencing, but

adult survival is reduced by 95% (±11 SE) compared to un-fenced sections (Figure 4-5) to 0.99 (±0.03 SE; Table 4-2).

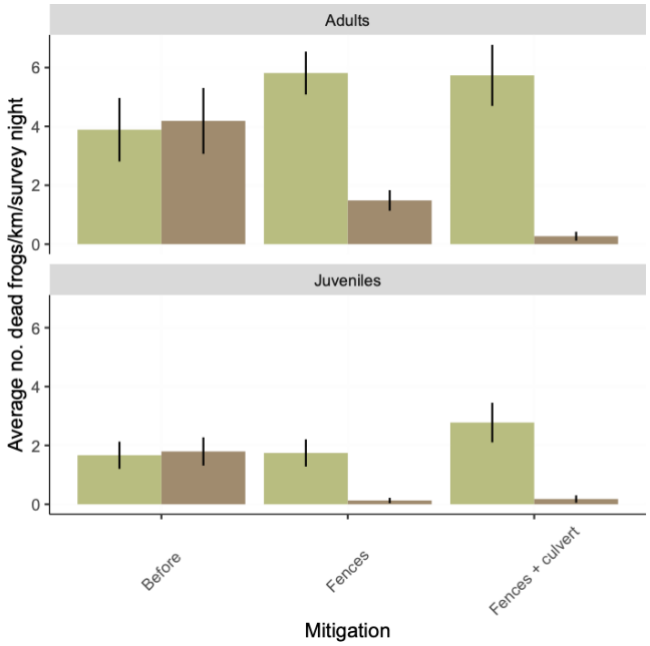

Figure 4-5 The observed mean number of dead frogs per kilometer per night in the most southeast control (90m un-fenced; green) vs. impact (90m fenced, 2005 – 2010; 90m fence + culvert, 2011 – 2015; brown) section of the highway near Swan Lake (see map Figure 1, fence 1) during the falll season (September – December). Numbers for the before period were aggregated juveniles and adults as age class data was not recorded during that time and are here corrected for using the ratio of age classes found during the fall season at the same section (fence 1) during the time period 2005 – 2010).

4.4.3. Matrix Models

Based on the mean number of adult female frogs predicted to cross the road from our abundance model each year (N = 341) and mean female population size estimated from egg mass counts at Swan Lake (N = 1380), we assume that 25% of the *R. aurora* population migrates across the road every year (Appendix C). Because of this, a *R. aurora* population modeled with road mortality but no mitigation and with current (2005-2015) vehicle traffic (Scenario 1, Table 4-1) has a stochastic growth rate (λ_s) of 0.98, equivalent to a 2% annual decrease, and a 30-year cumulative probability of quasi-extinction (CE) of 17% (Figure 4-6). When we model mitigation with roadside fencing (Scenario 2), λ_s increases to 0.99 and CE declines to 14%. When we apply the road crossing survival rates in the presence of both

roadside fencing and underpasses our models predict a positive population growth rate (λ_s) of 1.01, and CE = 12%.

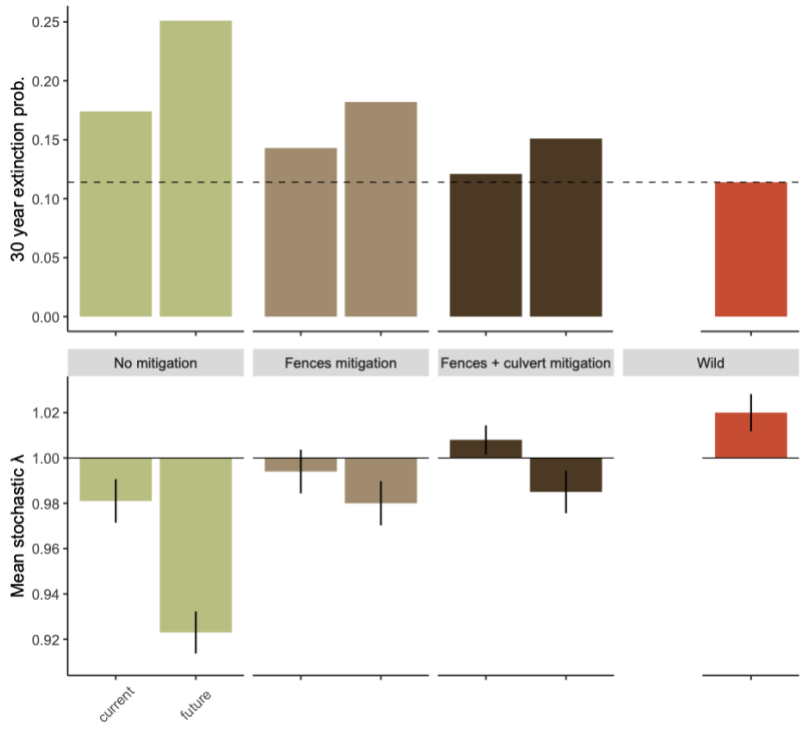

Figure 4-6 Mean stochastic lambda (λ_s) with standard error for the four population simulation scenarios for *R. aurora aurora* that experience road mortality with no mitigation, mitigation by roadside fences, or fences and an underpass for current (scenarios 1 – 3) and future (scenarios 4 – 6) vehicle traffic, compared to 'wild' a population (scenario 7) that does not experience road mortality (bottom panel), and the cumulative 30-year extinction probability for each scenario plus the wild population (dashed line; top panel).

We estimated that vehicle traffic from 2005 – 2015 increased by 6% annually (projected) or an 80% increase over the entire period. We assumed that by the 2040s, mean hourly traffic at night will increase by 160% (μ = 49 vehicles/hr; BC Ministry of Transportation Traffic Data Program). Using our model of road mortality as a function of hourly traffic, we estimate that annual mortality will increase by 130% for juveniles and 53% for adults by the 2040s (Figure 4-4, Table 4-2). When incorporated into our matrix projections we find that future vehicle traffic in the 2040s without mitigation (Scenario 4) results in a λ_s of 0.92 and CE = 0.25 (Figure 4-6). When we model future vehicle traffic with roadside fencing (Scenario 5), λ_s increases to 0.98 and CE declines to 18%. When we model both roadside fencing and underpass (Scenario 6)

with future vehicle traffic, we predict a negative population growth rate (λ_s) of 0.99 and CE = 15%. In contrast, a hypothetical 'wild' population (Scenario 7) that does not experience any road mortality has a stochastic population growth rate of 1.02, equivalent to a 2% annual increase, and a 30-year probability of quasi-extinction of 11%.

4.4.4. Elasticity analysis

Both the deterministic and simulation-based elasticity analysis revealed that vital rates contributed unequally to *R. aurora* population growth. The most elastic parameter in the simulated elasticity analysis was adult survival (ϕ_{adult}), followed by overwintering metamorph survival (ϕ_{meta}), juvenile survival (ϕ_{juv}), embryonic survival (ϕ_{embryo}), and larval survival (ϕ_{larval}). Adult fecundity (F) was the least elastic vital rate, although there was no significant difference in elasticity values between the latter five vital rates (Figure 4-7). Our simulation-based elasticity results were highly correlated with the deterministic elasticity ($Elasticity_{sim}$ = 0.728, r^2 = 0.95; Figure 7).

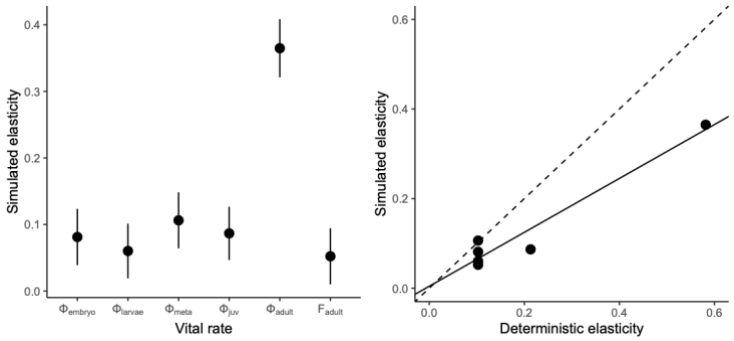

Figure 4-7 Simulated mean elasticity values and 95% confidence intervals for 'wild' *R. aurora aurora* population vital rates (left panel), and correlation between the deterministic and simulated elasticity values ($Elasticity_{sim}$ = 0.728, r^2 = 0.9; solid line) and the 1:1 correlation (dashed line; bottom right panel).

4.5. Discussion

Our analyses and models suggest that amphibian life history is sensitive to road mortality and that strategies such as roadside fencing and underpasses can be effective at mitigating road mortality for *R. aurora* populations in particular. We highlight that mitigation efficacy is dependent on the dynamic nature of road impacts, which frequently increase over time with highly-connected and growing human populations (e.g.; vehicle traffic). When our simulated *R. aurora* population was subjected to road mortality with current vehicle traffic and

no mitigation, the 30-year extinction probability was 1.5 times higher than a population without road mortality. When intensive mitigation infrastructure was installed (roadside fencing and underpasses), the 30-year extinction probability decreased substantially (Figure 5). We found that mitigation under all traffic scenarios helped to reduce population vulnerability, but that because the impact of the road is not static, and because traffic is very likely to increase between now and the 2040's, mitigation efficacy will lessen with time, leading to 30-year extinction probabilities of over 25% by the 2040s, or 1.3 times higher than a population that does not experience road mortality (Figure 4-5). These findings imply that current mitigation efforts in our *R. aurora* study population at Swan Lake are likely to reverse an otherwise declining population due to elevated road mortality, but that further conservation measures will need to be implemented, such as increased roadside fencing and underpasses, in the near future in order to maintain stable population dynamics.

Here we used demographic parameters and experimental mitigation primarily from a single population of *R. aurora* on the west coast of Vancouver Island, Canada to evaluate how (1) road mortality to increases population vulnerability and (2) the degree to which mitigation structures (fences and underpass) can reduce population vulnerability. Developing tools and metrics to evaluate conservation strategies to decrease extinction risk are critical for populations at risk of extinction from human impacts. Stage-based demographic models provide a unique opportunity to couple the complexities of species' life histories with quantitative models to identify life stages with the highest potential to affect population dynamics (Heppell et al. 2000, Sæther and Bakke 2000). Post-metamorphic amphibian life stages have been demonstrated to contribute more to overall population growth rates than early stages (Biek et al. 2002, Vonesh and De la Cruz 2002, Govindarajulu et al. 2005, Kissel et al. 2019). Here, our analysis supports this trend where the most elastic life-stage (adult survival) is negatively impacted by road mortality and has a disproportionate effect on the population growth rate (λ_s). For example, we found that road mortality imposed modest decreases (2-15% reduction) in survival for a quarter of the adult population that migrates across the road, equaling a 0.5 – 3.8% reduction in overall adult survival, but those changes drove strong population declines in the absence of mitigation infrastructure (decrease in λ_s of 4 – 10%). This reduction in adult survival scales to a reduction in population growth because it effects the most sensitive life stage (adults), and because density dependent bottlenecks in amphibian populations typically happen at earlier life history stages (Vonesh and De la Cruz 2002, Altwegg 2003, Patrick et al. 2008) that are not impacted by road mortality in our population (embryonic, larval, metamorphic). However, some amphibian

populations exhibit positive density dependence at the juvenile stage, such that increased mortality could allow survivors to grow faster and reach reproductive stages faster (Harper and Semlitsch 2007). Because juvenile stages in our *R. aurora* model are subject to road mortality, including such intrinsic factors in our model could allow for compensation such that road mortality is equivalent to a sustainable harvest (Hels and Buchwald 2001). However, parameterizing such a nuanced model is often difficult because it requires long-term field monitoring or manipulative experiments that often come with high uncertainty; and furthermore, require cautionary interpretation because overestimating compensatory effects can lead to overconfidence in the state of population growth (Rose et al. 2001). Therefore, understanding the impacts of road mortality to migrating adults (and juveniles) and the change in risk for the population, allows us to target important life stages for mitigation. Furthermore, by using a model without density dependence, we evaluate mitigation by taking a precautionary approach. By doing so we, increase our confidence that well designed mitigation strategies, used in combination, have the potential to increase the persistence of *R. aurora* populations and likely other species with similar complex life histories.

Our demographic analysis provides evidence that road mortality puts *R. aurora* populations at increased risk of extinction and allows us to evaluate the efficacy of mitigation structures at reducing that risk. When we compared the reduction in 30-year extinction probability between the no mitigation scenario (scenario 1) and the fencing only mitigation scenario (scenario 2; 18% reduction) versus both mitigation measures combined (additional 15% reduction), we show that the underpass structure contributed almost as much to reducing extinction risk as fences alone, and the combination was the only scenario that produced a positive population growth rate (Figure 4-5). While other studies have suggested that fences have the greatest single effect of reducing amphibian road mortality, (Cunnington et al. 2014), here we suggest that mitigation should be evaluated based on how it will achieve specific conservation goals. If the goal is to simply stop road mortality, fencing appears to be an effective mitigation measure that is relatively inexpensive, even if they require constant maintenance (BC Ministry of Environment and Climate Change Strategy 2020). In addition, fences are being increasingly designed for specific amphibians that can effectively stop virtually all movement (Conan et al. 2022). However, habitat fragmentation by roads, for many taxa, can result in reduced connectivity and thus reduced population viability beyond that caused by direct road mortality due to genetic and meta-population isolation, and increased risk of stochastic events (Wilcox and Murphy 1985, Reh and Seitz 1990, Lesbarrères et al. 2006). Thus, while

initially expensive, underpass structures are relatively low maintenance and can increase connectivity (Boyle et al. 2021). Furthermore, while the combination of fences and an underpass appears beneficial in our study and others (Helldin and Petrovan 2019), others caution that the decreased connectivity caused by fences has the potential to do more harm to population persistence than the face-value reduction in mortality (Jaeger and Fahrig 2004). Our population model provides strong support for mitigation having a positive effect on long-term population dynamics, however because it does not consider density dependence, our results warrant some caution. If *R. aurora* populations experience strong density dependent growth and survival in terrestrial stages (juvenile, adult), our results may overestimate the long-term benefit of fencing (increased density from reduced migration), but may underestimate the long-term benefit of underpasses. Regardless, future increases in the movement of goods and services across the landscape leading to higher vehicle traffic (scenario's 4 – 6) will reduce the efficacy of both forms of mitigation. And while unknown density dependence may be the difference between positive or negative population growth, the uncertainty and our moral obligation to reduce impacts to ecosystems (Yamin 1995, Piccolo et al. 2022) would suggest that further work is needed to reduce risk to *R. aurora* populations in the future.

Here, we have shown that it is possible to improve the quantitative basis for decisions regarding mitigation implementation and effectiveness when basic demographic data are available. The framework we used with *R. aurora* provides an example of the relative biological gains to be made by employing alternative mitigation strategies. Such tools are not commonly available to conservation decision makers, especially when logistically complicated and lengthy field data are required to assess impacts of mitigation and gauge conservation outcomes. But we argue that adapting existing models for other species can be relatively straightforward and can be used to guide management decisions. Although we show that increasing vehicle traffic with growing human populations is likely to continue to endanger *R. aurora* populations given current mitigation techniques, we also demonstrate that mitigation is an effective tool to reduce the population-level impacts over a multi-decade time horizon. Further, our stochastic models provide a framework that can be easily updated to re-evaluate the level of mitigation effort needed to effectively buffer populations from extinction.

Chapter 5. General Conclusion

In this thesis I explore three specific conservation challenges: 1) understanding how river diversion hydropower development changes thermal regimes for amphibian populations and increases their vulnerability to additional warming, 2) forecasting the magnitude and impact of climate change for populations of a wide-ranged amphibian, and 3) quantifying the impact and identifying effective mitigation strategies for amphibian populations subject to increasing road mortality. In each of these data chapters I demonstrate that using scale independent measures of species responses to changing environments allows us to make predictions of vulnerability across multiple scales, despite complex amphibian life-cycles. I find that with respect to changing environmental temperatures, renewable energy development can have immediate and lasting impacts on *A. truei* populations equivalent to decades of continued warming due to accelerating climate change. Furthermore, for *A. truei*, regional climate adaptions across the species range contributes to accelerating climate vulnerability for some populations despite relatively low current climate risk for these populations. Finally, I find that even though the footprint of a highway does not change on the landscape, it's impact to *R. aurora* populations can scale with increasing rates of human activity (traffic), which in turn can erode the efficacy of existing conservation and mitigation efforts. By considering the non-stationary nature of human stressors, such as climate change and increasing human activity in degraded habitats, I illustrate that time is central to predicting the consequences of human impacts to wildlife as well as to identifying what conservation efforts will be most useful in preventing or reversing population declines.

5.1. Combining ecological frameworks to better predict vulnerability

Environmental change scales across space and time such that as stressors increase in spatial scale, so do they increase in temporal scale (Delcourt & Delcourt 1983). In addition, we have learned that many stressors caused by human activities are affecting larger and longer scales than previously understood (Delcourt & Delcourt 1983, Winkler et al. 2021), Consequently, in this thesis I show how three anthropogenic stressors impacting wildlife populations, climate change, habitat degradation, and direct mortality, scale spatiotemporally (Figure 5-1) and intersect with different levels of biological organization (Figure 5-2). Nested within this framework I suggest that although stressors scale with space and time, their impact

acts on individuals, which in aggregate determine population-scale dynamics, and range-wide changes (Figure 5-2).

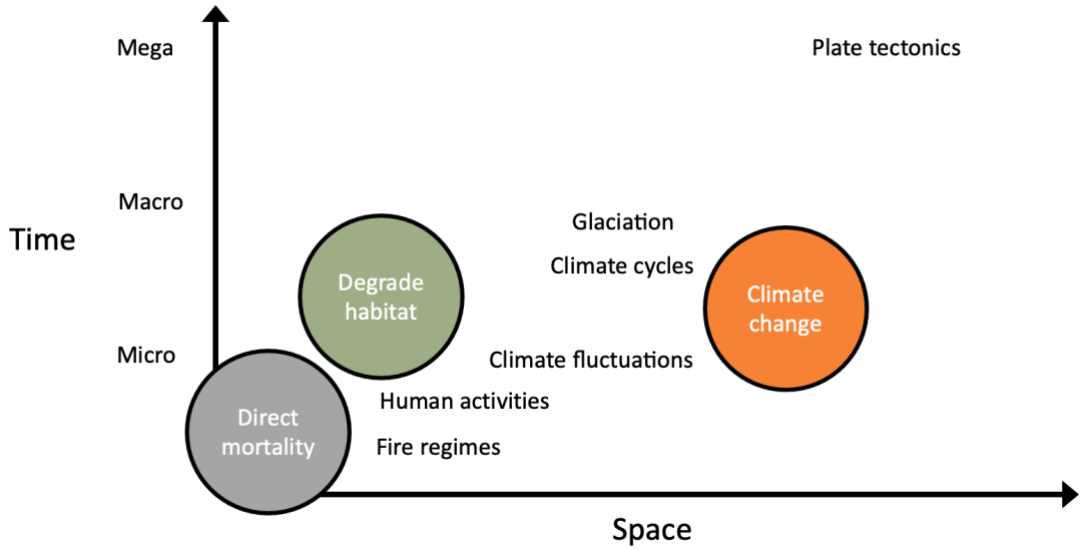

Figure 5-1 Three human impacts (climate change, habitat degradation, and direct mortality of wildlife) positioned within a spatiotemporal schematic of environmental change. Modified from Delecourt et al. 1983.

However, a central challenge of contemporary conservation lies in grappling with the accelerating nature of environmental change, the multiple scales at which change impacts populations, species, communities, and ecosystems, and how we best inform conservation decisions using imperfect data (Bawa 2006, Meffe 2006, Williams et al. 2020). A useful framework I have applied in each chapter defines vulnerability as the product of individual-level sensitivity, often dictated by physiology or behaviour, and environmental exposure to a specific stressor (Williams et al. 2008, Figure 5-2). This simple framework allows for the explicit consideration of the spatiotemporal nature of environmental change by scaling from the level of individuals to higher levels of biological organization (populations, species ranges). In this thesis, I have quantified the sensitivity of amphibian populations to specific stressors, the level of exposure to each based on current and predicted future environments in order to predict current and future vulnerability (Figure 5-2). For example, by assessing individual thermal performance of *A. truei* larvae, I can make conclusions about thermal sensitivity of *A. truei* populations to multiple stressors that each degrade thermal habitats including river diversion hydropower operations and climate change. An additional benefit of this framework is that conclusions on thermal vulnerability can be updated as conditions for populations, regions, or the species change through space and time. Furthermore, by assessing the exposure to

mortality that juvenile and adult *R. aurora* face from a highway that bisects an important migration corridor, I was able to predict the vulnerabilty of *R. aurora* populations to increased mortality in these important life stages and make conclusions not only on the vulnerability of populations to road mortality, but also the efficacy of existing conservation efforts.

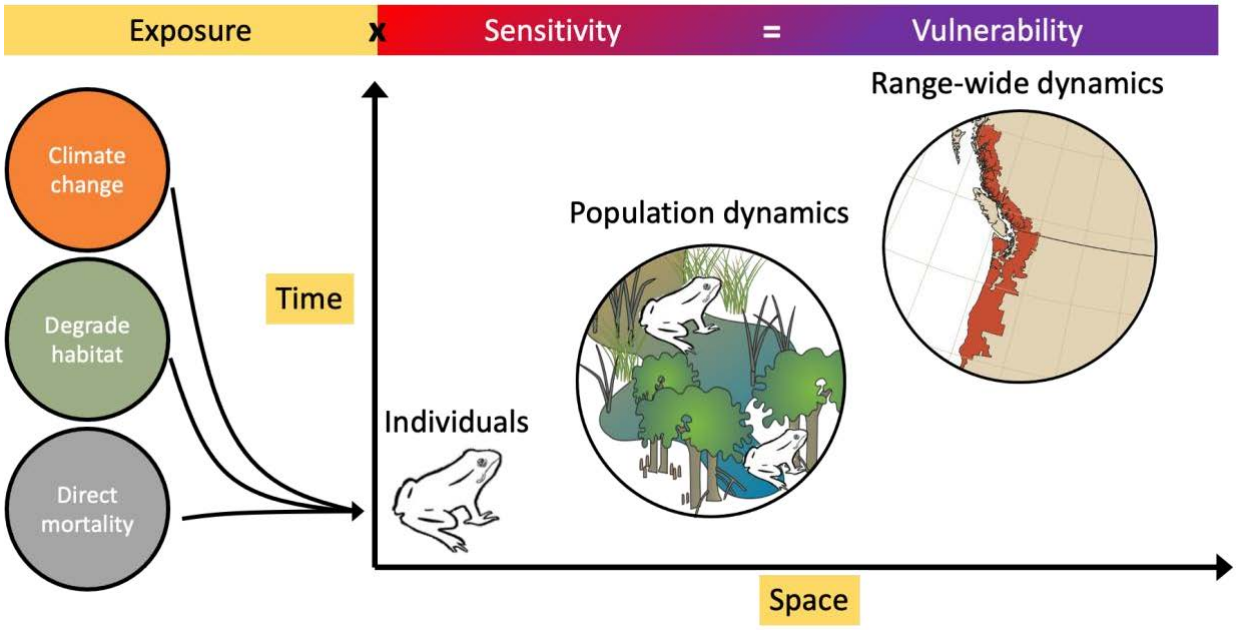

Figure 5-2 **Conceptual framework for the thesis including exposure to human stressors across space and time and across level of biological organization using scale-independent sensitivity (measured for individuals or populations) to make predictions of vulnerability at larger spatiotemporal scales (populations, species). Human stressors, such as climate change, habitat degradation, and direct mortality of wildlife, which range from small to large spatiotemporal scales (see Figure 5-1) act on individuals (e.g. physiological stress, direct mortality) and scale up to changes in population and potentially range-wide dynamics.**

5.2. Concluding remarks

It is my hope that in this thesis I provide support for the importance of assessing wildlife populations in ways that can be used to understand vulnerability to human stressors across space, time, and levels of biological organization. Furthermore, the tools and data used to accomplish such assessments can be easily updated as stressors change in magnitude, and though we are often limited by data, comparisons between snapshots in time can offer important insights into possible futures beyond what we can model. In Ted Chaing's "Story of Your Life" (2002), the character Louise learns to perceive past and future all at once from the visiting

Heptapod alien's teleological view of the universe. And while the goal of much of the conservation research of the past decades has been to understand what is to come, to predict the future, it is my hope that, unlike Louise and the Heptapods who must realize and perform the future, our quest for knowledge of what's to come allows us to change the future for the better.

References

Chapter 1

Angilletta, M. J. 2009. Thermal Adaptation: A Theoretical and Empirical Synthesis. Oxford University Press.

Antwi, E. K., J. Boakye-Danquah, W. Owusu-Banahene, K. Webster, A. Dabros, P. Wiebe, S. J. Mayor, A. Westwood, N. Mansuy, M. D. Setiawati, P. T. Yohuno (Apronti), K. Bill, A. Kwaku, S. Kosuta, and A. K. Sarfo. 2022. A Global review of cumulative effects assessments of disturbances on forest ecosystems. Journal of Environmental Management 317:115277.

Armstrong, C. G., J. Miller, A. McAlvay, P. M. Ritchie, and D. Lepofsky. 2021. Historical Indigenous Land-Use Explains Plant Functional Trait Diversity. Ecology and Society 26.

Bennett, E. M., P. Morrison, J. M. Holzer, K. J. Winkler, E. D. G. Fraser, S. J. Green, B. E. Robinson, K. Sherren, J. Botzas-Coluni, and W. Palen. 2021. Facing the challenges of using place-based social-ecological research to support ecosystem service governance at multiple scales. Ecosystems and People 17:574–589.

Braje, T. J., and J. M. Erlandson. 2013. Human acceleration of animal and plant extinctions: A Late Pleistocene, Holocene, and Anthropocene continuum. Anthropocene 4:14–23.

Buxton, R. T., E. A. Nyboer, K. E. Pigeon, G. D. Raby, T. Rytwinski, A. J. Gallagher, R. Schuster, H.-Y. Lin, L. Fahrig, J. R. Bennett, S. J. Cooke, and D. G. Roche. 2021. Avoiding wasted research resources in conservation science. Conservation Science and Practice 3:e329.

Campbell Grant, E. H., D. A. W. Miller, and E. Muths. 2020. A Synthesis of Evidence of Drivers of Amphibian Declines. Herpetologica 76:101–107.

Chown, S. L. 2012. Trait-based approaches to conservation physiology: forecasting environmental change risks from the bottom up. Philosophical Transactions of the Royal Society B: Biological Sciences 367:1615–1627.

Dahlke, F. T., S. Wohlrab, M. Butzin, and H.-O. Pörtner. 2020. Thermal bottlenecks in the life cycle define climate vulnerability of fish. Science 369:65–70.

Darimont, C. T., P. C. Paquet, A. Treves, K. A. Artelle, and G. Chapron. 2018. Political populations of large carnivores. Conservation Biology 32:747–749.

Deutsch, C. A., J. J. Tewksbury, R. B. Huey, K. S. Sheldon, C. K. Ghalambor, D. C. Haak, and P. R. Martin. 2008. Impacts of climate warming on terrestrial ectotherms across latitude. Proceedings of the National Academy of Sciences 105:6668–6672.

Echols, A., A. Front, and J. Cummins. 2019. Broadening conservation funding. Wildlife Society Bulletin 43:372–381.

Fletcher, R. 2020, September 28. Neoliberal Conservation. https://oxfordre.com/anthropology/display/10.1093/acrefore/9780190854584.001.0001/acrefore-9780190854584-e-300.

García-Barón, I., S. Giakoumi, M. B. Santos, I. Granado, and M. Louzao. 2021. The value of time-series data for conservation planning. Journal of Applied Ecology 58:608–619.

González-Tokman, D., A. Córdoba-Aguilar, W. Dáttilo, A. Lira-Noriega, R. A. Sánchez-Guillén, and F. Villalobos. 2020. Insect responses to heat: physiological mechanisms, evolution and ecological implications in a warming world. Biological Reviews 95:802–821.

Government of Canada, S. C. 2018, June 5. Government spending on environmental protection in Canada 2008 to 2016. https://www150.statcan.gc.ca/n1/pub/16-508-x/16-508-x2018002-eng.htm.

Hemery, G. 2014. In retrospect: Sylva. Nature 507:166–167.

Hoffman, K. M., E. L. Davis, S. B. Wickham, K. Schang, A. Johnson, T. Larking, P. N. Lauriault, N. Quynh Le, E. Swerdfager, and A. J. Trant. 2021. Conservation of Earth's biodiversity is embedded in Indigenous fire stewardship. Proceedings of the National Academy of Sciences 118:e2105073118.

Ma, G., A. A. Hoffmann, and C.-S. Ma. 2015. Daily temperature extremes play an important role in predicting thermal effects. Journal of Experimental Biology:jeb.122127.

Magurran, A. E., S. R. Baillie, S. T. Buckland, J. McP. Dick, D. A. Elston, E. M. Scott, R. I. Smith, P. J. Somerfield, and A. D. Watt. 2010. Long-term datasets in biodiversity research and monitoring: assessing change in ecological communities through time. Trends in Ecology & Evolution 25:574–582.

Meltzer, D. J. 2020. Overkill, glacial history, and the extinction of North America's Ice Age megafauna. Proceedings of the National Academy of Sciences 117:28555–28563.

Merow, C., J. P. Dahlgren, C. J. E. Metcalf, D. Z. Childs, M. E. K. Evans, E. Jongejans, S. Record, M. Rees, R. Salguero-Gómez, and S. M. McMahon. 2014. Advancing population ecology with integral projection models: a practical guide. Methods in Ecology and Evolution 5:99–110.

Pickett, S. T. A., V. T. Parker, and P. L. Fiedler. 1992. The New Paradigm in Ecology: Implications for Conservation Biology Above the Species Level. Pages 65–88 *in* P. L. Fiedler and S. K. Jain, editors. Conservation Biology: The Theory and Practice of Nature Conservation Preservation and Management. Springer US, Boston, MA.

Régnière, J., J. Powell, B. Bentz, and V. Nealis. 2012. Effects of temperature on development, survival and reproduction of insects: Experimental design, data analysis and modeling. Journal of Insect Physiology 58:634–647.

Simmons, B. I., P. S. A. Blyth, J. L. Blanchard, T. Clegg, E. Delmas, A. Garnier, C. A. Griffiths, U. Jacob, F. Pennekamp, O. L. Petchey, T. Poisot, T. J. Webb, and A. P. Beckerman. 2021. Refocusing multiple stressor research around the targets and scales of ecological impacts. Nature Ecology & Evolution 5:1478–1489.

Stuart, S. N., J. S. Chanson, N. A. Cox, B. E. Young, A. S. L. Rodrigues, D. L. Fischman, and R. W. Waller. 2004. Status and Trends of Amphibian Declines and Extinctions Worldwide. Science 306:1783–1786.

Taylor, E. N., L. M. Diele-Viegas, E. J. Gangloff, J. M. Hall, B. Halpern, M. D. Massey, D. Rödder, N. Rollinson, S. Spears, B. Sun, and R. S. Telemeco. 2021. The thermal ecology and physiology of reptiles and amphibians: A user's guide. Journal of Experimental Zoology Part A: Ecological and Integrative Physiology 335:13–44.

Thornton, R. 2005. Native American Demographic and Tribal Survival into the Twenty-first Century. American Studies 46:23–38.

Tuff, K.T., Tuff, T., and Davies, K.F. 2016. A framework for integrating thermal biology into fragmentation research. Ecology Letters. 19: 361 - 374.

Turner, M. G., W. J. Calder, G. S. Cumming, T. P. Hughes, A. Jentsch, S. L. LaDeau, T. M. Lenton, B. N. Shuman, M. R. Turetsky, Z. Ratajczak, J. W. Williams, A. P. Williams, and S. R. Carpenter. 2020. Climate change, ecosystems and abrupt change: science priorities. Philosophical Transactions of the Royal Society B: Biological Sciences 375:20190105.

Villellas, J., D. F. Doak, M. B. García, and W. F. Morris. 2015. Demographic compensation among populations: what is it, how does it arise and what are its implications? Ecology Letters 18:1139–1152.

Westwood, A. R., M. Olszynski, C. H. Fox, A. T. Ford, A. L. Jacob, J. W. Moore, and W. J. Palen. 2019a. The Role of Science in Contemporary Canadian Environmental Decision Making: The Example of Environmental Assessment. U.B.C. Law Review 52:243.

Westwood, A. R., S. P. Otto, A. Mooers, C. Darimont, K. E. Hodges, C. Johnson, B. M. Starzomski, C. Burton, K. M. A. Chan, M. Festa-Bianchet, S. Fluker, S. Gulati, A. L. Jacob, D. Kraus, T. G. Martin, W. J. Palen, J. D. Reynolds, and J. Whitton. 2019b. Protecting biodiversity in British Columbia: Recommendations for developing species at risk legislation. FACETS 4:136–160.

Wikelski, M., and S. J. Cooke. 2006. Conservation physiology. Trends in Ecology & Evolution 21:38–46.

Wright, A. D., R. F. Bernard, B. A. Mosher, K. M. O'Donnell, T. Braunagel, G. V. DiRenzo, J. Fleming, C. Shafer, A. B. Brand, E. F. Zipkin, and E. H. Campbell Grant. 2020. Moving from decision to action in conservation science. Biological Conservation 249:108698.

Chapter 2

Abbasi T. & Abbasi S.A. (2011) Small hydro and the environmental implications of its extensive utilization. Renewable and sustainable energy reviews, 15, 2134–2143.

Anderson E.P, Freeman M.C, & Pringle C.M. (2006) Ecological consequences of hydropower development in Central America: impacts of small dams and water diversion on neotropical stream fish assemblages. River Research and Applications, 22, 397–411.

Andrews R.M. & Schwarzkopf L. (2012) Thermal performance of squamate embryos with respect to climate, adult life history, and phylogeny. Biological Journal of the Linnean Society, 106, 851–864.

Angilletta M.J. Jr, Niewiarowski P.H, & Navas C.A. (2002) The evolution of thermal physiology in ectotherms. Journal of Thermal Biology, 27, 249–268.

Barnett T.P, Adam J.C, & Lettenmaier D.P. (2005) Potential impacts of a warming climate on water availability in snow-dominated regions. Nature, 438, 303–309.

Barnett T.P, Pierce D.W, Hidalgo H.G, Bonfils C, Santer B.D, Das T, Bala G, Wood A.W, Nozawa T, Mirin A.A, Cayan D.R, & Dettinger M.D. (2008) Human-Induced Changes in the Hydrology of the Western United States. Science, 319, 1080–1083.

Brown H.A. (1975) Temperature and development of the tailed frog, *Ascaphus truei*. Comparative Biochemistry and Physiology Part A: Physiology, 50, 397–405.

Caissie D. (2006) The thermal regime of rivers: a review. Freshwater Biology. 51: 1389-1406.

Cole E. & Newton M. (2013) Influence of streamside buffers on stream temperature response following clear-cut harvesting in western Oregon. Canadian Journal of Forest Research, 43, 993–1005.

Connors, M B, Marmorek D.R, Olson E, Hall A.W, la Cueva Bueno de P, Bensen A, Bryan K, Perrin C, Parkinson E, Abraham D, Alexander C, Murray C, Smith R, Grieg L, & Farrell G. (2014) Independent Review of Run-of-River Hydroelectric Projects and their Impacts on Salmonid Species in British Columbia.

Cooke S.J, Sack L, Franklin C.E, Farrell A.P, Beardall J, Wikelski M, & Chown S.L. (2013) What is conservation physiology? Perspectives on an increasingly integrated and essential science. Conservation Physiology. 1: 1-23.

COSWEWIC (2011). Assessment and status report on the Coastal Tailed Frog *Ascaphus truei* in Canada. xii–53.Carroll, Carol. (1999, July). Curating Curious Collections: An Interdisciplinary Perspective. *Predatory Publishing Quarterly, 16* (5)*,* 3-134.

Daugherty C.H. & Sheldon A.L. (1982) Age-determination, growth, and life history of a Montana population of the tailed frog (*Ascaphus truei*). Herpetologica.38: 461-468.

de Vlaming V.L. & Bury R.B. (1970) Thermal selection in tadpoles of the tailed-frog, *Ascaphus truei*. Journal of Herpetology. 4: 179-189.

Deutsch C.A, Tewksbury J.J, Huey R.B, Sheldon K.S, Ghalambor C.K, Haak D.C, & Martin P.R. (2008) Impacts of climate warming on terrestrial ectotherms across latitude. Proceedings of the National Academy of Sciences, 105, 6668–6672.

Dewson Z.S, James A.B.W, & Death R.G. (2007) A review of the consequences of decreased flow for instream habitat and macroinvertebrates. Journal of the North American Benthological Society, 26, 401–415.

Duarte H, Tejedo M, Katzenberger M, Marangoni F, Baldo D, Beltrán J.F, Martí D.A, Richter-Boix A, & Gonzalez-Voyer A. (2011) Can amphibians take the heat? Vulnerability to climate warming in subtropical and temperate larval amphibian communities. Global Change Biology, 18, 412–421.

Elsner M.M, Cuo L, Voisin N, Deems J.S, Hamlet A.F, Vano J.A, Mickelson K.E.B, Lee S.-Y, & Lettenmaier D.P. (2010) Implications of 21st century climate change for the hydrology of Washington State. Climatic Change, 102, 225–260.

Estay S.A, Clavijo-Baquet S, Lima M, & Bozinovic F. (2010) Beyond average: an experimental test of temperature variability on the population dynamics of Tribolium confusum. Population ecology, 53, 53–58.

Fry F. & Hart J.S. (1948) Cruising speed of goldfish in relation to water temperature. Journal of the Fisheries Board of Canada, 7b, 169–175.

Fuller T.K, Venditti J.G, Nelson P.A, Popescu V, & Palen W. (2014) Modeling Changes in Bed Surface Texture and Aquatic Habitat Caused by Run-of-River Hydropower Development. AGU Fall Meeting Abstracts.

Gallagher A.J, Hammerschlag N, Cooke S.J, Costa D.P, & Irschick D.J. (2015) Evolutionary theory as a tool for predicting extinction risk. Trends in Ecology & Evolution, 30, 61–65.

Gerick A.A, Munshaw R.G, palen W.J, Combes S.A, & O'Regan S.M. (2014) Thermal physiology and species distribution models reveal climate vulnerability of temperate amphibians. Journal of Biogeography, 41, 713–723.

Gibeau, P., B. M. Connors, and W. J. Palen. 2017. Run-of-River hydropower and salmonids: potential effects and perspective on future research. Canadian Journal of Fisheries and Aquatic Sciences 74:1135–1149.

Gibeau, P., and W. J. Palen. 2020. Predicted effects of flow diversion by Run-of-River hydropower on bypassed stream temperature and bioenergetics of salmonid fishes. River Research and Applications 36:1903–1915.

Gibeau, P., and W. J. Palen. 2021. Impacts of run-of-river hydropower on coho salmon (Oncorhynchus kisutch): the role of density-dependent survival. Ecosphere 12:e03684.

Gilchrist G.W. (1995) Specialists and generalists in changing environments. I. Fitness landscapes of thermal sensitivity. American Naturalist. 146: 252-270.

Gosner K.L. (1960) A simplified table for staging anuran embryos and larvae with notes on identification. Herpetologica. 16: 183–190.

Gray J. & Edington J.M. (1969) Effect of woodland clearance on stream temperature. Journal of the Fisheries Research Board of Canada. 26: 399-403.

Guitiérrez-Pesquera L.M. & Tejedo M. (2016) Testing the climate variability hypothesis in thermal tolerance limits of tropical and temperate tadpoles. Journal of Biogeography. 43: 1166-1178.

Hamlet A.F, Mote P.W, Clark M.P, & Lettenmaier D.P. (2005) Effects of Temperature and Precipitation Variability on Snowpack Trends in the Western United States*. dx.doi.org.proxy.lib.sfu.ca, 18, 4545–4561.

Hamlet A.F, Mote P.W, Clark M.P, & Lettenmaier D.P. (2007) Twentieth-Century Trends in Runoff, Evapotranspiration, and Soil Moisture in the Western United States*. dx.doi.org.proxy.lib.sfu.ca, 20, 1468–1486.

Hatfield T, Lewis A, Ohlson D, & Bradford M. (2003) Development of instream flow thresholds as guidelines for reviewing proposed water uses .British Columbia Ministry of Sustainable Resource Management, Victoria, BC.

Hedrick T.L. (2008) Software techniques for two-and three-dimensional kinematic measurements of biological and biomimetic systems. Bioinspiration & Biomimetics. doi: 10.1088/1748-3182/3/3/034001

Hossack B.R, Lowe W.H, Webb M.A.H, Talbott M.J, Kappenman K.M, & Corn P.S. (2013) Population-level thermal performance of a cold-water ectotherm is linked to ontogeny and local environmental heterogeneity. Freshwater Biology. 58: 2215-2225.

Huey R.B. & Kingsolver J.G. (1989) Evolution of thermal sensitivity of ectotherm performance. Trends in Ecology & Evolution, 4, 131–135.

Huey R.B. & Stevenson R.D. (1979) Integrating thermal physiology and ecology of ectotherms: a discussion of approaches. American Zoologist, 19, 357–366.

(2009) Why tropical forest lizards are vulnerable to climate warming. Proceedings of the Royal Society B: Biological Sciences, 276, 1939–1948.

Hunter M.A. (1992) Hydropower flow fluctuations and salmonids: a review of the biological effects, mechanical causes, and options for mitigation. 1–58.

Isaak D.J, Young M.K, Luce C.H, Hostetler S.W, Wenger S.J, Peterson E.E, Ver Hoef J.M, Groce M.C, Horan D.L, & Nagel D.E. (2016) Slow climate velocities of mountain streams portend their role as refugia for cold-water biodiversity. Proceedings of the National Academy of Sciences of the United States of America, 113, 4374–4379.

Jackson R.B, Carpenter S.R, & Dahm C.N. (2001) Water in a changing world. Ecological Applications. 11: 1027-1045.

Janzen D.H. (1967) Why mountain passes are higher in the tropics. The American Naturalist. 101: 233-249.

Johnson S.L. & Jones J.A. (2000) Stream temperature responses to forest harvest and debris flows in western Cascades, Oregon. Canadian Journal of Fisheries and Aquatic Sciences, 57, 30–39.

Köhler A, Sadowska J, Olszewska J, Trzeciak P, Berger-Tal O, & Tracy C.R. (2011) Staying warm or moist? Operative temperature and thermal preferences of common frogs (Rana temporaria), and effects on locomotion. The Herpetological Journal. 21:17-26.

Levins R. (1968) Evolution in changing environments: some theoretical explorations. Princeton University Press.

Lewis A, Hatfield T, Chilibeck B, & Roberts C. (2004) Assessment Methods for Aquatic Habitat and Instream Flow Characteristics in Support of Applications to Dam, Divert or Extract Water from Streams in British Columbia.

Lynch M. & Gabriel W. (1987) Environmental tolerance. American Naturalist. 129: 283-303.

Martin T.L. & Huey R.B. (2008) Why “Suboptimal” Is Optimal: Jensen’s Inequality and Ectotherm Thermal Preferences. The American Naturalist, 171, E102–E118.

Moore R.D. & Spittlehouse D.L. (2005) Riparian Microclimate and Stream Temperature Response to Forest Harvesting: A Review. Journal of the American Water Resources Association. 4: 813-834.

Mote P.W, Hamlet A.F, & Clark M.P. (2005) Declining mountain snowpack in western North America. Bulletin of the American Meteorological Society. 39: 39-46.

Poff N, Allan J.D, Bain M.B, Karr J.R, & Prestegaard K.L. (1997) The natural flow regime. BioScience. 47: 769-784.

Poff N.L. & Hart D.D. (2002) How Dams Vary and Why It Matters for the Emerging Science of Dam Removal. BioScience, 52, 659–668.

Poff N.L. & Ward J.V. (1989) Implications of streamflow variability and predictability for lotic community structure: a regional analysis of streamflow patterns. Canadian Journal of Fisheries and Aquatic Sciences. 45: 1805-1818.

Poole G.C. & Berman C.H. (2001) An Ecological Perspective on In-Stream Temperature: Natural Heat Dynamics and Mechanisms of Human-Caused Thermal Degradation. Environmental Management, 27, 787–802.

Schnorbus M, Werner A, & Bennett K. (2014) Impacts of climate change in three hydrologic regimes in British Columbia, Canada. Hydrological Processes. 28: 1170-1189.

Schulte P.M, Healy T.M, & Fangue N.A. (2011) Thermal Performance Curves, Phenotypic Plasticity, and the Time Scales of Temperature Exposure. American Zoologist, 51, 691–702.

Sinervo B, Méndez-de-la-Cruz F, Miles D.B, Heulin B, Bastiaans E, Cruz M.V.-S, Lara-Resendiz R, Martínez-Méndez N, Calderón-Espinosa M.L, Meza-Lázaro R.N, Gadsden H, Avila L.J, Morando M, la Riva De I.J, Sepulveda P.V, Rocha C.F.D, Ibargüengoytía N, Puntriano C.A, Massot M, Lepetz V, Oksanen T.A, Chapple D.G, Bauer A.M, Branch W.R, Clobert J, & Sites J.W. (2010) Erosion of Lizard Diversity by Climate Change and Altered Thermal Niches. Science, 328, 894–899.

Sinokrot B.A. & Stefan H.G. (1993) Stream temperature dynamics: measurements and modeling. Water Resources Research. 29: 2299-2312.

Stewart I.T, Cayan D.R, Dettinger M.D, & Stewart I.T. (2005) Changes toward Earlier Streamflow Timing across Western North America. dx.doi.org.proxy.lib.sfu.ca, 18, 1136–1155.

Stocker T.F, Qin D, Plattner G.K, Tignor M, & Allen S.K. (2013) Climate change 2013: the physical science basis. Contribution of working group I to the fifth assessment report of the intergovernmental panel on climate change.

van Vliet M.T.H, Franssen W.H.P, Yearsley J.R, Ludwig F, Haddeland I, Lettenmaier D.P, & Kabat P. (2013) Global river discharge and water temperature under climate change. Global Environmental Change, 23, 450–464.

Vugts H.F. (1974) Calculation of temperature variations of small mountain streams. Journal of Hydrology. 23: 267-278.

Watkins T.B. (1996) Predator-mediated selection on burst swimming performance in tadpoles of the Pacific tree frog, Pseudacris regilla. Physiological Zoology. 69: 154-167.

Wikelski M. & Cooke S.J. (2006) Conservation physiology. Trends in Ecology & Evolution, 21, 38–46.

Wohl E. (2006) Human impacts to mountain streams. Geomorphology, 79, 217–248.

Yin, X., J. Goudriaan, E. A. Lantinga, J. Vos, and H. J. Spiertz. 2003. A flexible sigmoid function of determinate growth. Annals of Botany 91:361–371.

Zuur A.F, Ieno E.N, Walker N.J, Saveliev A.A, & Smith G.M. (2009) Mixed effects models and extensions in ecology with R. Gail M, Krickeberg K, Samet JM, Tsiatis A, Wong W, editors. New York

Chapter 3

Addo-Bediako, A., S. L. Chown, and K. J. Gaston. 2000. Thermal tolerance, climatic variability and latitude. Proceedings of the Royal Society of London. Series B: Biological Sciences 267:739–745.

Ames, E. M., M. R. Gade, C. L. Nieman, J. R. Wright, C. M. Tonra, C. M. Marroquin, A. M. Tutterow, and S. M. Gray. 2020. Striving for population-level conservation: integrating physiology across the biological hierarchy. Conservation Physiology 8.

Angert, A. L., S. N. Sheth, and J. R. Paul. 2011. Incorporating Population-Level Variation in Thermal Performance into Predictions of Geographic Range Shifts. Integrative and Comparative Biology 51:733–750.

Angilletta, M. J. 2006. Estimating and comparing thermal performance curves. Journal of Thermal Biology 31:541–545.

Angilletta, M. J. 2009. Thermal Adaptation: A Theoretical and Empirical Synthesis. Oxford University Press.

Angilletta, M. J., P. H. Niewiarowski, and C. A. Navas. 2002. The evolution of thermal physiology in ectotherms. Journal of Thermal Biology 27:249–268.

Bates, D., M. Mächler, B. Bolker, and S. Walker. 2015. Fitting Linear Mixed-Effects Models Using **lme4**. Journal of Statistical Software 67.

Bennett, J. M., J. Sunday, P. Calosi, F. Villalobos, B. Martínez, R. Molina-Venegas, M. B. Araújo, A. C. Algar, S. Clusella-Trullas, B. A. Hawkins, S. A. Keith, I. Kühn, C. Rahbek, L. Rodríguez, A. Singer, I. Morales-Castilla, and M. Á. Olalla-Tárraga. 2021. The evolution of critical thermal limits of life on Earth. Nature Communications 12:1198.

van Berkum, F. H. 1988. Latitudinal Patterns of the Thermal Sensitivity of Sprint Speed in Lizards. The American Naturalist 132:327–343.

Bolker, B., and R. D. C. Team. 2017. bbmle: Tools for General Maximum Likelihood Estimation.

Bozinovic, F., M. J. M. Orellana, S. I. Martel, and J. M. Bogdanovich. 2014. Testing the heat-invariant and cold-variability tolerance hypotheses across geographic gradients. Comparative Biochemistry and Physiology Part A: Molecular & Integrative Physiology 178:46–50.

Brattstrom, B. H. 1965. Body Temperatures of Reptiles. The American Midland Naturalist 73:376–422.

Brattstrom, B. H. 1968. Thermal acclimation in Anuran amphibians as a function of latitude and altitude. Comparative Biochemistry and Physiology 24:93–111.

Brown, H. A. 1975. Temperature and development of the tailed frog, *Ascaphus truei*. Comparative Biochemistry and Physiology Part A: Physiology 50:397–405.

Buckley, L. B., J. C. Ehrenberger, and M. J. Angilletta. 2015a. Thermoregulatory behaviour limits local adaptation of thermal niches and confers sensitivity to climate change. Functional Ecology 29:1038–1047.

Buckley, L. B., and R. B. Huey. 2016. How Extreme Temperatures Impact Organisms and the Evolution of their Thermal Tolerance. Integrative and Comparative Biology 56:98–109.

Buckley, L. B., C. R. Nufio, E. M. Kirk, and J. G. Kingsolver. 2015b. Elevational differences in developmental plasticity determine phenological responses of grasshoppers to recent climate warming. Proceedings of the Royal Society B: Biological Sciences 282:20150441.

Burnham, K. P., and D. R. Anderson, editors. 2004. Model Selection and Multimodel Inference. Springer New York, New York, NY.

Carbonell, J. A., and R. Stoks. 2020. Thermal evolution of life history and heat tolerance during range expansions toward warmer and cooler regions. Ecology 101:e03134.

Chisholm, S. P. 2022. SATELLITE REMOTE SENSING FOR THE ASSESMENT OF PROTECTED AREAS: A GLOBAL APPLICATION.

Christian, K. A., and C. R. Tracy. 1981. The Effect of the Thermal Environment on the Ability of Hatchling Galapagos Land Iguanas to Avoid Predation during Dispersal. Oecologia 49:218–223.

Clusella-Trullas, S., T. M. Blackburn, and S. L. Chown. 2011. Climatic Predictors of Temperature Performance Curve Parameters in Ectotherms Imply Complex Responses to Climate Change. The American Naturalist 177:738–751.

Coristine, L. E., and J. T. Kerr. 2011. Habitat loss, climate change, and emerging conservation challenges in Canada [1] This review is part of the virtual symposium “Flagship Species – Flagship Problems” that deals with ecology, biodiversity and management issues, and climate impacts on species at risk and of Canadian importance, including the polar bear (*Ursus maritimus*), Atlantic cod (*Gadus morhua*), Piping Plover (*Charadrius melodus*), and caribou (*Rangifer tarandus*). Canadian Journal of Zoology 89:435–451.

Coristine, L. E., and J. T. Kerr. 2015. Temperature-related geographical shifts among passerines: contrasting processes along poleward and equatorward range margins. Ecology and Evolution 5:5162–5176.

COSEWIC. 2012. COSEWIC assessment and status report on the coastal tailed frog, *Ascaphus truei*, in Canada. Committee on the Status of Endangered Wildlife in Canada, Ottawa.

Dallas, H. F., and N. A. Rivers-Moore. 2012. Critical Thermal Maxima of aquatic macroinvertebrates: towards identifying bioindicators of thermal alteration. Hydrobiologia 679:61–76.

Daugherty, C. H., and A. L. Sheldon. 1982. Age-Determination, Growth, and Life History of a Montana Population of the Tailed Frog (*Ascaphus truei*). Herpetologica 38:461–468.

Deutsch, C. A., J. J. Tewksbury, R. B. Huey, K. S. Sheldon, C. K. Ghalambor, D. C. Haak, and P. R. Martin. 2008. Impacts of climate warming on terrestrial ectotherms across latitude. Proceedings of the National Academy of Sciences 105:6668–6672.

Dillon, M. E., G. Wang, and R. B. Huey. 2010. Global metabolic impacts of recent climate warming. Nature 467:704–706.

Dupuis, L., and D. Steventon. 1999. Riparian management and the tailed frog in northern coastal forests. Forest Ecology and Management 124:35–43.

Feder, M. E. 1978. Environmental Variability and Thermal Acclimation in Neotropical and Temperate Zone Salamanders. Physiological Zoology 51:7–16.

Frazier, M. R., R. B. Huey, and D. Berrigan. 2006. Thermodynamics Constrains the Evolution of Insect Population Growth Rates: “Warmer Is Better.” The American Naturalist 168:512–520.

Gaitan-Espitia, J. D., L. D. Bacigalupe, T. Opitz, N. A. Lagos, T. Timmermann, and M. A. Lardies. 2014. Geographic variation in thermal physiological performance of the intertidal crab Petrolisthes violaceus along a latitudinal gradient. Journal of Experimental Biology 217:4379–4386.

Gerick, A. A., R. G. Munshaw, W. J. Palen, S. A. Combes, and S. M. O’Regan. 2014. Thermal physiology and species distribution models reveal climate vulnerability of temperate amphibians. Journal of Biogeography 41:713–723.

Ghalambor, C. K. 2006. Are mountain passes higher in the tropics? janzen's hypothesis revisited. Integrative and Comparative Biology 46:5–17.

Gosner, K. L. 1960. A Simplified Table for Staging Anuran Embryos and Larvae with Notes on Identification. Herpetologica 16:183–190.

Greenberg, D. A., and W. J. Palen. 2021. Hydrothermal physiology and climate vulnerability in amphibians. Proceedings of the Royal Society B: Biological Sciences 288:20202273.

Gutiérrez-Pesquera, L. M., M. Tejedo, M. Á. Olalla-Tárraga, H. Duarte, A. Nicieza, and M. Solé. 2016. Testing the climate variability hypothesis in thermal tolerance limits of tropical and temperate tadpoles. Journal of Biogeography 43:1166–1178.

Higgins, J. K., H. J. MacLean, L. B. Buckley, and J. G. Kingsolver. 2014. Geographic differences and microevolutionary changes in thermal sensitivity of butterfly larvae in response to climate. Functional Ecology 28:982–989.

Hof, C., M. B. Araújo, W. Jetz, and C. Rahbek. 2011. Additive threats from pathogens, climate and land-use change for global amphibian diversity. Nature 480:516–519.

Hossack, B. R., W. H. Lowe, M. A. H. Webb, M. J. Talbott, K. M. Kappenman, and P. S. Corn. 2013. Population-level thermal performance of a cold-water ectotherm is linked to ontogeny and local environmental heterogeneity. Freshwater Biology 58:2215–2225.

Huey, R. B., C. A. Deutsch, J. J. Tewksbury, L. J. Vitt, P. E. Hertz, H. J. Álvarez Pérez, and T. Garland. 2009. Why tropical forest lizards are vulnerable to climate warming. Proceedings of the Royal Society B: Biological Sciences 276:1939–1948.

Huey, R. B., M. R. Kearney, A. Krockenberger, J. A. M. Holtum, M. Jess, and S. E. Williams. 2012. Predicting organismal vulnerability to climate warming: roles of behaviour, physiology and adaptation. Philosophical Transactions of the Royal Society B: Biological Sciences 367:1665–1679.

Huey, R. B., and J. G. Kingsolver. 1993. Evolution of Resistance to High Temperature in Ectotherms. The American Naturalist 142:S21–S46.

Isaak, D. J., M. K. Young, C. H. Luce, S. W. Hostetler, S. J. Wenger, E. E. Peterson, J. M. Ver Hoef, M. C. Groce, D. L. Horan, and D. E. Nagel. 2016. Slow climate velocities of mountain streams portend their role as refugia for cold-water biodiversity. Proceedings of the National Academy of Sciences 113:4374–4379.

Janzen, D. H. 1967. Why Mountain Passes are Higher in the Tropics. The American Naturalist 101:233–249.

Kingsolver, J. G., and L. B. Buckley. 2017. Quantifying thermal extremes and biological variation to predict evolutionary responses to changing climate. Philosophical Transactions of the Royal Society B: Biological Sciences 372:20160147.

Lee, T. M., and W. Jetz. 2008. Future battlegrounds for conservation under global change. Proceedings of the Royal Society B: Biological Sciences 275:1261–1270.

Leroux, S. J., and J. T. Kerr. 2013. Land Development in and around Protected Areas at the Wilderness Frontier. Conservation Biology 27:166–176.

Lertzman-Lepofsky, G. F., A. M. Kissel, B. Sinervo, and W. J. Palen. 2020. Water loss and temperature interact to compound amphibian vulnerability to climate change. Global Change Biology 26:4868–4879.

Lutterschmidt, W. I., and V. H. Hutchison. 1997. The critical thermal maximum: history and critique. Canadian Journal of Zoology 75:1561–1574.

Ma, G., A. A. Hoffmann, and C.-S. Ma. 2015. Daily temperature extremes play an important role in predicting thermal effects. Journal of Experimental Biology:jeb.122127.

Mitchell, W. A., and M. J. Angilletta. 2009. Thermal Games: Frequency-Dependent Models of Thermal Adaptation. Functional Ecology 23:510–520.

O'Regan, S. M., W. J. Palen, and S. C. Anderson. 2014. Climate warming mediates negative impacts of rapid pond drying for three amphibian species. Ecology 95:845–855.

Oregon Department of Fish and Wildlife. 2019. Sensitive Species List and Associated Frequently Asked Questions.

Payne, N. L., and J. A. Smith. 2017. An alternative explanation for global trends in thermal tolerance. Ecology Letters 20:70–77.

de Perez, E. C., M. van Aalst, K. Bischiniotis, S. Mason, H. Nissan, F. Pappenberger, E. Stephens, E. Zsoter, and B. van den Hurk. 2018. Global predictability of temperature extremes. Environmental Research Letters 13:054017.

Pinsky, M. L., A. M. Eikeset, D. J. McCauley, J. L. Payne, and J. M. Sunday. 2019. Greater vulnerability to warming of marine versus terrestrial ectotherms. Nature 569:108–111.

R Core Team. 2019. R: A Language and Environment for Statistical Computing. R Foundation for Statistical Computing, Vienna, Austria.

Riggio, J., J. E. M. Baillie, S. Brumby, E. Ellis, C. M. Kennedy, J. R. Oakleaf, A. Tait, T. Tepe, D. M. Theobald, O. Venter, J. E. M. Watson, and A. P. Jacobson. 2020. Global human influence maps reveal clear opportunities in conserving Earth's remaining intact terrestrial ecosystems. Global Change Biology 26:4344–4356.

Rohr, J. R., D. J. Civitello, J. M. Cohen, E. A. Roznik, B. Sinervo, and A. I. Dell. 2018. The complex drivers of thermal acclimation and breadth in ectotherms. Ecology Letters 21:1425–1439.

Rohr, J. R., and T. R. Raffel. 2010. Linking global climate and temperature variability to widespread amphibian declines putatively caused by disease. Proceedings of the National Academy of Sciences 107:8269–8274.

Shah, A. A., B. A. Gill, A. C. Encalada, A. S. Flecker, W. C. Funk, J. M. Guayasamin, B. C. Kondratieff, N. L. Poff, S. A. Thomas, K. R. Zamudio, and C. K. Ghalambor. 2018. Climate variability predicts thermal limits of aquatic insects across elevation and latitude. Functional Ecology:2118–2127.

Sinervo, B. 1990. Evolution of thermal physiology and growth rate between populations of the western fence lizard (Sceloporus occidentalis). Oecologia 83:228–237.

Sinervo, B., F. Mendez-de-la-Cruz, D. B. Miles, B. Heulin, E. Bastiaans, M. Villagran-Santa Cruz, R. Lara-Resendiz, N. Martinez-Mendez, M. L. Calderon-Espinosa, R. N. Meza-Lazaro, H. Gadsden, L. J. Avila, M. Morando, I. J. De la Riva, P. V. Sepulveda, C. F. D. Rocha, N. Ibarguengoytia, C. A. Puntriano, M. Massot, V. Lepetz, T. A. Oksanen, D. G. Chapple, A. M. Bauer, W. R. Branch, J. Clobert, and J. W. Sites. 2010. Erosion of Lizard Diversity by Climate Change and Altered Thermal Niches. Science 328:894–899.

Spicer, R., A. Herman, J. Yang, and T. Spicer. 2013. Why Future Climate Change is likely to be Underestimate: evidence from Palaeobotany. Journal of the Botanical Society of Bengal 67:75–88.

Stuecker, M. F., C. M. Bitz, K. C. Armour, C. Proistosescu, S. M. Kang, S.-P. Xie, D. Kim, S. McGregor, W. Zhang, S. Zhao, W. Cai, Y. Dong, and F.-F. Jin. 2018. Polar amplification dominated by local forcing and feedbacks. Nature Climate Change 8:1076–1081.

Sunday, J. M., A. E. Bates, and N. K. Dulvy. 2011. Global analysis of thermal tolerance and latitude in ectotherms. Proceedings of the Royal Society B: Biological Sciences 278:1823–1830.

Sunday, J. M., A. E. Bates, and N. K. Dulvy. 2012. Thermal tolerance and the global redistribution of animals. Nature Climate Change 2:686–690.

Sunday, J. M., A. E. Bates, M. R. Kearney, R. K. Colwell, N. K. Dulvy, J. T. Longino, and R. B. Huey. 2014. Thermal-safety margins and the necessity of thermoregulatory behavior across latitude and elevation. Proceedings of the National Academy of Sciences 111:5610–5615.

Sunday, J. M., G. T. Pecl, S. Frusher, A. J. Hobday, N. Hill, N. J. Holbrook, G. J. Edgar, R. Stuart-Smith, N. Barrett, T. Wernberg, R. A. Watson, D. A. Smale, E. A. Fulton, D. Slawinski, M. Feng, B. T. Radford, P. A. Thompson, and A. E. Bates. 2015. Species traits and climate velocity explain geographic range shifts in an ocean-warming hotspot. Ecology Letters 18:944–953.

Tewksbury, J. J., R. B. Huey, and C. A. Deutsch. 2008. ECOLOGY: Putting the Heat on Tropical Animals. Science 320:1296–1297.

Thompson, P. L., and A. Gonzalez. 2017. Dispersal governs the reorganization of ecological networks under environmental change. Nature Ecology & Evolution 1:1–8.

Thomson, R. C., A. N. Wright, H. B. Shaffer, B. Bolster, K. Cripe, S. J. Barry, R. N. Fisher, and H. H. Welsh. 2016. California Amphibian and Reptile Species of Special Concern. First edition. University of California Press.

Van Der Have, T. M. 2002. A proximate model for thermal tolerance in ectotherms. Oikos 98:141–155.

VanDerWal, J., H. T. Murphy, A. S. Kutt, G. C. Perkins, B. L. Bateman, J. J. Perry, and A. E. Reside. 2013. Focus on poleward shifts in species' distribution underestimates the fingerprint of climate change. Nature Climate Change 3:239–243.

Vasseur, D. A., J. P. DeLong, B. Gilbert, H. S. Greig, C. D. G. Harley, K. S. McCann, V. Savage, T. D. Tunney, and M. I. O'Connor. 2014. Increased temperature variation poses a greater risk to species than climate warming. Proceedings of the Royal Society B: Biological Sciences 281:20132612.

Vaughan, T. A., J. M. Ryan, and N. J. Czaplewski. 2013. Mammalogy. Jones & Bartlett Publishers.

de Vlaming, V. L., and R. B. Bury. 1970. Thermal Selection in Tadpoles of the Tailed-Frog, *Ascaphus truei*. Journal of Herpetology 4:179–189.

Wang, T., A. Hamann, D. Spittlehouse, and C. Carroll. 2016. Locally Downscaled and Spatially Customizable Climate Data for Historical and Future Periods for North America. PLOS ONE 11:e0156720.

Wiens, J. J. 2016. Climate-Related Local Extinctions Are Already Widespread among Plant and Animal Species. PLoS Biology 14.

Yin, X., J. Goudriaan, E. A. Lantinga, J. Vos, and H. J. Spiertz. 2003. A flexible sigmoid function of determinate growth. Annals of Botany 91:361–371.

Zhang, Y.-P., and X. Ji. 2004. The thermal dependence of food assimilation and locomotor performance in southern grass lizards, Takydromus sexlineatus (Lacertidae). Journal of Thermal Biology 29:45–53.

Chapter 4

Adams, M. J., C. A. Pearl, S. Galvan, and B. McCreary. 2011. Non-Native Species Impacts on Pond Occupancy by an Anuran. Journal of Wildlife Management 75:30–35.

Altwegg, R. 2003. Multistage density dependence in an amphibian. Oecologia 136:46–50.

Beasley, B. 2006. A STUDY ON THE INCIDENCE OF AMPHIBIAN ROAD MORTALITY BETWEEN UCLUELET AND TOFINO, BRITISH COLUMBIA. Wildlife Afield 1:1.

Beebee, T. J. C. 2013. Effects of Road Mortality and Mitigation Measures on Amphibian Populations. Conservation Biology 27:657–668.

Bender, D. J., T. A. Contreras, and L. Fahrig. 1998. Habitat Loss and Population Decline: A Meta-Analysis of the Patch Size Effect. Ecology 79:517–533.

Biek, R., W. C. Funk, B. A. Maxell, and L. S. Mills. 2002. What is Missing in Amphibian Decline Research: Insights from Ecological Sensitivity Analysis. Conservation Biology 16:728–734.

Blaustein, A., J. Beatty, D. Olson, and R. Storm. 1995. Biology of amphibians and reptiles in old-growth forests in the Pacific northwest. Forest Service general technical report.

Bond, A. R. F., and D. N. Jones. 2013. Roads and macropods: interactions and implications. Australian Mammalogy 36:1–14.

Boyle, S. P., M. G. Keevil, J. D. Litzgus, D. Tyerman, and D. Lesbarrères. 2021. Road-effect mitigation promotes connectivity and reduces mortality at the population-level. Biological Conservation 261:109230.

Carroll, C., R. F. Noss, and P. C. Paquet. 2001. Carnivores as Focal Species for Conservation Planning in the Rocky Mountain Region. Ecological Applications 11:961–980.

Caswell, H. 2010. Life Table Response Experiment Analysis of the Stochastic Growth Rate. Journal of Ecology 98:324–333.

Conan, A., J. Fleitz, L. Garnier, M. L. Brishoual, Y. Handrich, and J. Jumeau. 2022. Effectiveness of wire netting fences to prevent animal access to road infrastructures: an experimental study on small mammals and amphibians. Nature Conservation 47:271–281.

Cunnington, G. M., E. Garrah, E. Eberhardt, and L. Fahrig. 2014. Culverts alone do not reduce road mortality in anurans. Écoscience 21:69–78.

Cushman, S. A. 2006. Effects of habitat loss and fragmentation on amphibians: A review and prospectus. Biological Conservation 128:231–240.

Czech, B., and P. R. Krausman. 1997. Distribution and Causation of Species Endangerment in the United States. Science 277:1116–1117.

Denneboom, D., A. Bar-Massada, and A. Shwartz. 2021. Factors affecting usage of crossing structures by wildlife – A systematic review and meta-analysis. Science of The Total Environment 777:146061.

Eberhardt, E., S. Mitchell, and L. Fahrig. 2013. Road kill hotspots do not effectively indicate mitigation locations when past road kill has depressed populations. The Journal of Wildlife Management 77:1353–1359.

Elton, K., and M. Drescher. 2019. Implementing wildlife-management strategies into road infrastructure in southern Ontario: a critical success factors approach. Journal of Environmental Planning and Management 62:862–880.

Environment Canada. 2016. Management Plan for the Northern Red-legged Frog (Rana aurora) in Canada [Proposed]. Environment Canada, Ottawa. 4 pp.+ A.

Fahrig, L., J. H. Pedlar, S. E. Pope, P. D. Taylor, and J. F. Wegner. 1995. Effect of road traffic on amphibian density. Biological Conservation 73:177–182.

Fahrig, L., and T. Rytwinski. 2009. Effects of Roads on Animal Abundance: an Empirical Review and Synthesis. Ecology and Society 14.

Fardila, D., L. T. Kelly, J. L. Moore, and M. A. McCarthy. 2017. A systematic review reveals changes in where and how we have studied habitat loss and fragmentation over 20 years. Biological Conservation 212:130–138.

Fiske, I., and R. Chandler. 2011. unmarked: An R Package for Fitting Hierarchical Models of Wildlife Occurrence and Abundance. Journal of Statistical Software 43:1–23.

Forman, R. T. T., and L. E. Alexander. 1998. ROADS AND THEIR MAJOR ECOLOGICAL EFFECTS. Annual Review of Ecology and Systematics 29:207–231.

Garcia-Gonzalez, C., D. Campo, I. G. Pola, and E. Garcia-Vazquez. 2012. Rural road networks as barriers to gene flow for amphibians: Species-dependent mitigation by traffic calming. Landscape and Urban Planning 104:171–180.

Gibbs, J. P., and W. G. Shriver. 2005. Can road mortality limit populations of pool-breeding amphibians? Wetlands Ecology and Management 13:281–289.

Glista, D. J., T. L. DeVault, and J. A. DeWoody. 2009. A review of mitigation measures for reducing wildlife mortality on roadways. Landscape and Urban Planning 91:1–7.

Gonçalves-Souza, D., P. H. Verburg, and R. Dobrovolski. 2020. Habitat loss, extinction predictability and conservation efforts in the terrestrial ecoregions. Biological Conservation 246:108579.

Govindarajulu, P. 2004. Introduced bullfrogs (Rana catesbeiana) in British Columbia : impacts on native Pacific treefrogs (Hyla regilla) and red-legged frogs (Rana aurora).

Govindarajulu, P., R. Altwegg, and B. R. Anholt. 2005. Matrix Model Investigation of Invasive Species Control: Bullfrogs on Vancouver Island. Ecological Applications 15:2161–2170.

van der Grift, E. A., R. van der Ree, L. Fahrig, S. Findlay, J. Houlahan, J. A. G. Jaeger, N. Klar, L. F. Madriñan, and L. Olson. 2013. Evaluating the effectiveness of road mitigation measures. Biodiversity and Conservation 22:425–448.

Gu, W., R. Heikkilä, and I. Hanski. 2002. Estimating the consequences of habitat fragmentation on extinction risk in dynamic landscapes. Landscape Ecology 17:699–710.

Haddad, N. M., L. A. Brudvig, J. Clobert, K. F. Davies, A. Gonzalez, R. D. Holt, T. E. Lovejoy, J. O. Sexton, M. P. Austin, C. D. Collins, W. M. Cook, E. I. Damschen, R. M. Ewers, B. L. Foster, C. N. Jenkins, A. J. King, W. F. Laurance, D. J. Levey, C. R. Margules, B. A. Melbourne, A. O. Nicholls, J. L. Orrock, D.-X. Song, and J. R. Townshend. 2015. Habitat fragmentation and its lasting impact on Earth's ecosystems. Science Advances 1:e1500052.

Hanski, I. 1998. Metapopulation dynamics. Nature 396:41–49.

Harding, E. K. 2002. Modelling the influence of seasonal inter-habitat movements by an ecotone rodent. Biological Conservation 104:227–237.

Harper, E. B., and R. D. Semlitsch. 2007. Density dependence in the terrestrial life history stage of two anurans. Oecologia 153:879–889.

Hayes, M., T. Quinn, K. Richter, J. Schuett-Hames, and J. Shean. 2008. Maintaining lentic-breeding amphibians in urbanizing landscapes: the case study of the northern red-legged frog (Rana aurora). Pages 445–461.

Helldin, J. O., and S. O. Petrovan. 2019. Effectiveness of small road tunnels and fences in reducing amphibian roadkill and barrier effects at retrofitted roads in Sweden. PeerJ 7:e7518.

Hels, T., and E. Buchwald. 2001. The effect of road kills on amphibian populations. Biological Conservation 99:331–340.

Henry, A. C., D. A. Hosack, C. W. Johnson, D. Rol, and G. Bentrup. 1999. Conservation corridors in the United States: Benefits and planning guidelines. Journal of Soil and Water Conservation 54:645–650.

Heppell, S. S., H. Caswell, and L. B. Crowder. 2000. Life Histories and Elasticity Patterns: Perturbation Analysis for Species with Minimal Demographic Data. Ecology 81:654–665.

Jacobson, S. L., L. L. Bliss-Ketchum, C. E. de Rivera, and W. P. Smith. 2016. A behavior-based framework for assessing barrier effects to wildlife from vehicle traffic volume. Ecosphere 7:e01345.

Jaeger, J. a. G., and L. Fahrig. 2004. Effects of Road Fencing on Population Persistence. Conservation Biology 18:1651–1657.

Jennings, M. R., and M. P. Hayes. 1994. Amphibian and reptile species of special concern in California.

Kiesecker, J. M., and A. R. Blaustein. 1997. Population Differences in Responses of Red-Legged Frogs (Rana Aurora) to Introduced Bullfrogs. Ecology 78:1752–1760.

Kissel, A. M., W. J. Palen, M. E. Ryan, and M. J. Adams. 2019. Compounding effects of climate change reduce population viability of a montane amphibian. Ecological Applications 29:e01832.

Kociolek, A. V., A. P. Clevenger, C. C. St. Clair, and D. S. Proppe. 2011. Effects of Road Networks on Bird Populations. Conservation Biology 25:241–249.

Krebs, C. J. 1996. Population Cycles Revisited. Journal of Mammalogy 77:8–24.

Lannoo, M., editor. 2005. Amphibian Declines: The Conservation Status of United States Species.

Laurance, W. F., and A. Balmford. 2013. A global map for road building. Nature 495:308–309.

Lesbarrères, D., C. R. Primmer, T. Lodé, and J. Merilä. 2006. The effects of 20 years of highway presence on the genetic structure of Rana dalmatina populations. Écoscience 13:531–538.

Loss, S. R., T. Will, and P. P. Marra. 2014. Estimation of bird-vehicle collision mortality on U.S. roads. The Journal of Wildlife Management 78:763–771.

Malt, J. 2011. Effectiveness of Amphibian Mitigation on the Sea to Sky Highway.

Malt, J. 2013. Red-legged Frog (Rana aurora) occupancy monitoring – Metro Vancouver and Fraser Valley. Unpublished data analysis. described in COSEWIC. 2015. COSEWIC assessment and status report on the Northern Red-legged Frog Rana aurora in Canada. Ottawa. xii + 69 pp. Forests Lands and Natural Resource Operations, Surrey, BC.

McDonald, W., and C. C. St Clair. 2004. Elements that promote highway crossing structure use by small mammals in Banff National Park. Journal of Applied Ecology 41:82–93.

Mills, L. S., D. F. Doak, and M. J. Wisdom. 1999. Reliability of Conservation Actions Based on Elasticity Analysis of Matrix Models. Conservation Biology 13:815–829.

Morris, W. F., and D. F. Doak. 2002. Quantitative conservation biology. Sinauer, Sunderland, Massachusetts, USA.

Muths, E., R. D. Scherer, and D. S. Pilliod. 2011. Compensatory effects of recruitment and survival when amphibian populations are perturbed by disease. Journal of Applied Ecology 48:873–879.

Newbold, T., L. N. Hudson, S. L. L. Hill, S. Contu, I. Lysenko, R. A. Senior, L. Börger, D. J. Bennett, A. Choimes, B. Collen, J. Day, A. De Palma, S. Díaz, S. Echeverria-Londoño, M. J. Edgar, A. Feldman, M. Garon, M. L. K. Harrison, T. Alhusseini, D. J. Ingram, Y. Itescu, J. Kattge, V. Kemp, L. Kirkpatrick, M. Kleyer, D. L. P. Correia, C. D. Martin, S. Meiri, M. Novosolov, Y. Pan, H. R. P. Phillips, D. W. Purves, A. Robinson, J. Simpson, S. L. Tuck, E. Weiher, H. J. White, R. M. Ewers, G. M. Mace, J. P. W. Scharlemann, and A. Purvis. 2015. Global effects of land use on local terrestrial biodiversity. Nature 520:45–50.

Patrick, D. A., E. B. Harper, M. L. Hunter Jr., and A. J. K. Calhoun. 2008. Terrestrial Habitat Selection and Strong Density-Dependent Mortality in Recently Metamorphosed Amphibians. Ecology 89:2563–2574.

Perumal, L., M. G. New, M. Jonas, and W. Liu. 2021. The impact of roads on sub-Saharan African ecosystems: a systematic review. Environmental Research Letters 16:113001.

Petrovan, S. O., and B. R. Schmidt. 2019. Neglected juveniles; a call for integrating all amphibian life stages in assessments of mitigation success (and how to do it). Biological Conservation 236:252–260.

Piccolo, J. J., B. Taylor, H. Washington, H. Kopnina, J. Gray, H. Alberro, and E. Orlikowska. 2022. “Nature’s contributions to people” and peoples’ moral obligations to nature. Biological Conservation 270:109572.

Polak, T., J. R. Rhodes, D. Jones, and H. P. Possingham. 2014. Optimal planning for mitigating the impacts of roads on wildlife. Journal of Applied Ecology 51:726–734.

Popescu, V. D., and M. L. Hunter Jr. 2011. Clear-cutting affects habitat connectivity for a forest amphibian by decreasing permeability to juvenile movements. Ecological Applications 21:1283–1295.

Puky, M. 2003. Amphibian mitigation measures in Central-Europe. UC Davis: Institute of the Environment. Retrieved from https://escholarship.org/uc/item/5bb7k6t9

Raimer, F., and T. Ford. 2005. Yellowstone to Yukon (Y2Y) – einer der größten internationalen Wildtierkorridore. GAIA - Ecological Perspectives for Science and Society 14:182–185.

Reh, W., and A. Seitz. 1990. The influence of land use on the genetic structure of populations of the common frog Rana temporaria. Biological Conservation 54:239–249.

Rico, A., P. Kindlmann, and F. Sedláček. 2007. Barrier effects of roads on movements of small mammals.

Roedenbeck, I. A., L. Fahrig, C. S. Findlay, J. E. Houlahan, J. A. G. Jaeger, N. Klar, S. Kramer-Schadt, and E. A. van der Grift. 2007. The Rauischholzhausen Agenda for Road Ecology. Ecology and Society 12.

Rose, K. A., J. H. Cowan Jr, K. O. Winemiller, R. A. Myers, and R. Hilborn. 2001. Compensatory density dependence in fish populations: importance, controversy, understanding and prognosis. Fish and Fisheries 2:293–327.

Royle, J. A. 2004. N-Mixture Models for Estimating Population Size from Spatially Replicated Counts. Biometrics 60:108–115.

Rybicki, J., and I. Hanski. 2013. Species–area relationships and extinctions caused by habitat loss and fragmentation. Ecology Letters 16:27–38.

Rytwinski, T., and L. Fahrig. 2013. Why are some animal populations unaffected or positively affected by roads? Oecologia 173:1143–1156.

Sæther, B.-E., and Ø. Bakke. 2000. Avian Life History Variation and Contribution of Demographic Traits to the Population Growth Rate. Ecology 81:642–653.

Schwarz, C. J. 2001. The Jolly-seber model: More than just abundance. Journal of Agricultural, Biological, and Environmental Statistics 6:195–205.

Semlitsch, R. D., T. J. Ryan, K. Hamed, M. Chatfield, B. Drehman, N. Pekarek, M. Spath, and A. Watland. 2007. Salamander Abundance along Road Edges and within Abandoned Logging Roads in Appalachian Forests. Conservation Biology 21:159–167.

Serieys, L. E. K., M. S. Rogan, S. S. Matsushima, and C. C. Wilmers. 2021. Road-crossings, vegetative cover, land use and poisons interact to influence corridor effectiveness. Biological Conservation 253:108930.

Shepard, D. B., A. R. Kuhns, M. J. Dreslik, and C. A. Phillips. 2008. Roads as barriers to animal movement in fragmented landscapes. Animal Conservation 11:288–296.

Sijtsma, F. J., E. van der Veen, A. van Hinsberg, R. Pouwels, R. Bekker, R. E. van Dijk, M. Grutters, R. Klaassen, M. Krijn, M. Mouissie, and E. Wymenga. 2020. Ecological impact and cost-effectiveness of wildlife crossings in a highly fragmented landscape: a multi-method approach. Landscape Ecology 35:1701–1720.

Stuart, S. N., J. S. Chanson, N. A. Cox, B. E. Young, A. S. L. Rodrigues, D. L. Fischman, and R. W. Waller. 2004. Status and Trends of Amphibian Declines and Extinctions Worldwide. Science 306:1783–1786.

Teixeira, F. Z., A. V. P. Coelho, I. B. Esperandio, and A. Kindel. 2013. Vertebrate road mortality estimates: Effects of sampling methods and carcass removal. Biological Conservation 157:317–323.

Tuljapurkar, S. D. 1982. Population dynamics in variable environments. III. Evolutionary dynamics of r-selection. Theoretical Population Biology 21:141–165.

Van Buskirk, J. 2012. Permeability of the landscape matrix between amphibian breeding sites. Ecology and Evolution 2:3160–3167.

Vonesh, J. R., and O. De la Cruz. 2002. Complex life cycles and density dependence: assessing the contribution of egg mortality to amphibian declines. Oecologia 133:325–333.

Vos, C. C., A. G. Antonisse-de Jong, P. W. Goedhart, and M. J. M. Smulders. 2001. Genetic similarity as a measure for connectivity between fragmented populations of the moor frog (Rana arvalis). Heredity 86:598–608.

Whiteman, H. H., and S. A. Wissinger. 2005. Amphibian population cycles and long-term data sets. Amphibian declines: the conservation status of United States species. University of California Press, Berkeley:177–184.

Wiegand, T., E. Revilla, and K. A. Moloney. 2005. Effects of Habitat Loss and Fragmentation on Population Dynamics. Conservation Biology 19:108–121.

Wilcox, B. A., and D. D. Murphy. 1985. Conservation Strategy: The Effects of Fragmentation on Extinction. The American Naturalist 125:879–887.

Wilkinson, J. A., and J. M. Romansic. 2022. The effect of road-based mortality on a local population of newts along a narrow two-lane road in California. Frontiers in Ecology and Evolution 10.

Wisdom, M. J., L. S. Mills, and D. F. Doak. 2000. Life Stage Simulation Analysis: Estimating Vital-Rate Effects on Population Growth for Conservation. Ecology 81:628–641.

Yamin, F. 1995. Biodiversity, ethics and international law. International Affairs 71:529–546.

Chapter 5

Bawa, K. S. 2006. Globally Dispersed Local Challenges in Conservation Biology. Conservation Biology 20:696–699.

Delcourt, H. R., and P. A. Delcourt. 1988. Quaternary landscape ecology: Relevant scales in space and time. Landscape Ecology 2:23–44.

Meffe, G. K. 2006. The Success-and Challenges-of “Conservation Biology.” Conservation Biology 20:931–933.

Williams, D. R., A. Balmford, and D. S. Wilcove. 2020. The past and future role of conservation science in saving biodiversity. Conservation Letters 13:e12720.

Williams, S. E., L. P. Shoo, J. L. Isaac, A. A. Hoffmann, and G. Langham. 2008. Towards an Integrated Framework for Assessing the Vulnerability of Species to Climate Change. PLoS Biology 6:e325.

Appendix A.

Alternative TPC using a Generalized additive model

We fit thermal performance curves to V_{ave} for all individuals in all populations using Generalized Additive regression models (GAM) with a nonlinear locally weighted least squares smoother (LOESS; Zuur 2009) using population, weight, and larva volume as covariates. We ranked models using AICc and using the top ranked model, we estimated T_{opt} as the temperature coinciding with predicted maximum V_{ave} for each population. The top model (AICc w = 0.50; Table S5) for predicting larval burst swimming speed (V_{ave} within 0.5s) included treatment, temperature, and population identity. While population was important in predicting burst swimming speed, estimates of T_{opt} were consistent across populations (Figure S1; Table S6) at 23.0 ºC (Figure 2). For the final model we used maximum likelihood to estimate parameters from a modified beta curve (Yin et al. 2011; detailed in the main text).

Table S1. Natural flow regime of- and reduction in flow due to operation of river diversion hydropower dams on- the four streams where temperature and three where larvae were collected (except Douglas) in the South coast of British Columbia.

Stream	Mean Annual Discharge ($m^3 s^{-1}$)	Mean July Discharge Above Dam ($m^3 s^{-1}$)	July Minimum Discharge Requirement Below Dam ($m^3 s^{-1}$)	Percentage of Summer Flows Removed (%)
Tipella	7.4	4.6	0.9	80
Stokke	4.9	8.4	1.0	88
Fire	5.2	7.9	0.9	89
Douglas	6.5	6.5	0.9	85

Table S2. Average acclimation temperatures for the three populations of larvae that were kept in the lab waiting for thermal performance assays to be completed.

Population	Date of assay	Mean temperature over 21 days (°C)	+/- CI
Tipella	13-Dec-15	9.8	1.4
Stokke	09-Dec-15	9.7	1.4
Fire	11-Dec-15	9.7	1.4
	Total	**9.7**	**1.4**

Table S3. Model selection table for linear model set used to estimate the effect of warming at natural flow regimes and the warming rate due to diverted water and the presence of a dam.

Model	Degrees of Freedom	AICc	ΔAICc	AICc Weight	-Log Liklihood
Dist. From Headwater + Above or Below Dam + Interaction	5	3458.32	0	1	-1724.15
Dist. From Headwater + Above or Below Dam	4	3480.75	22.43	0	-1736.37
Dist. From Headwater	3	3703.24	244.92	0	-1848.62
Above or Below Dam	3	4555.43	1097.11	0	-2274.71
Null	2	5922.47	2464.15	0	-2959.23

Table S4. Model output for the top model describing rate of stream warming due to natural and reduced water flows and presence of a dam.

Parameter	Estimate	Std. Error	p Value
Intercept	0.17	0.02	0.00
Distance from headwaters (km)	0.17	0.01	0.00
Above or Below dam (Above = 0, Below = 1)	0.21	0.04	0.00
Interaction	0.06	0.01	0.00

Table S5. Model selection table for the Generalized additive model set used to estimate the effect of population, temperature, and individual size on smoothing Vmax. This model only shown as an alternative Topt estimator and to illustrate slight differences in the populations of larvae.

Model	Degrees of Freedom	AICc	ΔAICc	AICc Weight	-Log Liklihood
Population + Temperature	9	651.2	0.0	0.5	-315.3
Population + Temperature + Volume	10	653.8	2.6	0.1	-315.3
Population + Temperature + Mass	13	653.9	2.7	0.1	-310.2
Temperature	6	654.7	3.5	0.1	-320.0
Population + Temperature + Mass + Volume	14	655.2	3.9	0.1	-309.2
Temperature + Volume	7	656.7	5.5	0.0	-319.8
Temperature + Mass	11	656.9	5.7	0.0	-315.3
Temperature + Mass + Volume	12	659.0	7.8	0.0	-314.8
Population + Mass + Volume	11	684.2	33.0	0.0	-329.0
Mass + Volume	8	686.2	34.9	0.0	-333.0
Mass	7	687.9	36.7	0.0	-335.2
Population + Mass	10	688.4	37.2	0.0	-332.4
Null	2	690.8	39.6	0.0	-343.4
Volume	3	691.0	39.8	0.0	-342.4
Population + Volume	5	692.1	40.8	0.0	-340.7
Population	4	693.3	42.1	0.0	-342.4

Table S6. Model summary for the top GAM describing V_{max} as a function of population and treatment temperature.

Parameter	Estimate	Std. Error	p Value
Fire Population	31.80	1.80	0.00
Stokke Population	-6.51	2.56	0.01
Tipella Population	5.30	2.66	0.05

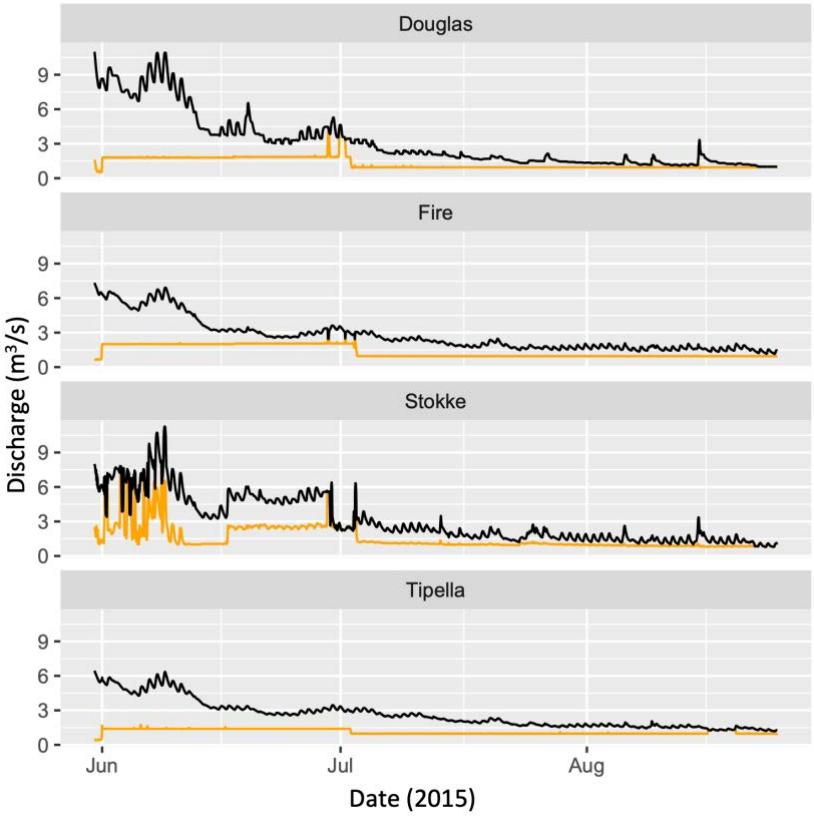

Figure S1. Summer discharge (m^3/s) (June 1 to August 25, 2015) above (black) and below dam (orange) for four streams in which temperatures were measured in the southcoast of British Columbia.

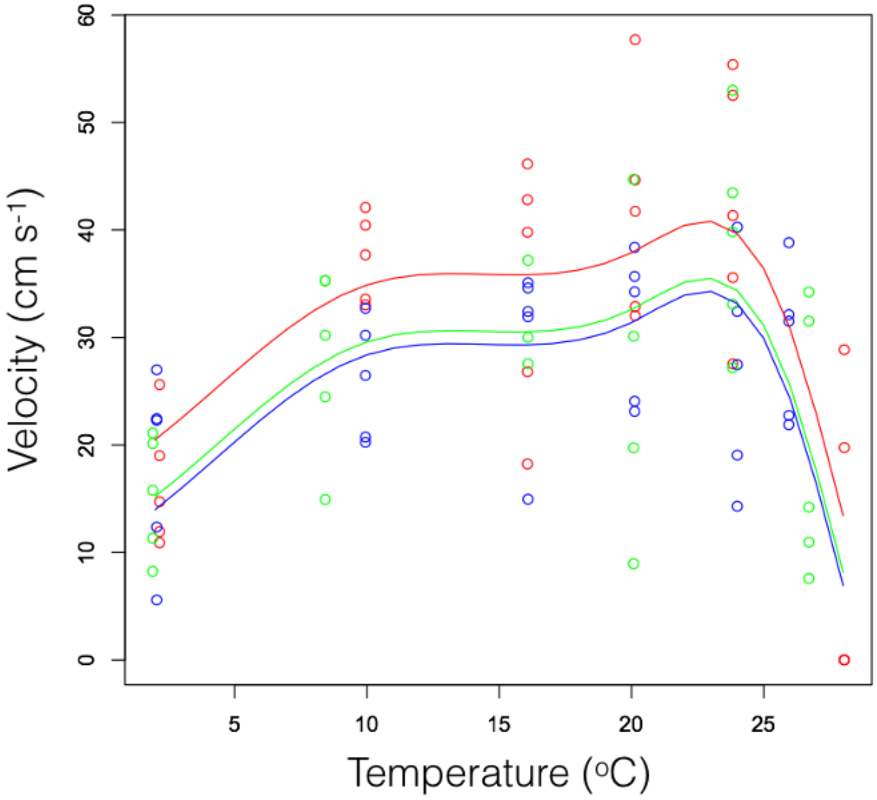

Figure S2. **Average burst swimming speeds (cm * sec^{-1}) for larval *A. truei* individuals (n = 30 per population) tested at six temperatures, and best fit thermal performance curves for each of three populations, Tipella (green), Stokke (blue), and Fire (red).**

Appendix B.

Measurement of stream temperature at the population level

At 22 of 27 streams (three in Northern California, 16 in Oregon, three in Southern British Columbia, and one in Northern British Columbia) we submerged temperature loggers (HOBO, Onset, Cape Cod, Massachusetts) to record hourly fluctuations in water temperature during the summer of 2015 (Southern British Columbia) and from summer 2016 to summer 2017 (Northern California, Oregon, Northern British Columbia). Loggers were also set at two additional streams in Northern California (Kleanza and Erlendsen Creeks) but were lost due to flooding or equipment failure during the time they were deployed. We used the data collected to calculate mean maximum daily summer (May to September) stream temperature, and summer stream temperature seasonality (the difference between mean maximum and minimum monthly temperatures for the coolest and warmest months of the summer) as predictors for differences in thermal physiology across populations.

Predicting riparian air temperatures across the species range

Using a model of riparian air temperatures as a function of landscape air temperatures, we transformed predictions of current and future landscape air temperatures downloaded from Climate NA (Wang et al. 2016) into riparian air temperatures. To make this transformation, we compared maximum daily riparian air temperatures from four streams in Southern British Columbia that have persistent *A. truei* populations between the years 2014 - 2017 with maximum daily air temperatures reported by the closest weather stations. Using a logistic curve fitted with a non-linear least squares algorithm in program R (Figure S3; $R^2 = 0.75$), we predicted riparian air temperature for each of the 4, 401 locations of *A. truei* occurrence chosen from the GBIF database with which we created frequency distributions across the species range of riparian temperatures for each region for both contemporary and future scenarios. We found that frequency of exceedance of T_{opt} using model predicted riparian air temperatures were similar to frequency of exceedance using empirical riparian air temperature data (Figure S6), suggesting that our model predictions of riparian air temperature are a good approximation across the landscape.

Table S1. ***A. truei*** **elevational range documented in each region, and midpoint used for cut-off between high and low elevations used in the analysis of thermal traits.**

Region	Elevation range (m)	Midpoint (m)	Reference
N.BC	0 - 800	400	Todd 2016
S.BC	0 - 1080	600	Hayes & Quinn 2015, Wallace & Diller 1998
OR	50 - 1800	700	Wallace & Diller 1998, Noble & Putnam 1931
N.CA	0 - 1980	900	Bury 1968

Table S2. Climatic correlates of latitude and elevation hypothesized to influence thermal traits.

Proxy for	Environmental variable	Correlation*	Reference
Latitude	30-year extreme max temperature (°C)	-0.73	
	Mean temperature of the warmest month (°C)	-0.58	Badgely & Fox 2000, Guralnick 2006, Gaston & Chown 1999
	Mean temperature of the coldest month (°C)	-0.9	As above, and: Ketterson & Nolan 1976
	Mean annual daytime temperature (°C)	-0.79	
	Degree days above 18°C	-0.52	
	Seasonality** (°C)	0.8	Badgely & Fox 2000, Guralnick 2006
	Glacier cover (% cover within 25km radius)	0.7	
	Snowfall (cm)	0.73	Ketterson & Nolan 1976
	Frostfree period (days)	-0.49	Badgely & Fox 2000
Elevation	Mean annual daytime temperature (°C)	-0.26	Buckley et al 2013
	Mean max summer stream temperature (°C)	-0.58	
	Seasonality** (°C)	0.54	Gaston & Chown 1999
	Stream seasonality** (°C)	0.14	Shah et al 2017

*Pearson's correlation coefficient **Difference between the mean temperature of the warmest month and coldest months

Table S3. Thermal optimum by population.

Region	Population	T_{opt} (°C)
N.BC	Erelendsen Tributary	24.9
	Erlendsen	19.5
	Kleanza	21
	Shames	20.2
	Kitimat	19.6
S.BC	Fire	22.4
	Tipella	19.3
	Stokke	23.1
OR	Noyo	26.1
	Bear	21.3
	Lookout	21.4
	Tidbits	26.5
N.CA	Trinity	24.2
	Stoney	23.1
	Jiggs	17.5

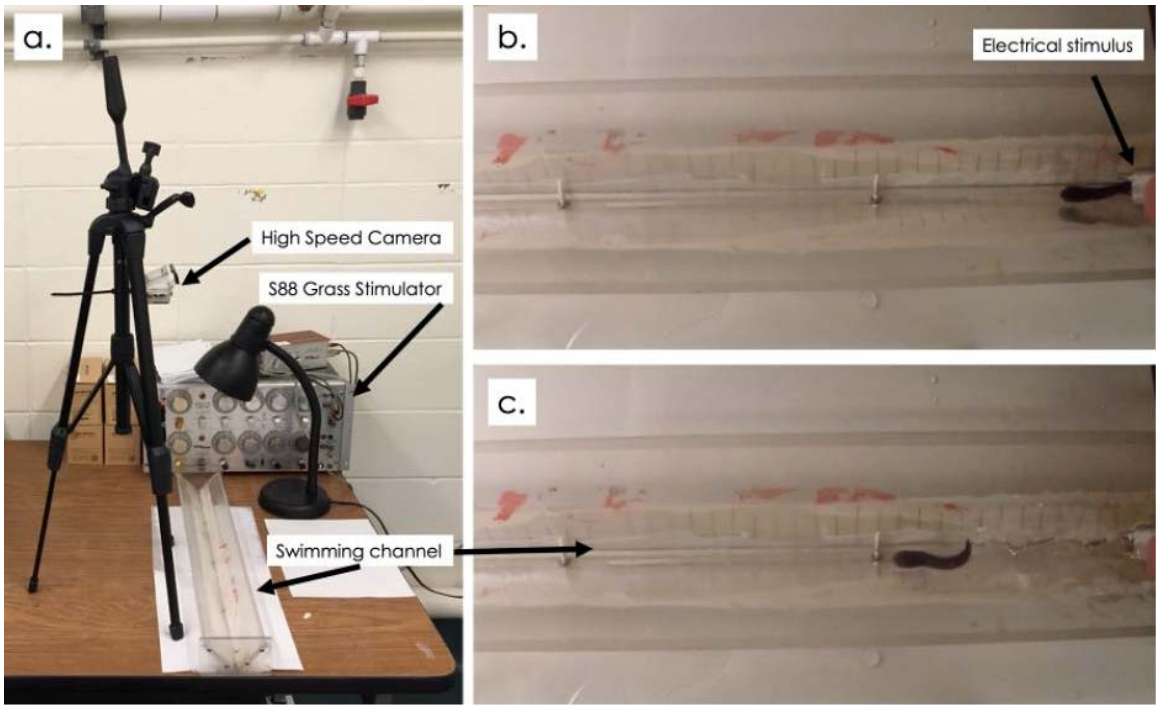

Figure S1. **Experimental apparatus for testing burst swimming speed in order to create thermal performance curves and estimate T_{opt} and TB_{80} (a). Tadpoles were placed in 2cm of water from each of their temperature treatments inside the swimming channel and given an electrical stimulus (b) at which point they swam forward (c) and were recorded with a high speed digital camera.**

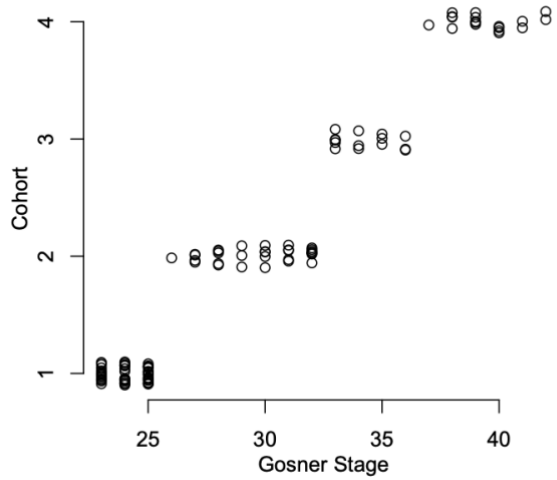

Figure S2. **Cohorts classified by Gosner Stage (based on Gosner, 1960).**

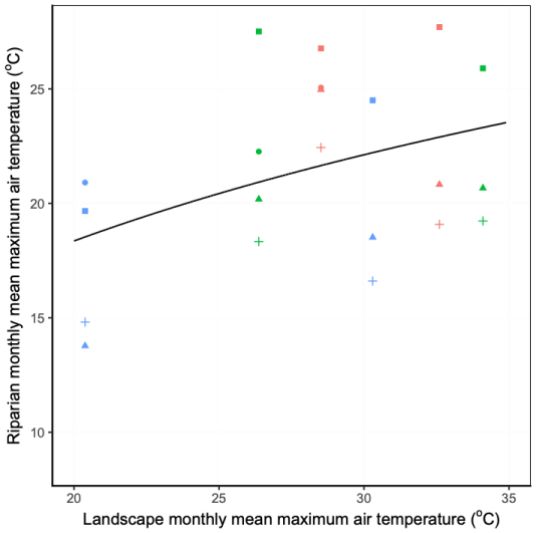

Figure S3. **Relationship of the monthly mean maximum landscape and riparian air temperatures calculated as mean of the daily maximums for each month (July, red; August, green; and September, blue) at four different streams (Douglas, circle; Fire, triangle; Stokke, square; and Tipella, cross) in Southern British Columbia in 2014 and 2015.**

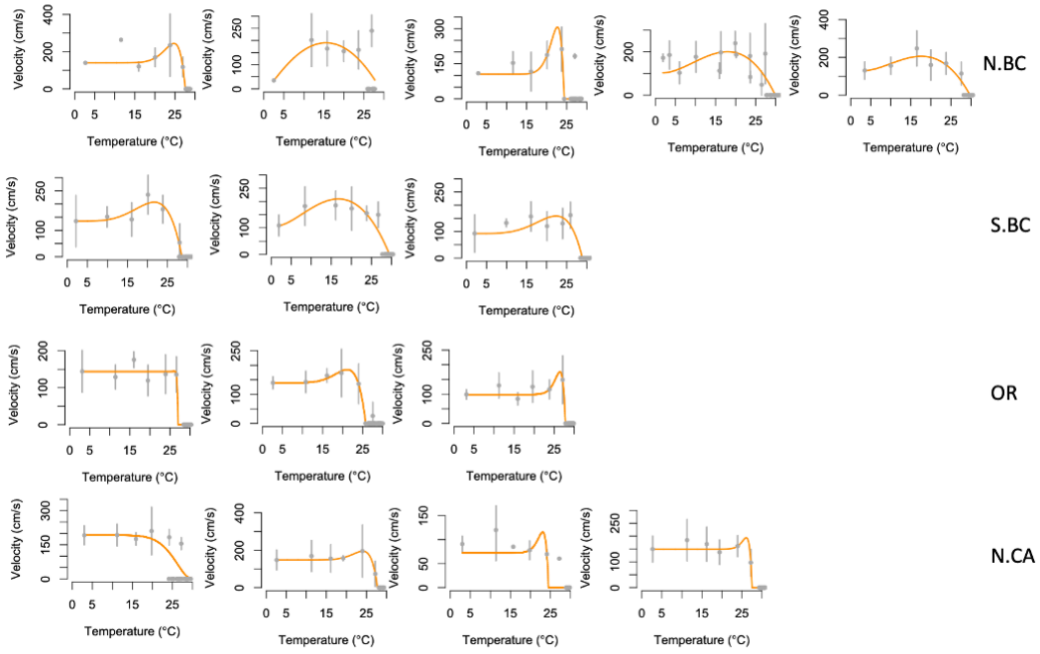

Figure S4. **Thermal performance curves by region and population with mean performance (grey dots) and standard deviation (grey lines) for each temperature treatment and performance (orange line) estimated from Equation (1).**

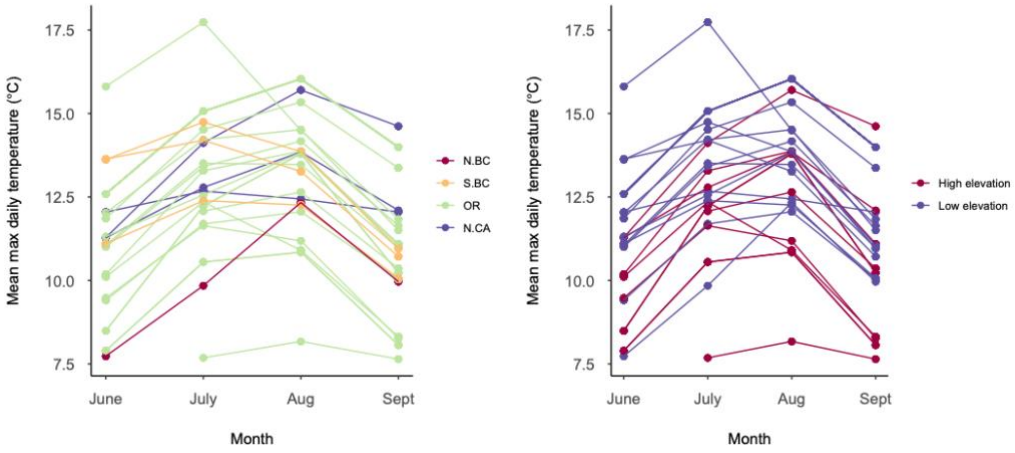

Figure S5. **Mean maximum daily stream temperatures during summer months (June - September) for 22 (of 27) streams across the *A. truei* range where we measured thermal traits (CT_{max}, T_{opt}, and TB_{80}).**

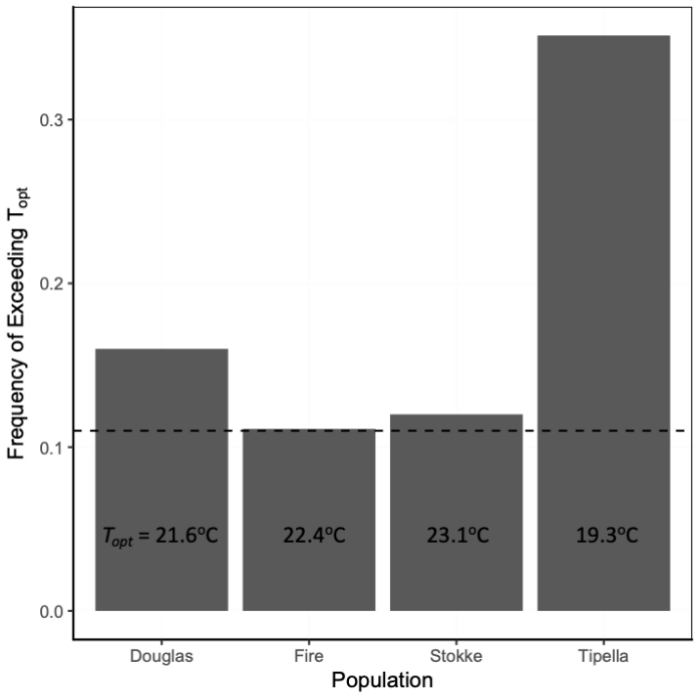

Figure S6. **Frequency of monthly mean maximum (mean of daily maximum) riparian air temperatures that exceeded T_{opt} in 2014 & 2015 at four populations in Southern British Columbia. T_{opt} for Douglas is the average between the values measured at the three nearby populations, but, frequency of exceedance, calculated from field observations of empirical temperature data, are site (population) specific. Average frequency of exceedance of modelled regional estimate of T_{opt} = 20.6°C calculated from Climate NA shown with dotted line.**

Appendix C

Overview of models used in support of matrix model scenarios

We used vital rates for *R. aurora* estimated from two populations (Swan Lake, BC, and Squaw Flat Research Natural Area) to parameterize the matrix model for the 'wild' population (scenario 7, Table 1). However, to estimate lower-level component vital rates for the proportion of the population of juveniles and adults that cross the road (scenarios 1-6, Table 1), we used experimental and survey data from the Swan Lake population (Table S1). We estimated the abundance of juveniles and adults that were at the roads edge and attempting to cross, which was then compared to our estimates of the number of individuals of each life stage that were killed on the road (carcass persistence), to estimate the per capita per crossing survival rate. We then estimated the effect of mitigation structures (BACI) on increasing survival, and the effect of increased vehicle traffic at reducing mitigation efficacy (traffic model).

Table S1. List and description of supporting models used in matrix model scenarios, including data sources, output, and use.

Model name	Description	Data source	Output	Subsequent use
Abundance at road edge	N-mixture model of abundance of juvenile and adult frogs at the roads edge and accounting for detection probability	Pitfall trap data 2005 - 2010	Juvenile and adult abundance/fence/season	per capita survival model
Carcass persistence	Binomial generalized linear mixed-effects model of probability of carcass persistence used to calculate the actual number of frogs killed on the road per night given vehicle traffic and weather variable	Road mortality surveys 2005-2010	Traffic, weather, and age specific coefficients of persistence	Multiplier of the number of frogs found in the morning to then use in per capita survival model
per capita survival	Linear model of dead frogs on the road (per fence per season) vs. alive frogs at the road edge (per fence per season)	Output from Abundance at road edge & Carcass persistence predictions of dead frogs (2005 - 2010)	per capita mortality rate of juveniles and adults crossing the road	Matrix model (road crossing survival)
BACI	BACI comparison of mean changes in mortality before and after mitigation, between control and impact stretches of road, with bootstrapped variance, not modelled	Raw road mortality at fence 1 (2000 - 2015)	Relative difference in mortality before and after mitigation, and between control and impact (mitigated).	Predicting change in mortality when mitigation is installed, matrix model lower-level component vital rate
Traffic	Number of dead frogs (corrected for persistence) as a function of the nightly hourly traffic from sunset to sunrise	Road mortality surveys & BC Ministry of Transportation Traffic Data Program (2005 - 2015)	Number of frogs killed/hourly traffic	Predicting increase in mortality in 2040's (increased vehicle traffic), matrix model lower-level component vital rate

Estimating proportion of migrating population

We assumed that approx. 25% of the *R. aurora* population was subject to potential road mortality based on the geography of our study site and observations of adult migration patterns (Figure 1). Swan Lake has been historically surrounded by forest typical of Coastal Western Hemlock Biogeoclimatic Zone (CWHvh1; B.C. Ministry of Forests 1994), However, currently the national park protects only the forest west of the lake (north and south) of the highway. Directly north of the lake is ongoing forestry, while east - southeast are active and fallow quarries and active industrial yards. A creek running south from Swan Lake to the highway to the southeast most fenced section acts as a migration corridor particularly for juveniles in the late summer, but also for adults in the spring and fall. While the forestry and industry block migration to the north and east, migration is unimpacted to the northwest where years of observation have seen migrating juveniles and adults moving into the forest protected by the national park. The 1.69km of highway over which road mortality has been observed from 2000 – present bisects possibly 25 - 50% of the landscape over which individuals may disperse and migrate across. Furthermore, by comparing our mean yearly estimates of adult frogs crossing the road, and correcting for sex ratio (341 females), to our average yearly estimates of egg masses laid and assuming every female breeds every year (1380 egg masses), we estimate that 24.7% of the female population crosses the road, and apply that number to the juvenile population as well.

Background on mitigation treatments

In May 2011, a concrete box culvert (1.8m x 0.5m interior) was installed under the highway to serve as an amphibian underpass where we had repeatedly captured the highest number of Northern Red-legged Frogs in pitfall traps. This location was along the southeast roadside fence (fence 1) 50 m from an existing drainage culvert where intermittent storm water has created a channel to Swan Lake. We added fencing to lead amphibians from the forest to the box culvert and drainage culvert (Figure S1). The initial fencing material was the same as the plastic sheeting used for the roadside fences, held up by wooden stakes to a height of 40 cm, and buried into the ground 10 cm. Each arm of fencing extended 15 to 60 m into the forest from the entrances of the two culverts on each side of the highway. In 2014, we replaced the plastic with durable polyethylene fabric to improve the integrity and function of the fencing.

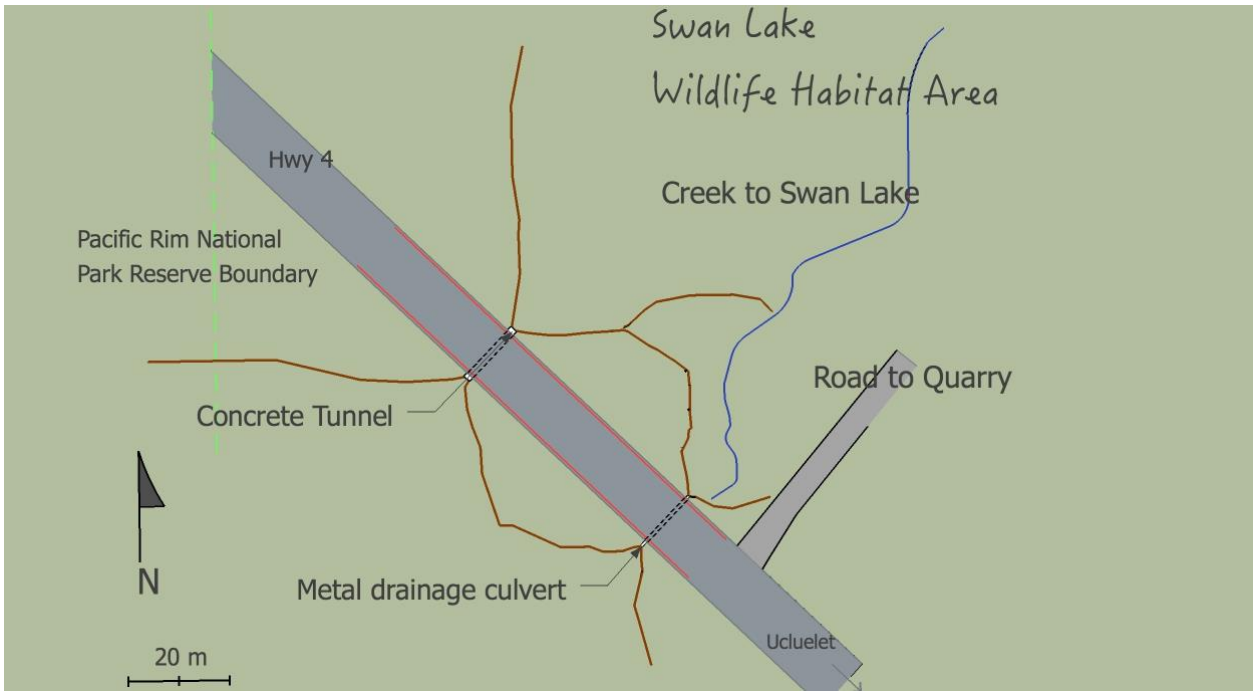

Figure S1. Layout of mitigation that included a new concrete box-culvert, and angled fencing leading amphibians to it and a nearby existing drainage culvert.

Quasi-extinction threshold

We chose a quasi-extinction threshold (Ginzburg 1982) of $n \leq 20$ adult females because it is the lower threshold recommendation given by Morris and Doak (2002) that is sufficiently high to take into account the stochasticity of the population.

Estimating vital rates

Here we describe the sources and field studies from which we derived vital rates for our population model for *R. aurora.* We estimated fecundity and embryonic survival for the Swan Lake *R. aurora* population between 2012 – 2018 by enclosing 4 – 21 (μ = 12) egg masses each year in separate floating mesh containers and counting the number of hatched and non-hatched tadpoles. Larval survival, first-year overwintering juvenile survival (called metamorph), second-year juvenile survival, and adult survival were each estimated from a *R. aurora* population in the Squaw Flat Research Natural Area in Umpqua National Forest, Oregon, USA (42° 58’ 14.3394”, -122° 40’ 43.2114”), at a 0.6-ha breeding pond surrounded by relatively undisturbed mixed coniferous forest and savanna-like first- and second- order drainages that carry surface water

into early summer (Hayes 2001). Specifically, larval survival was estimated from changes in larval density between sampling occasions. Overwintering metamorph, juvenile, and adult survival was estimated from a 3-year capture-mark-recapture study, where capture bouts occurred every 2 – 4 weeks throughout the spring, summer, and early fall, or every week during peak breeding and metamorph emergence and estimated using program MARK with a robust design. Specifics of the capture-mark-recapture data and model were lost in a fire at Washington State Department of Fish and Wildlife, Olympia, Washington. Variance around the mean vital rate estimates for fecundity and embryonic survival was obtained from 6 years of field data (B. Beasley – Swan Lake), and larval and juvenile suevival from the variance around 3 years of mean estimates (M. Hayes – Squaw Flats), and from previously published literature for overwintering metamorph and adult survival (*Rana luteiventris;* McCaffery & Maxell 2010).

Estimating abundance at road edge

The top models for detection and abundance for juveniles and adults were similar for each season (Table S2). Spring season detection was affected by overnight rain, summer detection by the combination of rain and overnight temperatures and fall season detection by the combination of all three detection variables: overnight rain, overnight temperatures, and the number of hours the traps were left open. Detection varied by season and by age and ranged from 5 – 15%, with the highest detection of adults and juveniles during the spring season (Table S2). The top models for detection and abundance for juveniles and adults were similar for each season (Table S2). Spring season detection was affected by overnight rain, summer detection by the combination of rain and overnight temperatures and fall season detection by the combination of all three detection variables: overnight rain, overnight temperatures, and the number of hours the traps were left open. Detection varied by season and by age and ranged from 5 – 15%, with the highest detection of adults and juveniles during the spring season (Table S3).

Estimating abundance of road mortality

The top model to predict carcass persistence was age and overnight rain and carried 42% of the AICc weight, however, a model that included the amount of traffic was less than 2 ΔAICc units from the top and carried an additional 22% AICc weight, therefore we used a model average of the two models within 2 ΔAICc units to predict persistence of carcasses on the road (Table S3). Persistence was negatively correlated with juveniles (they disappeared more often

between night and morning surveys), overnight rain was also negatively correlated with persistence (it helped to wash away the caracasses), and finally, hourly traffic was also negatively correlated with persistence (the more traffic during the night decreased the likelihood of re-finding a carcass between night and morning surveys; Figure S2). The average persistence (at average hourly traffic observed and average rainfall) for juveniles was 0.19 (0.13 – 0.27 95%CI) and for adults was 0.71 (0.65 – 0.76 95%CI).

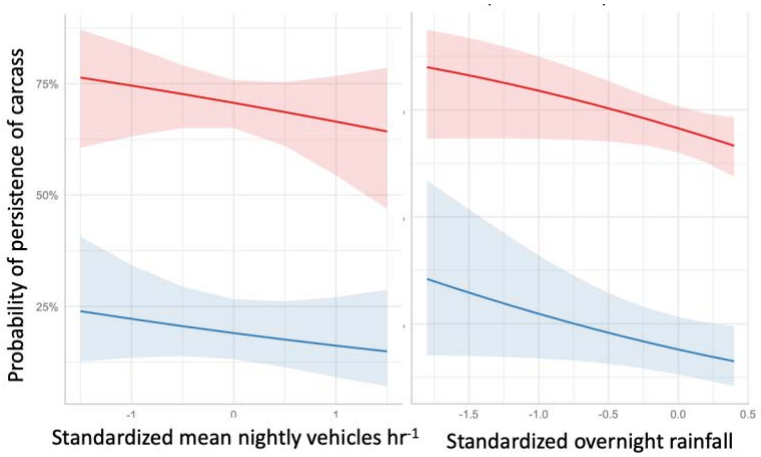

Figure S2. Predicted probability of persistence of adult (red) and juvenile (blue) *R. aurora* carcasses on the highway as a function of the standardized (minus the mean and divided by two standard deviations) mean number of cars per hour at night and the standardized total overnight rainfall.

Estimating road survival

We used a linear model of the mean density of dead frogs per kilometer at night throughout each of the three seasons (spring, summer, fall) as a function of the density of frogs attempting to cross the road per kilometer at night throughout each season to estimate the per capita mortality rate of juvenile and adult Red legged frogs that cross the road to complete the migratory portion of their lifecycle. The slope of the regression is the mortality rate, i.e. the number of frogs that are killed on the road per number of frogs found at the edge of the road attempting to cross. Adults: y = 0.0754 ($\pm$ 0.04 SE) x + 6.7 ($\pm$ 7.9), r^2 = 0.3, α < 0.05, Juveniles: y = 0.0214 ($\pm$ 0.01 SE)x + 0.7 ($\pm$ 1.1), r^2 = 0.4, α < 0.05.

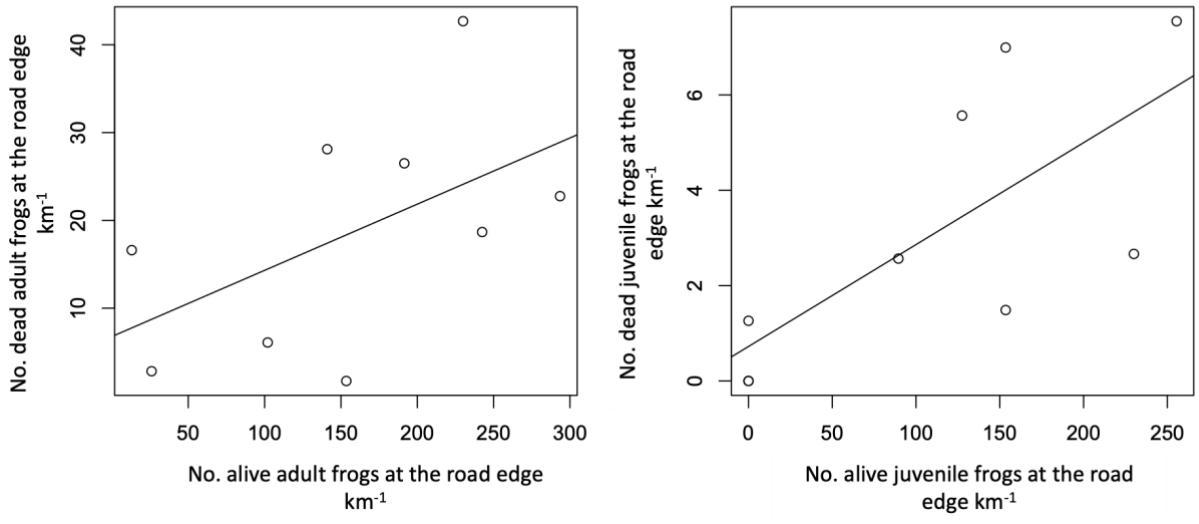

Figure S3. Mean predicted number of dead frogs per kilometer per fence (n = 3) per season (breeding, summer, dispersal) as a function of the mean predicted number of frogs alive at the road edge per kilometer per fence per season for adults (left) and juveniles (right).

Wild population size & correcting egg mass counts for detection

Egg masses were counted at Swan Lake between the years 2007 – 2022 using a kayak, and from 2014 to 2022using a stand-up paddle board (SUP) which was found to have better detection of egg masses under water due to its higher angle of observation. To correct for the lower detection of kayak egg mass counts in the earlier years, we implemented a study in 2019 and 2020 to compare the differences between the two methods. We created a nested design within each year: we delineated 30 different sections of egg laying habitat within Swan Lake with pin flags at the beginning of each breeding season and left the markers up until the end of breeding season. We chose 10 sections accessible to both types of vessels and re-counted each using multiple observers and the two different vessels (kayak, SUP). We implemented all possible combinations of re-counting: some re-counts were by the same observer with the same vessel, some re-counts by different observers with the same vessel, and some re-counts by the same observer with different vessels. Using the egg mass re-counts over 2 years we fit a negative binomial generalized linear mixed effects model using method (kayak v. SUP), observer ID, and search minutes as fixed effects, and section ID as a random effect, we found that SUP counts were 2.2 (± 1.1 SE) times higher than kayak counts. We applied this correction factor to the earlier egg mass counts (2010 – 2013; Figure S3) and left out years

2007-2009 because these were years where we were learning where the egg masses were laid and likely did not count all possible sections containing egg masses. Using the corrected yearly egg mass counts, we calculated a geometric mean λ and evaluated the general performance of the deterministic matrix by comparing it to the real geometric mean λ (a population with current levels of traffic and some mitigation).

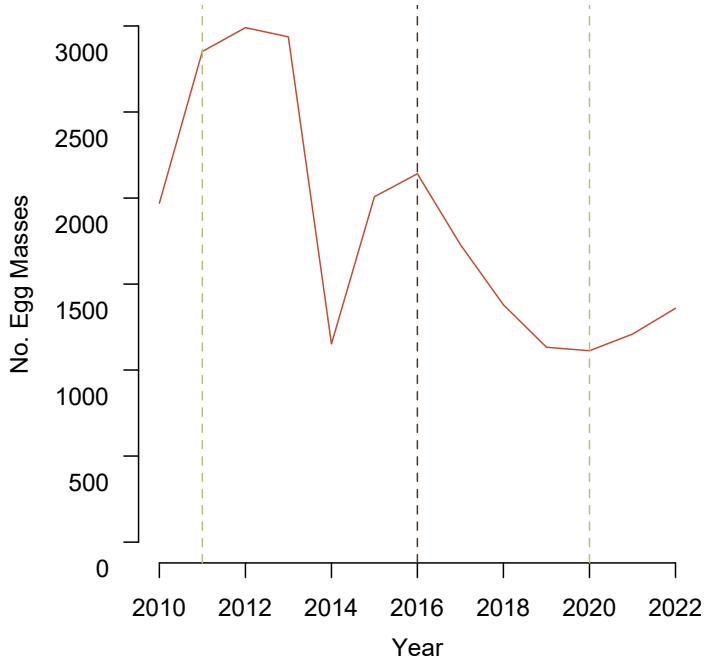

Figure S3. **Annual number of *R. aurora* egg masses detected in Swan Lake, BC surveyed over 12 years. Underpasses were added in 2011 (n = 1) and in 2020 (n = 3; light dashed lines) within the 1.69km stretch of road that bisects the Swan Lake population migration corridor for juveniles and adults. In 2016, 59.6-ha of forest and suspected foraging habitat for juveniles and adults was logged to the north & northeast of Swan Lake (dark dashed line).**

Table S2. Top, global, and null models for detection and abundance of juveniles and adults in pitfall traps.

Model	Detection parameters	Site parameters	ΔAICc	*w*	Total # of models
Spring					
Adults					
Top	Overnight rain	Fence + Side of road	0	0.34	8
Global	Overnight rain + Mean overnight temperature + Hours open	Fence + Side of road	1.6	0.15	
Null	~	Fence + Side of road	3.7	0.05	
Juveniles					
Top	Overnight rain	Fence + Side of road	0	0.34	8
Global	Overnight rain + Mean overnight temperature + Hours open	Fence + Side of road	0.55	0.21	
Null	~	Fence + Side of road	2.36	0.09	
Summer					
Adults					
Top	Overnight rain + Mean overnight temperature	Fence + Side of road	0	0.48	8
Global	Overnight rain + Mean overnight temperature + Hours open	Fence + Side of road	1.4	0.24	
Null	~	Fence + Side of road	13.78	0	
Juveniles					
Top	Overnight rain + Mean overnight temperature	Fence + Side of road	0	0.71	8
Global	Overnight rain + Mean overnight temperature + Hours open	Fence + Side of road	1.75	0.29	
Null	~	Fence + Side of road	299.83	0	
Fall					
Adults					
Top/Global	Overnight rain + Mean overnight temperature + Hours open	Fence + Side of road	0	0.99	8
Null	~	Fence + Side of road	421.3	0	
Juveniles					
Top/Global	Overnight rain + Mean overnight temperature + Hours open	Fence + Side of road	0	1	8
Null	~	Fence + Side of road	2700.06	0	

Table S3. Predicted detection probabilities for adults and juveniles in pitfall traps during the three seasons of capture at the road edge.

	Detection probability	SE
Spring		
Adult	0.15	0.02
Juvenile	0.14	0.02
Summer		
Adult	0.07	0.02
Juvenile	0.08	0.02
Fall		
Adult	0.07	0.03
Juvenile	0.05	0.08

Table S4. Model selection table for the persistence of carcasses on the road from night to morning surveys.

Parameters	DF	ΔAICc	*w*
Age + Overnight rain	4	0.0	0.42
Age + Hourly traffic + Overnight rain	5	1.3	0.22
Age	3	2.4	0.13
Age + Hourly traffic	4	3.0	0.09
Age + Season + Overnight rain	6	3.8	0.06
Age + Season + Hourly traffic + Overnight rain	7	5.0	0.04
Age + Season	5	6.1	0.02
Age + Season + Hourly traffic	6	6.4	0.02
Null	2	100.8	0
Overnight rain	3	101.7	0
Hourly traffic	3	102.8	0
Season	4	103.7	0
Hourly traffic + Overnight rain	4	103.7	0
Season + Overnight rain	5	104.6	0
Season + Hourly traffic	5	105.7	0
Season + Hourly traffic + Overnight rain	6	106.5	0

Table S5. Model selection table for the number of carcasses on the road as a function of the hourly nightly traffic and overnight rainfall. We used the top model (No. cars per hour only) to make predictions of the mean number of frogs killed during mean current traffic, and mean future traffic in the 2040's.

Parameters	DF	ΔAICc	*w*
No. cars per hour	2	0	0.58
No. cars per hour + Overnight rainfall	3	0.67	0.42
Overnight rainfall	2	29.04	0
Null	1	35.14	0

Conclusions on Swan Lake

While the utility of demographic models is in understanding how population dynamics arise from species life-histories generally, we also have the opportunity to make inferences about the Swan Lake *R. aurora* population in particular. We evaluated the risk posed by roads that bisect a *R. aurora* migration corridor in by using demographic rates estimated from two populations: one in Oregon, USA and one in British Columbia, Canada. By combining vital rates, borrowing some data from previously published literature, and in particular, having the unique opportunity to parameterize our 'wild' (scenario 7) population with previously unpublished data (Oregon, M. Hayes) from a pristine habitat, we can make comparisons to Swan Lake in order to understand the specific impacts of our conservation efforts. We expect that, in general, the Swan Lake population is responding to road mortality similar to other *R. aurora* populations impacted by roads (e.g. Malt 2011, 2013). It is tempting to further compare our estimate of geometric mean λ calculated from 12 years of egg mass surveys (2010 – 2022; Appendix S1, Figure S3) to the specific mitigation efforts at Swan Lake in order to evaluate our conservation goals, especially because geometric mean λ = 1.01 and is very similar to λ_s = 1.01. However, real impacts not reflected in our model may influence population growth at Swan Lake, such that a comparison of road impacts and mitigation efficacy cannot be directly drawn between our model and the observed population growth. For example, in winter 2016, 59.6-ha of forest was logged northwest of Swan Lake. The geometric mean λ for the period preceding logging (2010 – 2016) was 1.11, and afterwards (2017 – 2022) was 0.92, suggesting that the loss of habitat may induce negative density dependence in the older life stages, and/or that the sediment that subsequently flowed into Swan Lake could also negatively impact embryonic and larval stage survival. While geometric mean λ for the period after logging but before the

installation of three more underpasses (2016 – 2020) was 0.84, and after (2021 – 2022) was 1.11, similar to pre-logging, the population appears to exhibit periodicity in abundance much like other populations across diverse taxa (Krebs 1996, Whiteman and Wissinger 2005). Therefore, continuing to collect long-term data will be required to make any inference about impacts to the observed population abundance and dynamics. Thus, further illustrating the importance of demographic models and their potential to increase the speed of conservation efforts.